Echocardiographic assessment of the right heart in conditions with transient right ventricular pressure overload

PhD thesis

Ágnes Nógrádi MD

Supervisor: Réka Faludi MD, PhD

Head of the Doctoral School: Prof. Lajos Bogár MD, PhD, DSc

Head of the Doctoral Program: Prof. István Szokodi MD, PhD, DSc

University of Pécs, Medical School

Heart Institute

Pécs, 2023

Table of Contents

1 Abbreviations

2D	2-dimensional
2DE	2-dimensional echocardiography
3D	3-dimensional
3DE	3-dimensional echocardiography
6MWT/D	6-minute walk test/walking distance
A	late diastolic velocity of the mitral/tricuspid inflow
a’	annular late diastolic myocardial longitudinal velocity
ACR/EULAR	American College of Rheumatology/ European League Against Rheumatism
AEF	active emptying fraction
ASE/EACVI	American Society of Echocardiography/European Association of Cardiovascular Imaging
AUC:	area under the curve
BSA:	body surface area
CPET	cardiopulmonary exercise test
CO:	cardiac output
COPD:	chronic obstructive pulmonary disease
CT:	computed tomography
CTD	connective tissue diseases
CTD-P(A)H	pulmonary (arterial) hypertension associated with connective tissue diseases
CTEPH	chronic thromboembolic pulmonary hypertension
DcSSc:	diffuse cutaneous form of systemic sclerosis
DLCO:	diffusion capacity of carbon monoxide
E:	early diastolic velocity of the mitral/tricuspid inflow
e’:	annular early diastolic myocardial longitudinal velocity
EF:	ejection fraction
EI:	expansion index

ESC	European Society of Cardiology
ERS	European Respiratory Society
EIPH	exercise induced pulmonary hypertension
FEV1	forced expiratory volume in the first second
FVC	forced vital capacity
HFpEF:	heart failure with preserved ejection fraction
HFrEF	heart failure with reduced ejection fraction
ILD	interstitial lung disease
ILD-P(A)H	pulmonary (arterial) hypertension associated with interstitial lung disease
IVC	inferior vena cava
LA:	left atrium, left atrial
LHD	left heart disease
LHD-P(A)H	pulmonary (arterial) hypertension associated with left heart disease
LSD test	least significant difference test
LV:	left ventricle, left ventricular
LVMi:	left ventricular mass index
(m)PAP	(mean) pulmonary artery pressure
MPI	myocardial performance index
MRI:	magnetic resonance imaging
NT-proBNP:	N-terminal pro-B-type natriuretic peptide
NYHA:	New York Heart Association
P(A)H:	pulmonary (arterial) hypertension
PASP	pulmonary artery systolic pressure
PAWP:	pulmonary arterial wedge pressure
PEA	pulmonary endarterectomy
PEF:	passive ejection fraction
PH	pulmonary hypertension

PVR	pulmonary vascular resistance
RHC	right heart catheterization
ROC curve:	receiver operating characteristic curve
RV	right ventricle, right ventricular
RVFAC	right ventricular fractional area change
S:	annular systolic myocardial longitudinal velocity
SD:	standard deviation
SSc:	systemic sclerosis
SSc-P(A)H	pulmonary (arterial) hypertension associated with systemic sclerosis
STE:	speckle tracking echocardiography
SV	stroke volume
TAPSE	tricuspid annular plane systolic excursion
TDI:	tissue Doppler imaging
TEF:	total emptying fraction
TPG	transpulmonary gradient
TPR	total pulmonary resistance
TR	tricuspid regurgitation
Vae:	active emptying volume
VIF:	variance inflation factor
Vmax:	maximal atrial volume
Vmin:	minimal atrial volume
Vp:	pre-contraction atrial volume
Vpe:	passive emptying volume
Vte:	total emptying volume
SLE	systemic lupus erythematosus
WHO	World Health Organization
WU	Wood unit

2 Introduction

Elevated pulmonary arterial pressure, a condition with complex aetiology, results in an increased right ventricular (RV) afterload, which in turn triggers anatomical and biochemical responses, both adaptive and maladaptive. These processes lead in the end to the clinical syndrome of right heart failure, an important cause of morbidity and mortality [1].

Among conditions with right heart overload, chronic obstructive pulmonary disease (COPD) is significant as a growing global epidemic, one of the leading causes of death, as well as representing a large health care burden and being an important cause of disability [2, 3]. Dyspnoea and reduced functional capacity are common consequences with a multifactorial aetiology including parameters of the resting pulmonary function such as forced expiratory volume in the first second (FEV1), dynamic lung hyperinflation, pulmonary hypertension (PH), alterations of the cardiac function as well as other factors such as depression and skeletal muscle weakness [4-8]. Among the potential cardiac causes of exercise intolerance, RV systolic failure with low cardiac output (CO) is rare in patients with COPD, but they often develop RV diastolic dysfunction with stress induced or resting elevation of filling pressures [9]. Left ventricular (LV) diastolic dysfunction is also reported to be common in the COPD population [10, 11]. Nevertheless, data are scarce regarding the effect of the RV and LV diastolic dysfunction on the functional capacity in COPD.

Systemic sclerosis (SSc), another condition associated with PH, is a connective tissue disease (CTD) characterized by inflammation, microvascular damage, and generalized fibrosis of the skin and various internal organs. It has been proved that cardiac and pulmonary manifestations are present in a high proportion of patients and are recognized as powerful adverse prognostic factors [12]. LV diastolic dysfunction is frequent in SSc [13, 14] and is often accompanied by impaired left atrial (LA) function [15-17]. RV dysfunction was traditionally attributed to the development of pulmonary arterial hypertension (PAH) or pulmonary fibrosis [18]. Subclinical RV dysfunction, however, was also proved in SSc patients without the resting elevation of the pulmonary pressure, by using tissue Doppler or speckle tracking measurements [19-22]. Recent data suggest that right atrial (RA) size and mechanics correlate well with the functional capacity of the patients in conditions with known right heart

involvement, such as in idiopathic PAH [23]. In SSc, however, little is known about the RA mechanics and about its correlation with the functional capacity and survival of the patients.

Functional impairment of RV and RA is difficult to measure, but the novel echocardiographic methods such as tissue Doppler imaging (TDI) and the even more recently developed speckle tracking echocardiography (STE) are appropriately sensitive to recognise even the subclinical dysfunction of the right heart.

3 Objectives

The aim of the present work was the echocardiographic assessment of the right heart – focusing on the parameters of RA size and mechanics – in conditions with transient RV pressure overload, such as COPD and SSc. TDI and 2-dimensional (2D) STE-derived strain techniques were used to investigate the correlation between echocardiographic parameters and the functional capacity of the patients. Prognostic value of the RA size and mechanics was also investigated in SSc patients without manifest PAH.

4 Background

4.1 Pulmonary hypertension

Increased pressure in the pulmonary circulation from any cause will lead to an overload of the right heart and eventually to right heart failure. PH is therefore a significant cause of morbidity and mortality [24]. PH is defined by an elevated mean pulmonary artery pressure (mPAP) measured invasively with right heart catheterization (RHC). Historically, the cut off value defining PH was set at mPAP equal or higher than 25 mmHg, though it was changed in the recently published ESC guideline [24, 25]. Among the various conditions causing PH, two fundamentally different pathomechanisms can be differentiated: 1. Conditions with precapillary PH are caused by diseases affecting primarily the lung parenchyma and/or the pulmonary vasculature. These include PAH, PH caused by pulmonary diseases, chronic thromboembolic pulmonary hypertension (CTEPH) and some cases of PH of unclear or multifactorial origin. In these forms, diagnosis is based on a pulmonary arterial wedge pressure (PAWP) less than or equal to 15 mmHg (besides the elevated mPAP) [24]. 2. On the other hand, diseases of the left heart may cause an elevation of the LA filling pressure which in turn results in the increase of PAP. This form is therefore called postcapillary or venous PH and is characterized by PAWP exceeding 15 mmHg. It is to be noted that postcapillary PH is divided into 2 subgroups of isolated postcapillary PH with normal pulmonary vascular resistance (PVR) and combined pre-and postcapillary PH (with increased PVR) [24]. The World Health Organization (WHO) classification of PH are described in **Table 1**.

The traditional definition of PH was challenged in recent years: It was recognized that the cut off value of PH has been set arbitrarily at mPAP ≥ 25 mmHg. Based on the analysis of accumulated hemodynamic data of healthy subjects by Kovacs et al. [26], normal mPAP was found to be 14 ± 3 mmHg; thus, the upper normal limit should be 20 mmHg (mean + 2 SD). This was supported by the growing evidence that the so-called borderline range of PAP between 21-24 mmHg also has clinical and prognostic significance, especially in patients with an increased risk for developing PH [27-30].

Table 1. Clinical classification of pulmonary hypertension(Humbert, Kovacs et al. 2022).

1. **Pulmonary arterial hypertension (PAH)** 1.1. Idiopathic 1.1.1.Non-responders at vasoreactivity testing 1.1.2.Acute responders at vasoreactivity testing 1.2. Heritable 1.3. Associated with drugs and toxins 1.4. Associated with: 1.4.1.Connective tissue disease 1.4.2.HIV infection 1.4.3.Portal hypertension 1.4.4.Congenital heart disease 1.4.5.Schistosomiasis 1.5. PAH with features of venous/capillary (PVOD/PCH) involvement 1.6. Persistent pulmonary hypertension of the newborn
2. **PH associated with left heart disease** 2.1. Heart failure: 2.1.1.with preserved ejection fraction 2.1.2.with reduced ejection fraction 2.2. Valvular disease 2.3. Congenital/acquired cardiovascular conditions leading to post-capillary PH
3. PH associated with lung diseases and/or hypoxia 3.1. Obstructive lung disease or emphysema 3.2. Interstitial lung disease 3.3. Lung disease with mixed restrictive/obstructive pattern 3.4. Hypoventilation syndromes 3.5. Hypoxia without lung disease (e.g. high altitude) 3.6. Developmental lung disorders
4. PH associated with pulmonary artery obstructions 4.1. Chronic thromboembolic PH 4.2. Other pulmonary artery obstructions
5. PH with unclear and/or multifactorial mechanisms 5.1. Haematological disorders 5.2. Systemic disorders 5.3. Metabolic disorders 5.4. Chronic renal failure with or without haemodialysis 5.5. Pulmonary tumour thrombotic microangiopathy 5.6. Fibrosing mediastinitis

PCH: pulmonary capillary haemangiomatosis; PVOD: pulmonary veno-occlusive disease

In SSc it was shown that patients with mPAP in the borderline range have similar symptoms related to decreased exercise capability, a higher risk of developing PAH as well as an

increased risk of mortality [27]. Valerio described that 86 of 228 (37.7%) in a cohort of SSc patients had mPAP values in the borderline range. This group had an increased risk for progressing to manifest PH (HR 3.7) compared to the normal subgroup [29]. Kovacs et al. investigated a small cohort of SSc patients without significant pulmonary fibrosis, left heart dysfunction, or manifest PAH. In this group, resting mPAP above the median (17 mmHg) was predictive of reduced exercise capability (decreased 6-minute walking distance (6MWD) and peak VO2) [27]. Stamm et al. compared SSc patients with normal, borderline, and elevated mPAP and showed that the 1-, 3-, and 5-year survival differed significantly among the three subgroups. Lung transplant-free survival was similar in the borderline and manifest PH groups but significantly worse than in the group with normal mPAP [30]. Similarly, in patients with chronic thromboembolic disease without PH (mPAP ≤25 mmHg), significant exercise limitation may be found, and desobliteration with pulmonary endarterectomy (PEA) resulted in haemodynamic and clinical improvements [31, 32].

Recently, the focus of research shifted to patients with Group 2 and Group 3 PH (with chronic left heart disease and chronic lung disease) who make up the large majority of PH patients, and who also were shown to have a 2–3 fold increased mortality risk with the development of PH [9, 33]. In a group of patients with idiopathic pulmonary fibrosis, even the borderline mPAP forecasted a poorer outcome: patients with mPAP>17 mmHg experienced significantly higher 5-year mortality [34]. In a large cohort of unselected patients undergoing RHC, both upper-normal (mean+1SD to mean + 2SD: 17.4–20.6 mmHg) and borderline (20.6–24.9 mmHg) mPAP's were significantly associated with poor survival. In multivariate model, considering age and comorbidities, however, only borderline mPAP remained the independent predictor of all-cause mortality [35]. In a cohort of veterans including more than 21 000 patients undergoing RHC for any indication, those with borderline mPAP had an increase of mortality (HR 1.2) [36]. A retrospective study of a mixed cohort of patients undergoing RHC revealed similar results: borderline mPAP (18–24 mmHg) was associated with mortality with a HR of 1.3 [37].

Thus, in 2018, the 6th World Symposium on Pulmonary Hypertension published the expert consensus opinion that the definition of PH should be based on mPAP > 20 mmHg and PVR > 2

Wood units (WU) [38]. Thus, the recently published European Society of Cardiology Guidelines for the diagnosis and treatment of pulmonary hypertension amended the earlier definitions [24].

4.2 Pulmonary hypertension in COPD

4.2.1 Prevalence

In Thabut's cohort of patients evaluated for lung transplantation or lung volume reduction surgery, about half of COPD cases had a PH (mPAP > 25 mmHg), of whom 36.7% was mild (mPAP 26 to 35 mmHg), 9.8% moderate (mPAP 36 to 45 mmHg), and 3.7% was severe (mPAP > 45 mmHg) [39]. In Andersen's retrospective analysis (n=409), 51% of the patients evaluated for lung transplantation had normal pulmonary pressures, 13% had postcapillary PH (mPAP ≥ 25 mmHg, PAWP > 15 mmHg) whereas 36% had precapillary PH. Severe PH (mPAP > 35 mmHg), was shown in 16 patients (3.9%) [40] In a group of 362 patients evaluated for lung transplantation, 23% or 68% of the patients had PH, when using mPAP > 25 mmHg or >20 mmHg as cut-off, respectively [41]. Cuttica et al. showed that PH was present in 30% of 4930 patients included in the Organ Procurement Tissue Network database registry study, with severe PH in 4% [10]. These data suggest, that in up to 90% of COPD patients, mPAP exceeds 20 mmHg at rest [42]. In most of the cases, however, PH is relatively mild, between 20-35 mmHg. Only 1-5% of patients have a mPAP > 35-40 mmHg [43, 44].

4.2.2 Pathophysiology

By definition, PH in COPD belongs to Group 3 (PH due to chronic lung diseases and/or hypoxia). The pathophysiology of COPD (small airways' disease and parenchymal destruction, chronic inflammation) results in hyperinflation, airway obstruction, airway collapse and in the advanced phase, elevated intrathoracic pressure [3]. These factors may results in hypoxia and hypoxic vasoconstriction which are considered as main factors resulting in increased PVR in COPD [2, 3].

However, it is well known that PH in COPD is complex and multifactorial in origin [3]: concomitant left heart failure occurs in up to 30% of patients [3], and LV diastolic dysfunction is even more common [11, 45] which can lead to Group 2 PH. CTEPH, Group 4 PH may also occur, as COPD is associated with an increased risk of pulmonary embolism [46-48]. In addition, in some patients the pulmonary vascular changes are predominant, forming a PH subgroup who share some important clinical characteristics (severe PH, progressive right heart failure) with patients with PAH (Group 1). It is called as "pulmonary vascular phenotype" group by Kovacs et al. [49].

4.2.3 Clinical significance

4.2.3.1 Prognosis

In COPD, similarly to other groups of PH, even moderate elevation in pulmonary pressures is associated with worse survival [9]. In 1981, Weitzenblum et al. found that among 175 COPD patients, the presence of mPAP > 20 mmHg was associated with shorter survival [50]. Nevertheless, both this group and another study found that the rate of PH progression in COPD is relatively slow (an increase of 0.4 to 0.7 mmHg per year) [50, 51].

In patients receiving long term oxygen therapy, mPAP was the best prognostic factor of mortality, better than FEV1, hypoxia or hypercapnia: in this cohort, patients with mPAP > 25 mmHg had a 5-year survival of 36.3% compared to 62.2% in those with mPAP < 25 mmHg [52]. In a study reporting a 7-year follow-up of COPD patients, survival had a negative correlation with PVR [53]. Besides, in a large cohort of end-stage COPD patients evaluated for lung transplantation, patients with PH had a significantly worse survival than those without PH [40].

4.2.3.2 Worse clinical status

PH is also a marker of worse clinical status and the more frequent acute exacerbations in COPD. In the study of Kessler et al., mPAP > 18 mmHg carried a higher risk of severe exacerbations requiring hospital admission [54]. Dilated pulmonary artery trunk on computed tomography (CT) scan is an imaging parameter predictive of PH [55]. In the study by Wells et al., this finding predicted hospitalization for COPD acute exacerbations [56]. In the study of

Sims et al., elevated mPAP was proved to be an independent predictor of decreased exercise capability in COPD patients [41].

4.3 Pulmonary hypertension in connective tissue diseases

4.3.1 Prevalence

The association of Group 1 PH (PAH) with connective tissue diseases (CTD) is well known. In fact, PAH associated with CTD (CTD-PAH) is the second most prevalent form after idiopathic PAH in Western countries [25, 57]. SSc, mixed connective tissue disease and systemic lupus erythematosus (SLE) are the CTD's most frequently complicated with PAH. Among these, SSc is most prevalent in the Western countries [57] while in Asian countries, SLE-PAH is more common [58, 59]. The largest body of data exists about SSc-PAH, and the diagnosis was invasively confirmed in most of these studies. The prevalence of PAH in SSc is shown to be 7.8-12% [60-62]. Hachulla et al. found a 0.61 cases/100 patient years incidence of newly diagnosed PAH [63]. P(A)H prevalence in SLE is shown to be 3.3-5% [64, 65]. It is of note, that in most studies about PH in further types of CTD's other than SSc, the diagnosis was established non-invasively, by echocardiography, and pre-or postcapillary forms of PH were not distinguished [64-66].

4.3.2 Pathophysiology: various forms of PH in SSc

Although SSc-PAH is the most extensively researched form of PH in SSc, it is known that SSc may be associated with all the other PH groups [67]. Pulmonary fibrosis (interstitial lung disease, ILD) and left heart failure with preserved ejection fraction (HFpEF) occur frequently in SSc, but it is important to mention the rare forms of PH like pulmonary veno-occlusive disease (PVOD) or CTEPH [67]. LV diastolic dysfunction is one of the most common cardiac manifestations in SSc [13, 68], its prevalence reaches from 23% [69] to 43-67% in some cohorts [17, 70]. HFpEF, the manifest clinical syndrome caused by diastolic dysfunction was present in about 27% of SSc patients in a recent survey [71]. ILD is another frequent manifestation of SSc, occurring in about 25-50% of SSc patients [72].

In spite of the high prevalence of these complications in SSc, many of the studies report Group 1 PAH as the most common cause of SSc-PH: 50-70% of the invasively confirmed PH cases are

shown to be PAH while a smaller segment of patients is classified as Group 2 PH (9-21%) and Group 3 PH (19-36%) [61, 73, 74]. In other studies that excluded patients with clinically relevant ILD or differentiated only between pre-and postcapillary PH, postcapillary PH constituted 20-40% of the total PH count [75, 76]. It is to be noted that most of the registries and patient cohorts studied for PH were aimed at diagnosing PAH, and patients likely to have another cause for PH (ILD or HFpEF) were often excluded from studies and were less likely to undergo RHC. This heterogeneous patient selection and referral bias potentially obscures the true prevalence of Group 2 and Group 3 PH in SSc patients [61].

The significant overlap among the mechanisms leading to PH in SSc is further demonstrated by the results of Bourji et al., who found that among the left heart disease (LHD) associated PH patients, the majority (63%) was in the combined pre-and postcapillary PH haemodynamic category. Also, Fox et al. found that in their SSc-PH cohort about one third of the patients initially classified as precapillary PH should be reclassified to LHD-PH after fluid challenge as it resulted in a pathological elevation of the LV filling pressure [76].

PVOD is a rare form of PH in which echocardiographic findings and the haemodynamic parameters suggest PAH. The histopathological changes such as obliterating fibrosis, however, occur predominantly in the small pulmonary venules. Diagnosis is based on morphological parameters on CT scan. The clinical deterioration (manifestation of pulmonary oedema) after initiation of PAH-specific therapy is also characteristic. This condition is more prevalent in SSc than in the general population and it is supposed that some SSc-PAH patients have a prominent venous component of their disease [67].

4.3.3 Clinical significance of PH in SSc

4.3.3.1 Mortality

Cardiac involvement in general, the presence of lung disease, and the presence of PH are known to increase mortality in SSc [12, 70, 77]. Cardiac involvement is associated with a HR of 2.1-3.2 [12, 70] while the presence of PH carries a HR of 3.1-3.5 in metaanalyses evaluating 8-12 thousands of SSc patients [12, 78]. SSc-PAH has worse prognosis than idiopathic PAH [79, 80] while ILD-PH in SSc is shown to have even poorer survival rates: 3-year survival rate was

35% in a metaanalysis, compared to 56% in SSc-PAH [72]. Lefevre et al. observed similar results (1- and 3-year survival rates of 81% and 56%, respectively in SSc-PAH versus 1- and 3-year survival rates of 77% and 35%, respectively in ILD-PH) [81]. In the study of Bourji et al., LHD-PH in SSc patients had twofold worse mortality than SSc-PAH patients when adjusted for haemodynamic parameters [75].

4.3.3.2 Screening

The above prevalence and survival data underline the importance of early detection of PH in SSc. Screening methods have been proposed based on several studies [62, 74, 82-84]. The current guideline updated the recommendations on screening SSc patients. The risk of PH should be annually evaluated in all SSc patients based on clinical symptoms (breathlessness); echocardiogram or pulmonary function test including forced vital capacity (FVC) and diffusion capacity of carbon monoxide (DLCO); and brain natriuretic peptide or N-terminal pro-B-type natriuretic peptide (BNP/NT-proBNP) [24]. In patients with the characteristics of the DETECT study cohort (patients with SSc spectrum disorders associated with DLCO < 60% of predicted and disease duration >3 year), the DETECT diagnostic algorithm is recommended which includes a two-step approach using NT-proBNP, additional biomarkers, ECG and clinical parameters such as teleangiectasias and FVC%/DLCO% before echocardiography [74].

4.4 Exercise pulmonary hypertension

There is a subgroup of patients who have normal pulmonary pressures at rest, but they present with effort dyspnea and increased PAP during exercise. If the resting PAP was not elevated, early guidelines recommended to perform exercise RHC [85]. Mean PAP>30 mmHg on exercise was included in the definition of PH, often termed as exercise induced PH (EIPH).

However, the 4th World Symposium on Pulmonary Hypertension held in 2008 in Dana Point, California, concluded that there are several uncertainties in the methodology of the exercise RHC and the definition of EIPH [86]. Namely, the type, level, and posture of the exercise test were not standardized. Furthermore, it was recognized that the normal response to exercise varies with age in the pulmonary circulation, showing an increase in peak pulmonary pressures

even in the healthy elderly population. There is a significant overlap between the physiological and pathological levels of exercise-induced increase in mPAP. In a study, almost 50% of healthy subjects aged >50 years had an exercise induced mPAP>30 mmHg (the supposed upper normal limit) [26]. In this study it was also recognized that higher CO resulted in higher mPAP values on exercise. Thus, the concept of EIPH was omitted from the subsequent guidelines [25, 87].

Detailed analysis of the physiological response to exercise [88, 89] shows that increase of mPAP on exercise has a linear relationship with the increasing CO, and the slope (mPAP/CO ratio, i. e. total pulmonary resistance, TPR) distinguishes physiological increase from pathological. The excessive increase in mPAP in relation to CO during exercise may be caused by two distinct pathophysiological processes: 1. In left heart failure, exercise causes a steep elevation of LV filling pressure which will be transmitted backwards through the pulmonary circulation to cause PH. 2. In pulmonary vascular pathology, PVR elevation is responsible for mPAP increase, without PAWP elevation. Subclinical levels of pulmonary vasoconstriction and remodelling [88, 90] cause a transient elevation of PAP during exercise as pulmonary circulation no longer has the capacity to adapt to the increasing CO.

A recent review by Zeder et al. proposed cut-off values of prognostic relevance based on available evidence: mPAP/CO slope > 3 WU and PAWP/CO slope > 2 WU was associated with worse prognosis in two cohorts of patients with effort dyspnea [91, 92]. Considering these data, the recently published ESC guideline reintroduced the definition of exercise PH defined as mPAP/CO slope between rest and peak exercise > 3 WU [24].

Although mPAP/CO slope > 3 WU is shown to define a pathological response, it does not distinguish between precapillary and postcapillary causes [90]. These two can be distinguished with more detailed analysis using mPAP, PAWP, transpulmonary gradient (TPG) and CO in the following mathematical equations:

$$TPR=mPAP/CO$$

$$TPG=mPAP-PAWP$$

$$mPAP=TPG+PAWP$$

$$PVR=(mPAP-PAWP)/CO=TPG/CO$$

$$mPAP/CO=TPG/CO+PAWP/CO$$

which reflects the pathophysiological concept that mPAP/CO can be elevated if either TPG/CO increases due to the pathology of the pulmonary vasculature, or PAWP/CO increases due to let heart disease [93].

4.4.1 Exercise PH in COPD

Just as mildly elevated PAP is a common finding in COPD, normal resting PAP with a pathological response to exercise also occurs in a large proportion of these patients. Supposed mechanisms include pulmonary vascular disease as well as LV dysfunction or exercise-induced air trapping [49].

In the study of Cherneva et al., 67% of the patients had elevated mPAP on exercise, tested by stress echocardiography [94]. With invasive assessment, Christensen et al. found exercise PH (defined as mPAP > 30 mmHg) in 65% of their COPD patients during exercise equivalent to the activities of daily living, [95]. Skjørten et al. investigated 93 stable COPD patients, of whom 24% had PH at rest, 45% had exercise PH and 21% had normal hemodynamic results [96]. Portillo et al. observed a 71% prevalence of exercise PH in a group of 85 COPD patients; the ratio of exercise PH patients was 70%, 67% and 100% in GOLD 2, GOLD 3 and GOLD 4 stages, respectively [97]. In the cohort of Kessler et al., 131 stable COPD patients without hypoxemia or resting PH (using 20 mmHg as cut-off), 42% had normal hemodynamic response to exercise, and 58% had exercise PH [51]. Hilde et al. examined 98 stable COPD patients, among whom 27% had resting PH and 73% no PH. In this cohort, both the PH and the non-PH groups showed similar increase in PAP and PVR on exercise. Based on a threshold of mPAP/CO slope <3WU, only less than half of the non-PH group (30 patients) had normal hemodynamic response to

exercise and the remaining 42 patients (41%) could be considered as exercise PH. mPAP/CO slope was a predictor of exercise tolerance [98]. In the follow-up study of Kessler et al., COPD patients with exercise PH had a significantly higher risk of developing resting PH [51].

4.4.2 Exercise PH in CTD

Evidence is accumulating about the prevalence and significance of exercise PH in CTD, with particular focus on SSc patients who formed the majority of the investigated patient cohorts.

In the studies that evaluated SSc or CTD patient cohorts invasively, exercise PH was found in a significant number of the patients. Hager et al. examined 173 patients on exercise RHC who had previously undergone resting and stress echocardiography suggesting elevated PAP. In this cohort, 53 patients (35%) had increased mPAP and mPAP/CO slope on exercise. Based on detailed analysis including changes in TPG, PAWP, ΔTPG/ΔPAWP and PVR, this group was further divided into precapillary (n=6) and postcapillary (n=47) origin [99]. In Saggar et al.'s cohort of 80 SSc patients, 52% had exercise PH. The authors divided these into 3 groups: exercise LHD-PH (n=12), exercise PAH (n=21) and a group they called "exercise out of proportion PH", as both PAWP and TPG were elevated (combined pre-and postcapillary origin using the current nomenclature, n=9) [100]. Stamm et al. had a SSc patient group of similar size with clinical suspicion of PH, and they found 45% exercise PH with RHC, 12% in the postcapillary and 33% in the precapillary group [30]. Miyanaga et al. investigated a smaller group of CTD patients (n=34) including non-SSc type CTD's. Their proportion of exercise PH patients was slightly less: 21% [101]. These studies used various cut-off values and definitions: exercise mPAP > 30 mmHg, exercise TPR > 3 WU, or exercise TPG ≥ 15 mmHg [30, 99-101]. mPAP/CO slope cut-off was usually 3 WU but occasionally 2 WU [99]. Cut-off for PAWP on exercise was 18 [100], or 20 mmHg [30]. Besides the different inclusion criteria also may explain the differences in their results.

Clinical significance of exercise PH in SSc, similarly to that in COPD, includes worse exercise tolerance, a risk for developing resting PH and higher risk for mortality or adverse outcome: Kovacs et al. subgrouped their SSc patients using the median mPAP on moderate exercise (23 mmHg at 25 W, 28 mmHg at 50 W) as cut-off, lower than the usual threshold for exercise PH.

Patients with mPAP above the median (measured at either level of exercise) had worse exercise tolerance on 6MWT [27]. In the study of Miyanaga et al., mentioned above, the exercise PH group had higher resting mPAP, right atrial pressure (RAP) and PVR, but lower 6MWD and peak VO_2/kg than the subgroup with normal exercise response [101]. In another prospective study of 85 SSc patients showing clinical risk factors for PH, exercise PH detected by stress echocardiography predicted a high risk for developing resting PH [102].

Stamm et al. found that survival was significantly worse in the exercise PH group compared to SSc patients without PH, but similar to those with PH at rest. Exercise mPAP was a predictor of lung transplant-free survival [30]. In the study of Zeder et al., investigating 80 SSc patients without resting PH, both PVR and TPR on exercise as well as mPAP/CO slope and TPG/CO slope showed association with mortality while resting hemodynamic parameters did not [103].

4.5 Echocardiographic techniques for the assessment of transient and permanent pressure overload in the right heart

4.5.1 Stress echocardiography

Exercise RHC is the gold standard for evaluating hemodynamic response to exercise and to identify those patients with exercise PH [24]. However, the invasive nature of this examination as well as the well-known technical difficulties make it advisable to search for non-invasive diagnostic modalities which can detect cardiopulmonary involvement at an early stage in patients at high risk for PH. Echocardiography is potentially useful in this aspect.

Clinical data about assessing exercise hemodynamics with stress echocardiography in COPD are scarce. Two studies tested small groups of COPD patients with Doppler echocardiography during cardiopulmonary exercise test (CPET), using sitting [104] or supine [105] cycle ergometer. They concluded that COPD patients had significantly reduced exercise tolerance and higher PASP values on exercise compared to controls [105] but oxygen inhalation reduced the exercise related elevation of PASP [104]. Both studies required intravenous administration of agitated saline contrast to achieve adequate Doppler signals of the tricuspid regurgitation (TR). The difficulty of obtaining adequate echocardiographic images in COPD patients, in

particular during exercise, is generally acknowledged [104-106]. Cherneva et al. examined a larger group of non-severe COPD patients with CPET using supine cycle ergometer. Echocardiography was performed at rest and immediately (within 1-2 minutes) after peak exercise. Their goal was to investigate the prevalence of LV and RV diastolic dysfunction on exercise [107, 108]. The results showed a marked prevalence of LV diastolic dysfunction (64%) and RV diastolic dysfunction (78%) on exercise.

In SSc there were attempts to evaluate exercise hemodynamics noninvasively, with stress echocardiography. Results of these studies show a marked prevalence of exercise PH in SSc patients, between 36% and 55% [102, 109-114]. The criteria for diagnosing exercise PH were various: immediate post-stress pulmonary arterial systolic pressure (PASP) > 35+5 mmHg [109]; ΔPASP ≥ 20 mmHg [110]; PASP ≥ 50 mmHg at peak exercise [111-113]. Moreover, a recent metaanalysis reported significant variability in the methodology of these studies as well (cycloergometer or treadmill, supine, semi-supine or upright position, exercise PASP measured during or immediately after exercise) [115]. Some, but not all stress-echocardiographic studies assessed CO, PVR and markers of LV diastolic dysfunction or elevated LV filling pressure to differentiate between pre-and postcapillary origin of exercise PH. These non-invasive hemodynamic measurements, however, are technically challenging and not always standardized [115]. There are also some studies that use 6MWT as exercise to assess increase in PASP [114, 116] Thus, reliable and reproducible assessment of exercise PH in SSc and analysis of the underlying pathophysiology with stress echocardiography may need further research and standardization [115].

4.5.2 Resting echocardiography in P(A)H and exercise PH

4.5.2.1 Traditional methods for the detection of PH

Resting transthoracic echocardiography is the most important screening modality for PH [24, 84]. The primary echocardiographic parameter is estimated RV systolic pressure, calculated from the peak TR velocity utilizing the modified Bernoulli equation. Although a sensitivity of 87% and a specificity of 79% was shown for echo-measured PASP in predicting invasively measured PH [117], the potential pitfalls of this non-invasive estimation are well known [118].

Recent studies show considerable discordance between noninvasively estimated PASP and invasive results obtained by RHC [119, 120]. Therefore, additional echocardiographic parameters are required to assess the probability of PH. Elevated pressures in the right heart typically result in dilatation of the RV, RA or pulmonary artery. Besides, flattening of the interventricular septum, shortened RV outflow tract acceleration time, notching on the RV outflow tract Doppler curve, high early pulmonary regurgitation velocity and dilated inferior vena cava (IVC) with decreased inspiratory collapse may also occur [24]. However, in mild PH and especially in exercise PH, these overt signs of RV pressure overload are usually not detectable.

4.5.2.2 Assessment of RV systolic function

Transthoracic echocardiography can also be used to detect RV systolic dysfunction developing in consequence of RV pressure overload. The traditional parameters of RV systolic dysfunction include tricuspid annular plane systolic excursion (TAPSE) – an index of the longitudinal systolic function, and RV fractional area change (RVFAC) – a parameter of global RV function. Besides, myocardial performance index (MPI) or Tei index reflects both RV systolic and diastolic function [121].

Besides the traditional echocardiographic modalities, TDI also supplies information regarding RV function. Tricuspid annular systolic velocity (tricuspid S) has been added to the recommended parameters when investigating RV longitudinal systolic function [121].

There is a robust amount of accumulated data on RV function based on these parameters which have been validated against radionuclide ventriculography or magnetic resonance imaging (MRI), the current gold standard for determining RV function [121-124]. However, there are limitations to the use of each. Thus, the combined assessment of these parameters is recommended in the current guideline [121].

Echocardiographic parameters of RV systolic dysfunction predict adverse clinical events and mortality in a variety of conditions: in PAH [125-129], SSc [20, 130], HFpEF [131], Group 3 PH [132], COPD [133] Eisenmenger's syndrome [134], and HFrEF [130, 135].

The echocardiographic parameters of RV systolic function can also indicate a favourable response to therapy: in a group of untreated PAH patients tricuspid S was reduced compared to controls, but improved after receiving pulmonary vasodilator therapy [136].

In the context of PH, as the above studies show, RV systolic function has great diagnostic and prognostic significance. However, these studies included patients with manifest PH, often in advanced stage of the disease. Several studies show limited sensitivity of these traditional echocardiographic parameters especially when the studied PH patients are in early stage of the disease. In some studies, involving patients with pulmonary disease or with SSc, echocardiographic parameters of RV function did not show significant difference compared to controls. In the study of D'Andrea et al. comparing two subgroups of patients with idiopathic pulmonary fibrosis (with or without PH) to healthy controls, TAPSE and tricuspid S were within normal range across all subgroups, without significant differences. The only significant difference was found in the pulmonary fibrosis-PH subgroup: RV hypertrophy and dilatation [137]. In the study of Yiu et al., SSc patients with or without pulmonary fibrosis and/or PH exhibited preserved TAPSE, similarly to the healthy control group [18].

On the other hand, in some patient cohorts, traditional RV functional parameters showed significant difference but were still within the normal range across all subgroups. This was shown in the study of Hilde et al., comparing COPD patients with or without PH and controls. Although TAPSE, RVFAC and tricuspid S showed a small but significant difference, they were within the normal range even in patients with COPD-PH. RV MPI, however, was impaired in COPD patients both with and without PH suggesting the possibility of transient, exercise-related elevation of pulmonary pressures not manifesting on resting echocardiography [138]. Similarly, in comparing SSc patients to healthy controls, Durmus et al. found that RVFAC showed no significant difference, while TAPSE and tricuspid S was significantly decreased, but still within the normal range in the SSc cohort [20]. Cuttica et al. examined non-severe COPD patients (mild, moderate, and moderately severe subgroups were defined according to the American Thoracic Society guidelines). They found normal TAPSE and tricuspid S values across the whole cohort, without significant difference according to COPD severity [10]. Fukuda et al. investigated predictors of adverse outcome (death or hospitalization for right heart failure) in

PAH and CTEPH patients, and found that traditional RV functional parameters could not distinguish between the subgroups with and without adverse events [139].

As the above results show, traditional echocardiographic parameters of RV systolic function are often not sensitive enough to identify patients with exercise related transient elevation of pulmonary pressure in high-risk conditions, such as COPD or SSc.

4.5.2.3 Evaluation of RV diastolic dysfunction with tissue Doppler echocardiography

Similarly to that of LV diastolic function, the recommended method to evaluate RV diastolic function is a combined approach using tricuspid E/A, tricuspid e', and tricuspid E/e' [121, 140, 141]. In research, however, other parameters, including isovolumetric relaxation time, deceleration time and tricuspid e'/a' have also been used [134, 142-144].

The presence of RV diastolic dysfunction was confirmed in conditions associated with right heart involvement: in a group of SSc patients, RV diastolic dysfunction (diagnosed by tricuspid E/A and tricuspid E/e') was found in 25% of the cohort by Meune et al. [145]. Durmus et al. found impaired tricuspid e' in SSc patients compared to controls [20]. Impaired tricuspid e' compared to controls was also confirmed in COPD patients by Agoston-Coldea et al., along with increased tricuspid E/e' indicating an increase of RV filling pressure [146]. Seyfeli et al. investigated a group of rheumatoid arthritis patients and found significantly impaired RV diastolic function compared to controls. TDI parameter tricuspid e'/a' was more sensitive in recognising RV diastolic dysfunction than tricuspid E/A. Besides, the subgroup with elevated PASP had significantly worse RV diastolic function detected by TDI in this study [147]. Ozdemirel et al. found that in COPD patients, RV diastolic function parameters correlated with FEV1 and with various CPET parameters [148].

Huez et al. found reduced tricuspid E/A in SSc patients compared to controls, as well as impaired tricuspid e' with TDI [149]. The patients also showed decreased exercise capacity and decreased maximum workload on stress echocardiography. Noninvasively obtained estimation of pulmonary pressure-flow curve suggested that RV diastolic dysfunction was an early sign of latent pulmonary vascular pathological changes resulting in exercise PH in this

cohort [149]. Faludi et al. aimed to confirm this observation with the help of echocardiographic and invasive measurements in patients with various CTD's. [19]. Their findings showed that CTD patients with resting PH had both RV systolic and diastolic dysfunction based on TDI parameters, while the subgroup with exercise PH had only RV diastolic dysfunction, suggesting that RV diastolic dysfunction may be an early consequence of transient, exercise related PH [19]. In another cohort of SSc patients without resting PH, Gargani et al. found that tricuspid e'/a' was independent predictor of elevated PASP on exercise [112]. There are some data about prognostic significance of RV diastolic dysfunction: in a prospective study of CTD patients, tricuspid e' was among the predictors of the development of PH [116].

4.5.2.4 Speckle tracking derived strain: Right ventricular function

Speckle tracking echocardiography (STE) is a recently developed technique to assess myocardial mechanics. It is a sensitive technique allowing the exploration of subclinical, previously undetected myocardial dysfunction [150]. The usefulness of RV strain parameters (either RV free wall or RV global strain) is demonstrated in several conditions related to PH: RV strain was shown to be decreased compared to controls while conventional echocardiographic parameters of RV function were within normal range in SSc [18, 21]. Similar phenomenon was reported in patients with PAH and CTEPH [151, 152]. In the study of Morris et al., RV global and free wall systolic strain were able to detect subtle RV longitudinal systolic abnormalities in a significant proportion of patients with HFrEF and to a lesser extent in HFpEF despite the preserved TAPSE, tricuspid S and RVFAC values [153]. D'Andrea et al. demonstrated significantly impaired RV strain values in pulmonary fibrosis patients both with and without PH compared to controls [137]. Similarly, in the study of Hilde et al., COPD patients both with and without PH showed decreased RV strain values compared to controls [138].

RV strain was also shown to correlate with disease severity in these studies: In the above COPD cohort, RV strain correlated with invasively measured pulmonary pressures [138]. Regarding SSc patients, in the investigation of Yiu et al., all SSc patients (with or without pulmonary fibrosis and with or without PH) showed significantly impaired RV free wall strain compared

to controls, but the subgroup with both pulmonary fibrosis and PH had the most severely impaired RV free wall strain [18]. In HFpEF and HFrEF patients, Morris et al. showed significantly worse RV strain parameters parallel with the worsening of NYHA functional class. RV strain showed significant correlation with exercise tolerance demonstrated by 6MWD in patients with idiopathic pulmonary fibrosis [137]. Fukuda et al. proved similar correlation in PAH. In their study, RV free wall strain also correlated with invasively measured mPAP [152]. Similarly, in the study of Rice et al., in a group of COPD patients undergoing RHC, RV strain correlated with PVR. Moreover, PASP and RV strain could be estimated in 31% and 57% of the COPD patients, respectively [154].

RV strain also demonstrates excellent prognostic ability: it was found to predict adverse outcome in PAH [139, 155], and in HF [156, 157]. Fine et al. showed independent and incremental prognostic value of RV-free in a group of patients evaluated for PH [158]. Hardegree et al. reported that serial RV strain measurements were useful in monitoring therapeutic response and predicting outcome in PAH [159]. Similarly, in a group of COPD patients undergoing pulmonary rehabilitation, RV strain improved after completion of the program and showed significant correlation with the change in exercise capacity [160].

4.5.3 Right atrial size and mechanics

4.5.3.1 Pathophysiology

Understanding LA function and its role in the pathophysiology of left heart failure [161, 162] directed the focus on the evaluation of RA function [163].

RA function consists of three phases throughout the cardiac cycle: during ventricular systole, with closed tricuspid valves, RA receives the blood from the body (reservoir phase); after the opening of the tricuspid valve, in the early phase of ventricular relaxation it passively conveys the blood to the RV (conduit phase) and during late diastole the active contraction of the RA assists ventricular filling as a booster pump (contractile phase) [163-165].

Each of these phases is influenced both by intrinsic atrial properties and by interactions between the atrium and the ventricle [166]: the reservoir phase is influenced by the apical

displacement of the tricuspid annulus; the conduit phase by the ventricular relaxation; the contractile phase by ventricular compliance [163, 165].

The physiological role of the RA is to support RV filling by receiving and transmitting blood from systemic venous return towards the RV without filling pressure elevation and consequent systemic congestion. RV pressure or volume overload causes dynamic adaptive changes in function and size of the RA to preserve CO and prevent systemic congestion [163]. Gaynor et al. showed in an invasive experimental animal model that transient or permanent elevation of PAP results in early impairment of RV diastolic function. To compensate for this, RA contractility increases to maintain adequate RV filling and CO [167]. However, as the RA operates according to the Frank-Starling mechanism [165], RA functional reserve to increase preload is eventually exhausted by the progression of the RV diastolic dysfunction as it has been described regarding the LA [17].

4.5.3.2 Evaluation of RA size

Dilatation of the RA is a relatively late but easily measured sign of RA remodelling [162, 163]. RA size is routinely assessed by 2D echocardiography, measuring major and minor diameters or maximal RA area [121]. RA volume may be calculated by 2D echocardiography using the only 2D plane available [168]. 2D echo based volumetry of the RA was validated with cardiac CT or MRI, showing acceptable correlations between the different methods, although 2D echocardiography seems to underestimate RA volume [169, 170]. The introduction of 3D echocardiography (3DE) allows direct echocardiographic volumetric measurement. 3DE-derived RA volumes correlate more closely with cardiac CT and MRI findings and appear to be somewhat larger than 2D-echocardiography-derived RA volume data, but still significantly smaller compared to CT or MRI [170-174].

Maximal RA area or the RA to LA area ratio is a predictor of adverse outcome or mortality in several conditions: in HFrEF [175], Eisenmenger's syndrome [134], acute pulmonary embolism [176] as well as in PAH [139]. RA area predicts functional capacity in HCM [177], indicates response to therapy in CTEPH [178] and after ASD closure [179]. Maximal RA volume indexed for body surface area (BSA) correlates with the functional capacity of patients and is an

independent predictor of mortality and adverse events in HFrEF [180-184] and in PAH [185, 186]

4.5.3.3 Evaluation of RA phasic function

Alterations of the atrial function occur earlier than the enlargement of the atrial volume: it is an early sign of atrial remodelling that is more difficult to demonstrate [162, 163, 165, 166, 187]. The traditional way of investigating atrial function is to measure atrial volumes in certain points of the cardiac cycle: namely, maximal atrial volume (Vmax), minimal atrial volume (Vmin) at the time of the closure of the tricuspid valve, and pre-atrial contraction volume defined by the start of the P-wave on ECG [163, 165, 188, 189]. Parameters reflecting the phasic function of the atrium may be calculated using these static volume values [163, 172, 190]. The total, passive and active emptying volumes and fractions reflect the reservoir, conduit, and contractile function of the RA, respectively. Expansion index (EI), the ratio of atrial expansion to the minimal atrial volume is an alternative parameter to describe reservoir function. **Table 2** shows the phasic atrial volumes and the formulae to calculate them. This 2DE based approach is time consuming and requires geometrical assumptions which may result in inaccuracy. Thus, often cardiac CT or MRI and more recently, 3DE is used for the evaluation of RA phasic function [170, 191, 192].

Table 2. Phasic atrial volumes (based on Willens et al. [190] and Peluso et al. [172]

Reservoir function	Total emptying volume (Vte)	Vte = Vmax – Vmin
	Total emptying fraction (TEF)	TEF= Vte /Vmax x 100 (%)
	Expansion index (EI)	EI= Vte/ Vmin x 100 (%)
Conduit function	Passive emptying volume (Vpe)	Vpe = Vmax – Vp
	Passive emptying fraction (PEF)	PEF= Vpe /Vmax x100 (%)
Contractile function	Active emptying volume (Vae)	Vae = Vp - Vmin
	Active emptying fraction (AEF)	AEF = Vae /Vp x 100 (%)

Examination of phasic RA volumes has been used in various conditions: In PAH patients, TEF and AEF was shown to have a strong negative correlation with mortality [193, 194]. Willens et al. showed increased atrial volumes, decreased PAF and increased AEF in PAH. In other PAH

studies, impaired TEF and conversely, increased AEF was found in patients with less advanced disease, while in the subgroup of patients with the worst functional status and impaired RV function both TEF and AEF were impaired [195, 196]. In a population of heart failure patients TEF was significantly impaired and associated with the risk for death and hospitalization [183]. In patients with inferior myocardial infarction, the subgroup with concomitant RV myocardial infarction had increased RV volumes and decreased PEF [197].

4.5.3.4 Evaluation of RA mechanics with STE

Speckle tracking-derived strain analysis results in a strain curve that shows specific strain values in each phase of the RA function: a reservoir, conduit and contractile strain value can be determined. RA strain has been shown to be feasible and reliable in several studies [172, 198], and there is an increasing body of evidence of its potential usefulness in different clinical situations. Several cohorts of PAH patients showed correlations between RA strain and invasive hemodynamics: negative associations with RA pressure and PVR as well as positive correlations with SV and CO were found [23, 199-202]. RA reservoir correlated with the functional capacity [23, 203], and was proved to be a predictor of adverse outcome and mortality in various PAH cohorts [199, 200, 203, 204].

RA reservoir strain was also impaired in heart failure patients, significantly correlated with PAP [198, 204], or showed good discriminatory power to indicate patients with high pulmonary pressures [198]. In the study of Jain et al., comparing HFpEF and HFrEF patients with controls, RA function was progressively impaired from controls through HFpEF to HFrEF. Reservoir and conduit strain were independent predictors of mortality in heart failure patients [205].

4.5.3.5 Right atrial stiffness

Atrial stiffness represents the change in pressure required to increase the volume of the atrium in a given measure [206]. Atrial stiffness as a noninvasively assessed parameter is defined as the ratio of E/e' and reservoir strain. Kurt et al. reported LA stiffness as a useful index to differentiate between HFpEF and asymptomatic diastolic dysfunction [206]. Our group has reported, that LA stiffness was superior to maximal LA volume index and reservoir strain in predicting elevated NT-proBNP levels in SSc patients [207]. LA stiffness was also

investigated as a potential marker for early organ damage in patients with hypertension [208]. Regarding the RA, Teixeira et al. showed a correlation between RA stiffness and the degree of tricuspid regurgitation in HFrEF patients [209].

5 Methods

5.1 Correlation between echocardiographic parameters of LV and RV diastolic function and the functional capacity of the patients in COPD

5.1.1 Study population

Eighty outpatients with stable COPD of varying severity were consecutively screened for this study. Diagnosis and pulmonological management of the COPD were based on the GOLD strategy document [210]. In patients with borderline FEV1/FVC (below 0.70 but above the lower limit of normal) the diagnosis of COPD was based on the clinical symptoms (dyspnoea, chronic cough and/or sputum production) and a history of exposure to risk factors for the disease. All patients underwent spirometry within one month before the inclusion. They had to be free of exacerbations for the two months before inclusion. Patients with moderate-to-severe LV systolic dysfunction (ejection fraction (EF) <45%), atrial fibrillation, neuromuscular disorders affecting exercise capacity, significant left sided valvular abnormalities or prosthetic valves were excluded. Detailed medical history was obtained. Significant ischemic heart disease was defined as coronary artery stenosis >50% proved by invasive measurements or as history of previous myocardial infarction. Heart failure was diagnosed when the patient was regularly treated with loop diuretics and/or at any symptoms of heart failure.

Data of 34 healthy volunteers without any cardiac disease were used as control. The study complied with the Declaration of Helsinki. The institutional ethics committee approved the study. All subjects had given written informed consent prior to inclusion.

5.1.2 Echocardiography

Echocardiography was performed using Philips CX50 ultrasound system (Philips Healthcare, Best, The Netherlands). Studies were performed by a single cardiologist blinded to all other data.

LV EF was measured by Simpson's method. End-diastolic thickness of the septum and the posterior wall as well as the end-diastolic diameter of the LV were measured from parasternal long axis view, by M-mode. LV mass was calculated according to the Devereux formula and indexed for BSA. Maximal LA and RA areas were measured in apical 4-chamber view at the time of mitral/tricuspid valve opening. Atrial appendages and pulmonary veins were excluded from the measurements. Atrial areas were corrected for BSA (LA and RA area index) [121, 211]. Basal, mid-cavity, and longitudinal dimensions of the RV were obtained at end-diastole in RV–focused apical 4-chamber view and corrected for BSA. As parameters of the RV systolic function, TAPSE and RVFAC were measured. Spectral Doppler based MPI (Tei index) was also obtained. Maximal and minimal diameters of the IVC were measured in subxiphoid view and collapsibility index (the percent decrease in the diameter during inspiration) was calculated. RV wall thickness was obtained from subxiphoid window by 2D echocardiography at end-diastole [121].

Transmitral and transtricuspid flow velocities were assessed from the apical 4-chamber view. Peak of the early (E) and late (A) diastolic velocities were measured. PASP was estimated as a sum of the pressure difference across the tricuspid valve calculated using the modified Bernoulli equation and an estimate of mean RA pressure (5 to 15 mmHg) using the diameter and collapsibility index of the IVC. Myocardial systolic (S), early- (e') and late- (a') diastolic velocities were measured from apical 4-chamber view at the lateral and septal border of the mitral as well as at the lateral border of the tricuspid annulus using pulsed TDI. Mitral and tricuspid E/A, E/e' and e'/a' ratios were calculated. Doppler measurements were obtained from ≥ 3 consecutive beats during end-expiratory apnoea [121, 211, 212]. LV diastolic function was evaluated in accordance with the current guideline. Diastolic dysfunction was identified if mitral lateral e'< 10 cm/s and septal e'< 8 cm/s while elevated LV filling pressure was defined as mean E/e'≥ 9 [212]. Elevated RV filling pressure was diagnosed if tricuspid E/e'> 6 [121].

5.1.3 Six-minute walk test

Functional capacity of the patients was estimated using 6MWT, on the day of the echocardiography. Borg dyspnoea index (0–10) was used for subjective assessment of shortness of breath during the exercise [213].

5.1.4 Statistical analysis

Categorical data were expressed as frequencies and percentages; continuous data were expressed as mean ± SD. Intraclass correlation coefficient was calculated to assess intraobserver reliability. Comparisons of data between two groups were performed using independent-sample t-tests for continuous variables and chi^2 tests for categorical variables. Comparisons of data between more groups were performed using ANOVA with LSD post hoc test. A p-value of < 0.05 was considered significant.

Univariate predictors of 6MWD were assessed using linear regression analysis. Multiple stepwise linear regression analysis was performed by entering those variables that were considered significant ($p<0.05$) on univariate analysis. In this method the variable with the smallest probability of its F-statistic ($p<0.05$) is entered into the model first. This process continues to add variables to the model until there are no variables left that have F statistics that meet the criteria. As this process progresses, the F statistics for variables already in the model may change. If the significance level of these F statistics exceeds the criterion (if $p \geq 0.1$), then these variables are removed from the model. Variance inflation factor (VIF) values above 2.5 were considered to have potential multicollinearity.

IBM SPSS 22 statistical software was used.

5.2 Significance of RA size and mechanics in SSc: correlation with functional capacity and prognostic value

5.2.1 Study population

Seventy consecutive patients diagnosed with SSc in the tertiary centre of the Department of Rheumatology and Immunology, Medical School, University of Pécs were enrolled into our prospective study. All cases complied with the updated ACR/EULAR classification criteria [214].

Patients were systematically screened for PAH. RHC was initiated in the presence of abnormalities suggestive of PAH (velocity of tricuspid regurgitation higher than 2.8 m/s or

consistent with 2.5–2.8 m/s in the presence of unexplained dyspnoea, signs of RV hypertrophy/dilatation, or a systolic D-sign; disproportional decrease of DLCO compared with the forced vital capacity (FVC/DLCO > 1.6), and/or DLCO < 60% of predicted) [215]. The diagnosis of PAH was based on results obtained by RHC (mPAP ≥ 25 mmHg and PAWP ≤ 15 mmHg and PVR > 3 Wood units) [25]. Patients with atrial fibrillation, significant left sided valvular disease as well as with significant peripheral artery disease, cognitive issues, neuromuscular or musculoskeletal problems were excluded from the study. Detailed medical history was obtained.

An age and gender matched group of 25 healthy volunteers without any signs or symptoms of cardiac disease was used as control.

The study complied with the Declaration of Helsinki. The institutional ethics committee approved the study. All subjects had given written informed consent before inclusion.

5.2.2 Follow-up

Patients underwent echocardiography during a 9-month period in the year 2015 and were followed for 5 years after the initial investigation with yearly scheduled visits. Patients refusing or not able to attend the visit were consented for telephone visit for the assessment of the vital status. To avoid misclassification of the cause of death, all-cause mortality was selected as endpoint. Follow-up time was defined as the time between the date of echocardiography and the date of death or the last clinical visit.

5.2.3 Echocardiography

Echocardiography was performed using Philips Epiq 7G ultrasound system (Philips Healthcare, Best, The Netherlands) by a single investigator. LV EF was measured by biplane Simpson's method. Basal, mid-cavity, and longitudinal dimensions of the RV were obtained at end-diastole in RV–focused apical 4-chamber view and corrected for BSA. TAPSE and RVFAC were measured, as parameters of the RV systolic function. Maximal and minimal diameters of the IVC were measured in subxiphoid view. Collapsibility index was calculated. RV wall thickness was obtained from subxiphoid view by 2D echocardiography at end-diastole, in a zoomed

subcostal view, by 0.5 mm increments. Severity of tricuspid regurgitation was assessed according to the current recommendations and classified as mild, moderate, or severe. PASP was estimated as a sum of the pressure difference across the tricuspid valve (calculated using the modified Bernoulli equation) and an estimate of mean RA pressure (5 to 15 mmHg) using the diameter and collapsibility index of the IVC [121]. In addition to the spectral Doppler parameters of the transmitral and transtricuspid flow (E, A) **(Figure 1d)**, myocardial systolic (S), early (e') and late (a') diastolic velocities were measured in apical 4-chamber view at the septal and lateral border of the mitral annulus as well as on the lateral border of the tricuspid annulus **(Figure 1e)** using pulsed TDI. Mitral and tricuspid E/A and E/e' ratios were calculated. Doppler measurements were obtained from ≥ 3 consecutive beats during end-expiratory apnoea. LV diastolic function was evaluated in accordance with the current recommendation [140]. Impaired RV longitudinal systolic function was defined as tricuspid S < 10 cm/s (19). Elevated RV filling pressure was diagnosed if tricuspid E/e' > 6 [121]

5.2.4 Right atrial strain and volume measurements

For atrial speckle tracking analysis, RA-focused apical 4-chamber view movies were obtained. Care was taken to obtain true apical images using standard anatomic landmarks to avoid foreshortening (a situation where the ultra-sound plane is not appropriate, and RA is not opened up to its fullest size). Image contrast, depth and sector size were adjusted to achieve adequate frame rate (80 and 90 frames/s) and optimize RA border visualization. Three consecutive heart cycles were recorded digitally and processed by a single investigator blinded to standard echocardiographic and clinical data of the patients, using a dedicated software (QLab 10.5, Philips Healthcare, Andover, MA, USA), allowing off-line semi-automated analysis of speckle tracking-based strain **(Figure 1a)**. The beginning of the QRS was predefined by the software as reference point. The first positive peak of the curve was measured at the end of the reservoir phase, just before tricuspid valve opening (reservoir strain). This was followed by a plateau and a second late peak at the onset of the P wave on the electrocardiogram (RA contractile strain). RA conduit strain was defined as the difference between reservoir and contractile strain [216]. **(Figure 1c)**. RA stiffness was calculated as ratio of tricuspid E/e' to RA reservoir strain [206, 209, 217].

Using the atrial borders created for speckle tracking analysis, RA volume curves were generated by the same software **(Figure 1b),** based on Simpson's single plane method of disks. Maximal RA volume was measured at the end of T wave on electrocardiogram, just before the opening of the tricuspid valve, and indexed for BSA (RA Vmax index).

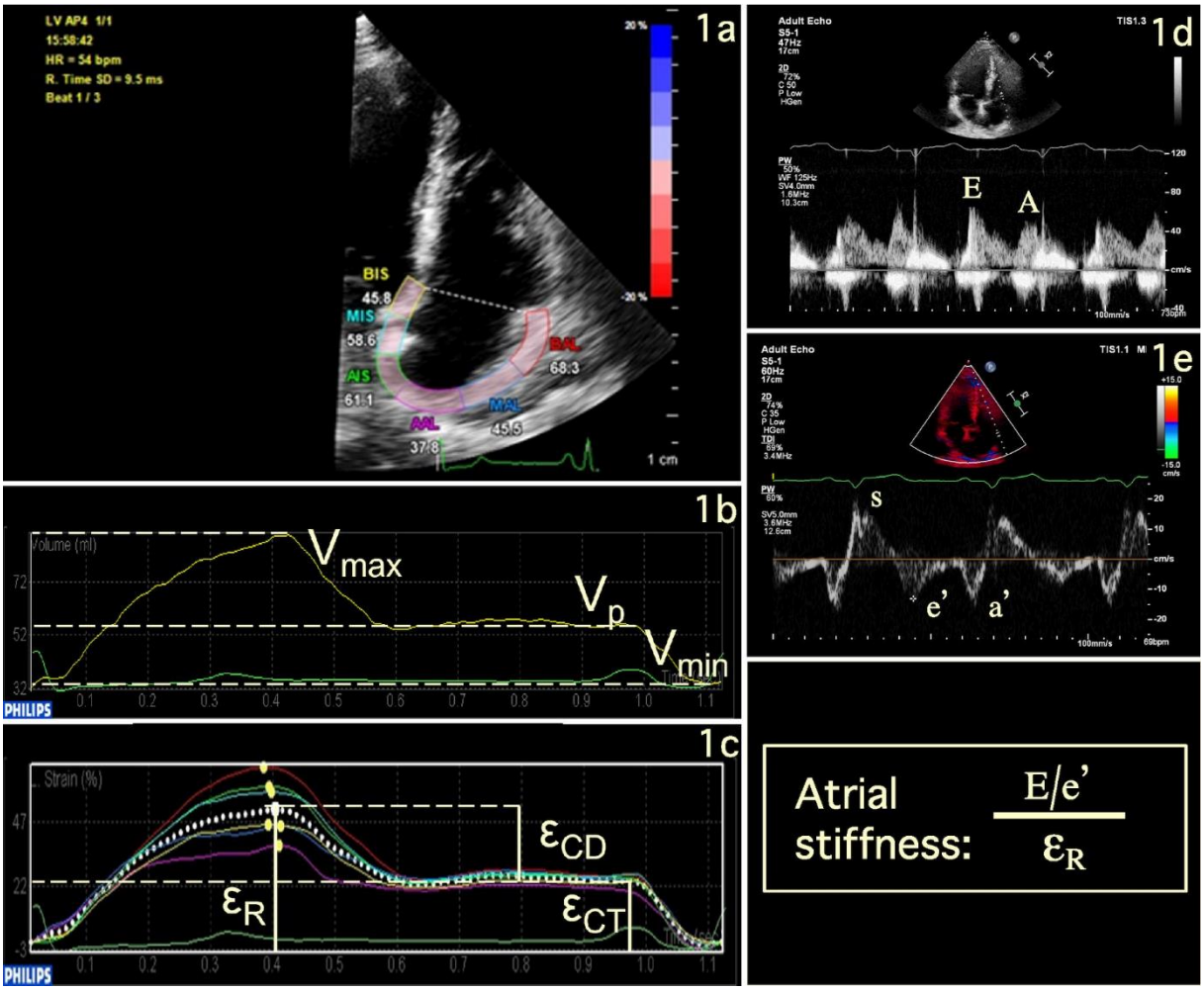

Figure 1. *RV–focused apical 4-chamber view depicting the region of interest* ***(1a)*** *and the RA strain curve created by the speckle-tracking software* ***(1c)****. Using the atrial borders created for speckle-tracking analysis, RA volume curves were generated by the same software* ***(1b)****. Spectral Doppler curve of the transtricuspid flow* ***(1d).*** *Pulsed tissue Doppler curve measured on the lateral border of the tricuspid annulus* ***(1e)****.*

ε_R: RA reservoir strain; ε_{CD}: RA conduit strain; ε_{CT}: RA contractile strain

5.2.5 Six-minute walk test

See 5.1.3.

5.2.6 Statistical analysis

Categorical data were expressed as frequencies and percentages; continuous data were expressed as mean ± SD. Comparisons of data between two groups were performed using independent-sample t tests or Mann-Whitney test for continuous variables and chi^2 tests for categorical variables.

Univariate predictors of 6MWD were assessed using linear regression analysis. A p value of < 0.05 was considered significant. Multiple stepwise linear regression analysis was performed by entering those variables that were considered significant on univariate analysis. VIF values above 2.5 were considered to have potential multicollinearity. Receiver operating characteristic (ROC) curve analysis was used to derive the optimal cut-off values for predicting 6MWD < 300m.

For survival analysis, univariable and multiple Cox proportional-hazards models were applied. HR-s were calculated with 95% confidence intervals (CI). Models were set up based on variables with $p < 0.1$ in univariable analysis. Sequential chi^2 analysis was used to evaluate the incremental prognostic benefit of adding RA volume, strain or stiffness to tricuspid S. C-statistics were applied to compare multivariable Cox models, with values greater than 0.7 representing acceptable models. In order to input them into Cox models, RA stiffness and NT-proBNP data were standardized by calculating a z-score for each value.

ROC curves were used to examine the diagnostic performance of RA stiffness in predicting all-cause mortality. Area under the curve (AUC) value was calculated. Optimal cut-off value was chosen to maximize sensitivity and specificity. Based on this cut-off value, Kaplan-Meier survival curve was created and differences between groups were tested by Mantel-Cox log rank test.

Prognostic power of concordant versus discordant values for tricuspid S and RA stiffness were also evaluated: three groups were created defined by dividing each variable at the cut-off

value (high tricuspid S AND low RA stiffness; low tricuspid S OR high RA stiffness; low tricuspid S AND high RA stiffness). Kaplan-Meier survival curve was created and differences between groups were tested by Mantel-Cox log rank test.

To determine intraobserver variability, assessment of RA strain and volume parameters was repeated 2 and 4 weeks after the index measurements in 30 randomly selected patients by the same investigator. To calculate interobserver variability, assessment of RA strain and volume parameters was repeated by another experienced cardiologist in 20 randomly selected patients. Intraobserver and interobserver variability was assessed by the intraclass correlation coefficient.

Data were analysed using IBM SPSS 22 and 27 statistical software.

6 Results

6.1 Correlation between echocardiographic parameters of LV and RV diastolic function and the functional capacity of the patients in COPD

Of a total of 80 patients with COPD, 65 were eligible for the study. Fifteen patients were excluded due to atrial fibrillation (4 patients), poor acoustic window (2 patients), severe sinus tachycardia (1 patient), moderate-to-severe left-sided valve disease (1 aortic stenosis, 1 mitral regurgitation), severely reduced LV systolic function (1 patient with dilated cardiomyopathy, 1 patient with previous myocardial infarction), and severe pericardial constriction (1 patient). Three patients (all in GOLD stage IV) did not attempt to perform 6MWT because of their weak physical condition.

Systemic hypertension, heart failure and diabetes were common in our COPD population. In 1 case percutaneous coronary intervention was performed while 4 patients underwent coronary artery bypass surgery. In 3 cases prior myocardial infarction was reported, but coronary intervention was not feasible. Clinical and echocardiographic data of the 65 patients are reported in **Table 3.**

Thirty-five patients were in GOLD stage II, 27 patients in GOLD stage III, and 3 patients in GOLD stage IV. Borg dyspnoea index was significantly higher in GOLD III patients compared with GOLD II. On the other hand, no significant difference was found between the 6MWD covered by the patients in GOLD stage II and III **(Figure 2).**

Spectral Doppler and TDI measurements were feasible in all patients. Intraclass correlation coefficients were 0.988 and 0.981 for mitral and tricuspid E, respectively. Intraclass correlation coefficients for e', a' and S were 0.984, 0.984 and 0.917 on mitral lateral annulus; 0.983, 0.978 and 0.977 on mitral septal annulus and 0.970, 0.982 and 0.986 on tricuspid annulus.

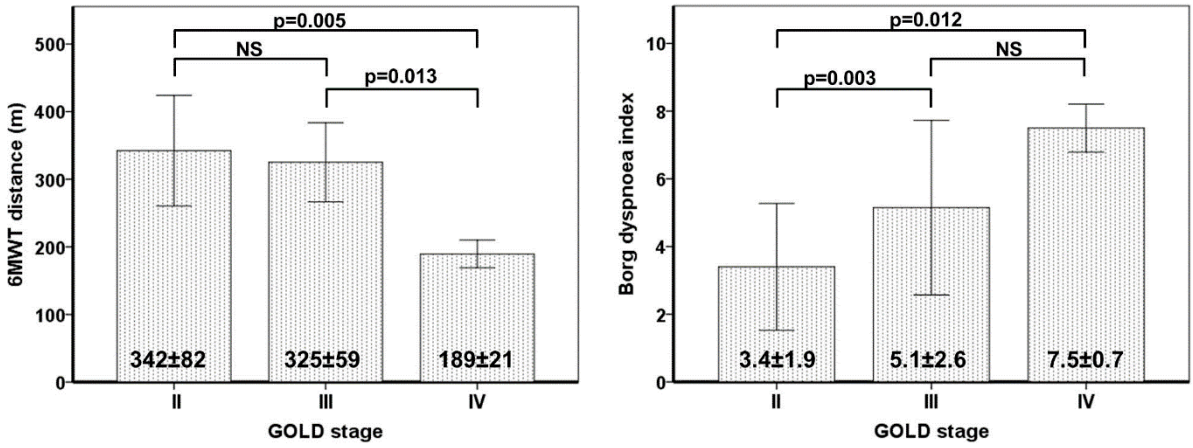

Figure 2. *6MWT and Borg dyspnoea index results in different GOLD stages (Mean ± SD; ANOVA with LSD post hoc test)*

6.1.1 Comparison of COPD population with healthy controls

Our patients and healthy controls were matched in age and gender distribution **(Table 3)**. BSA was significantly larger in patients with COPD, but the difference was clinically not remarkable. LV EF was preserved (EF ≥ 55%) in 59 (91%), while mildly reduced (45–54%) in 6 (9%) patients. LVM index was significantly higher in patients with COPD. Both lateral and septal myocardial early diastolic velocities (e') were significantly lower, while mean E/e' was significantly higher in the COPD population. LV diastolic dysfunction was found in 48 (74%), while LV filling pressure was elevated in 28 (43%) patients. (Grade I and grade II diastolic dysfunction in 20 (31%) and in 28 (43%) patients, respectively.)

Assessment of the tricuspid regurgitation's velocity was feasible in 41 (63%) patients. RV systolic pressure was significantly higher in patients with COPD. Resting PH (PASP ≥ 35 mmHg) was found in 9 (14%) patients. RV wall thickness, RA area and RV basal diameter were significantly increased in patients with COPD. IVC was dilated, while collapsibility index was significantly lower in the COPD group. TAPSE and tricuspid S were significantly lower in our patients as compared with controls. RV systolic dysfunction was rare in the COPD population: RVFAC < 35%, TAPSE < 16 mm and tricuspid S < 10 cm/s were found in 1 (1.5%), 3 (5%) and 7 (11%) patients, respectively. RV MPI was prolonged (> 0.4) in 31 (47%) patients. Tricuspid e'

and tricuspid e'/a' were significantly decreased in the COPD population. RV filling pressure was elevated in 29 (45%) patients.

Table 3. Baseline characteristics of the COPD population and comparison with healthy subjects.

	COPD patients (n=65)	**Healthy volunteers (n=34)**	**p**
Clinical data			
Age (years)	60.8±9.0	58.0±8.3	0.092
Male sex n (%)	39 (60%)	18 (53%)	0.500
BSA (m^2)	1.9±0.3	1.8±0.2	**0.023**
FEV_1 % predicted	54.6±14.8		
FEV_1/FVC (%)	57.2±10.5		
Pack-years of smoking	33.5±26.2		
Co-morbidities			
Coronary artery disease n (%)	9 (12%)		
Systemic arterial hypertension n (%)	51 (78%)		
Diabetes mellitus n (%)	18 (28%)		
Heart failure n (%)	51 (78%)		
Medication			
Angiotensin convertase enzyme inhibitors n (%)	32 (49%)		
Beta-blockers n (%)	29 (45%)		
Spironolactone n (%)	3 (5%)		
Other diuretics n (%)	27 (42%)		
Echocardiography			
LV ejection fraction (%)	60.2±4.8	61.9±3.3	**0.044**
LVM index (g/m^2)	106.5±25.3	95.0±14.0	**0.003**
LA area index (cm^2/m^2)	8.9±1.5	8.5±1.0	0.065
Mitral E/A	0.9±0.2	1.3±0.3	**0.000**
Lateral S (cm/s)	9.5±1.9	10.8±2.0	**0.000**
Lateral e' (cm/s)	8.7±1.9	11.1±3.1	**0.000**
Lateral a' (cm/s)	11.2±2.1	11.0±2.3	0.744
Septal S (cm/s)	8.2±1.4	9.2±1.4	**0.001**
Septal e' (cm/s)	7. 0±1.4	9.0±2.1	**0.000**

	COPD patients (n=65)	Healthy volunteers (n=34)	p
Septal a' (cm/s)	9.6±1.6	9.6±1.8	0.982
Mean LV E/e'	8.8±2.1	6.4±1.4	**0.000**
RV basal diameter index (mm/m^2)	16.2±2.0	14.3±2.1	**0.000**
RV mid-cavity diameter index (mm/m^2)	11.5±1.5	11.2±1.6	0.301
RV longitudinal diameter index (mm/m^2)	28.5±3.1	27.4±4.3	0.121
RVFAC (%)	49.1±7.4	51.2±5.9	0.092
TAPSE (mm)	20.8±2.5	25. 1±3.5	**0.000**
MPI	0.43±0.19	0.31±0.04	**0.000**
RA area index (cm^2/m^2)	8.3±1.5	7.2±1.3	**0.000**
RV wall thickness (mm)	6.0±1.3	3.6±1.0	**0.000**
PASP (mmHg)	27.9±6.5	22.7±3.0	**0.000**
IVC (mm)	13.3±3.1	9.5±2.2	**0.000**
Collapsibility index (%)	59.1±14.4	64.4±9.0	**0.018**
Tricuspid E/A	1.1±0.2	1.4±0.2	**0.000**
Tricuspid S (cm/s)	12.6±2.0	13.9±2.1	**0.001**
Tricuspid e' (cm/s)	7.9±1.3	11.4±2.3	**0.000**
Tricuspid a' (cm/s)	13.4±2.2	13.0±4.3	0.618
Tricuspid e'/a'	0.6±0.1	0.9±0.3	**0.000**
Tricuspid E/e'	6.0±1.8	3.8±1.3	**0.000**

Statistically significant p-values are formatted in bold ($p<0.05$)

6.1.2 Determinants of functional capacity in patients with COPD

Among all clinical parameters, 6MWD showed significant negative correlation with age and significant positive correlation with BSA. FEV1% and FEV1/FVC did not show significant correlation with 6MWD, but they were significant predictors of Borg dyspnea index (FEV1%: r= − 0.474; p = 0.000 and FEV1/FVC: r = − 0.374; p = 0.002). Among all echocardiographic parameters, significant negative correlation was found between LA area index and 6MWD. Other parameters of LV systolic and diastolic function did not show correlation with the functional capacity. Several parameters representing RV size, RV diastolic function and filling pressure were proven to be significant predictors of 6MWD. No correlation was found between 6MWT results and the echocardiographic parameters of RV systolic function. Univariate and multivariate predictors of the 6MWD are reported in **Table 4**.

Table 4. Predictors of the 6MWD (m) in patients with COPD: univariate and multivariate regression analyses (Unstandardized (B) and standardized (β) regression coefficients).

	Univariate analysis			**Multivariate analysis**		
	B	**r**	**p**	**B**	**β**	**p**
Age (years)	-2.297	-0.273	**0.029**			
BSA (m^2)	91.399	0.314	**0.011**	96.914	0.359	**0.000**
LA area index (cm^2/m^2)	-15,515	-0.319	**0.011**			
RV basal diameter index (mm/m^2)	-10.627	-0.290	**0.021**			
RV longitudinal diameter index (mm/m^2)	-6.357	-0.271	**0.031**			
RA area index (cm^2/m^2)	-22.522	-0.445	**0.000**	-15.606	-0.304	**0.001**
Collapsibility index (%)	2.677	0.505	**0.000**	1.384	0.270	**0.005**
Tricuspid a' (cm/s)	-17.858	-0.525	**0.000**			
Tricuspid e'/a'	355.493	0.611	**0.000**	213.688	0.377	**0.000**

Statistically significant p-values are formatted in bold (p<0.05)

In stepwise multiple linear regression analysis tricuspid e'/a', BSA, RA area index and collapsibility index were independent predictors of 6MWD (multiple r = 0.764; p = 0.000; F = 19.269) **(Figure 3).** VIF values for all variables were below 2.5.

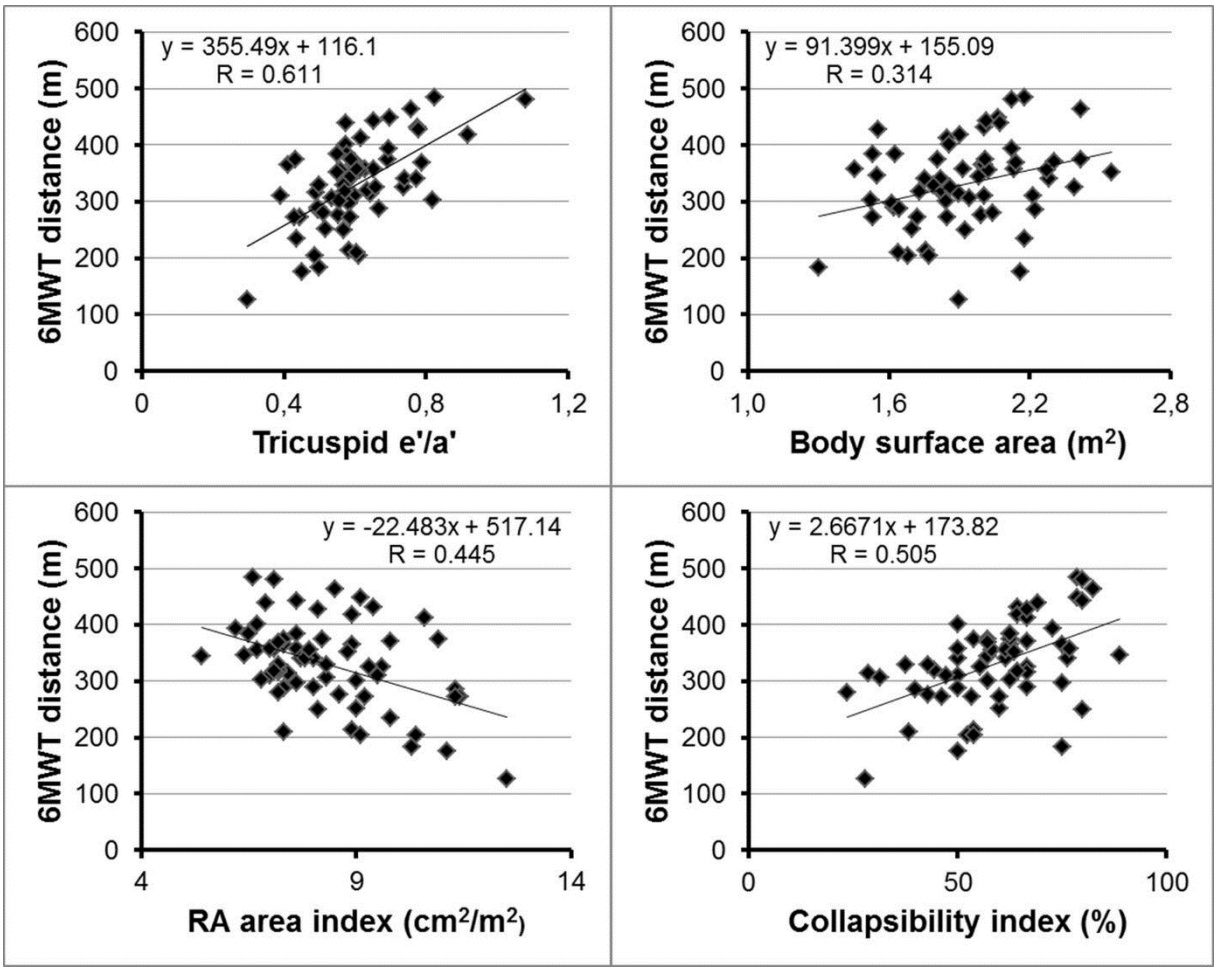

Figure 3. *Main predictors of the 6MWD in patients with COPD*

6.2 Significance of RA size and mechanics in SSc: correlation with functional capacity and prognostic value

Seventy SSc patients were enrolled into the study. At baseline, mean age of the study cohort was 57±12 years. 32 (46%) patients had limited cutaneous, while 38 (54%) patients had diffuse cutaneous form of the disease. **Table 5** summarizes the clinical characteristics of the population.

Intraclass correlation coefficients for intraobserver variability were 0.91, 0.96, 0.91 and 0.93 for reservoir, contractile and conduit strain and for RA Vmax, respectively. Regarding interobserver variability, intraclass correlation coefficients for reservoir, contractile and conduit strain and for RA Vmax were 0.89, 0.88, 0.87 and 0.91, respectively.

Table 5. Clinical characteristics of the SSc population

Variable		**All patients (n=70)**
Age (years)		57±12
BSA (m^2)		1.75±0.19
Female gender n (%)		63 (90)
Disease duration (years)		7.2±5.8
Limited cutaneous form n (%)		32 (46)
Modified Rodnan skin score		11.3±8.0
Anti-Centromere Antibody n (%)		18 (26)
Anti-Topoisomerase I Antibody n (%)		20 (29)
Coronary artery disease n (%)		2 (3)
Systemic arterial hypertension n (%)		36 (51)
Angiotensin convertase enzyme inhibitors n (%)		33 (47)
Calcium channel blockers n (%)		36 (51)
Loop diuretics n (%)		31 (44)
Mineralocorticoid receptor antagonists n (%)		18 (26)
New York Heart Association functional class n (%)	I	20 (28)
	II	32 (46)
	III	18 (26)
6MWD (m)		391±95
Modified Borg dyspnoea index		1.7±1.6
Erythrocyte sedimentation rate (mm/h)		21.9±16.0
C-reactive protein (mg/l)		3.6±5.5
Creatinine (µmol/l)		70.6±23.7
N-terminal pro-B-type natriuretic peptide (pg/ml)		192.0±163.0
Troponin-T (ng/l)		12.0±11.2
Forced vital capacity (%)		100.5±15.0
Diffusing capacity of carbon monoxide (%)		64.5±15.1

6.2.1 Echocardiographic parameters of SSc patients and healthy controls

LV EF was preserved (≥ 55%) in 68 (97%) and mildly reduced (45–54%) in 2 (3%) patients. LV diastolic function was preserved in 20 (28.6%) patients whereas elevated LV filling pressure was found in 15 (21.4%) patients. Detailed echocardiographic data characterizing LV and LA size and function and their comparison with an age and gender matched healthy population has already been reported [17].

Significant differences were found between the SSc group and control group in the parameters reflecting RV systolic function. Real RV systolic dysfunction, however, was rare in the SSc population: RVFAC < 35%, TAPSE < 16 mm and tricuspid S < 10 cm/s were found in 3 (4.6%), 1 (1.4%), and 8 (11.4%) patients, respectively. Tricuspid E/e' suggested elevated RV filling pressure in 22 (31.4%) SSc patients. RA reservoir and conduit strain values were significantly lower in the SSc population, while RA stiffness was significantly increased in SSc patients compared with the control group. Detailed echocardiographic data characterizing RV and RA size and function and their comparison with healthy controls are reported in **Table 6**.

Table 6. Echocardiographic data of the SSc population and comparison with healthy subjects

Variable		**Systemic sclerosis (n=70)**	**Healthy subjects (n=25)**	**p**
Age (years)		57±12	54±7	0.239
BSA (m^2)		1.75±0.19	1.83±0.18	0.071
Female gender n (%)		63 (90%)	19 (76%)	0.082
LV ejection fraction (%)		60.8±4.5	63.3±2.5	**0.011**
LV diastolic function n (%)	Normal	20 (28.6)	25 (100)	**<0.001**
	Impaired relaxation	35 (50)		
	Pseudonormal	15 (21.4)		
Grade of tricuspid regurgitation n (%)	Mild	63 (90)	25 (100)	0.259
	Moderate	5 (7)		
	Severe	2 (3)		
PASP (mmHg)		26.2±5.7	25.8±2.9	0.724

Variable	Systemic sclerosis (n=70)	Healthy subjects (n=25)	p
RV basal diameter index (mm/m^2)	18.4±2.4	17.5±1.6	0.924
RV mid-cavity diameter index (mm/m^2)	13.5±2.1	13.0±1.5	0.175
RV longitudinal diameter index (mm/m^2)	31.7±3.6	32.3±2.8	0.392
IVC (mm)	14.0±3.8	14.8±4.7	0.469
Collapsibility index (%)	55.5±11.5	55.0±13.4	0.874
RV wall thickness (mm)	5.0±1.0	4.8±0.8	0.329
RVFAC (%)	47.5±7.2	54.1±6.6	**0.000**
TAPSE (mm)	21.1±2.6	23.6±1.6	**0.000**
Tricuspid E (cm/s)	47.5±9.2	54.3±8.9	**0.002**
Tricuspid A (cm/s)	39.5±8.8	39.0±5.6	0.771
Tricuspid e’ (cm/s)	9.5±2.3	11.7±2.8	**0.002**
Tricuspid a’ (cm/s)	13.2±2.6	13.6±3.3	0.533
Tricuspid S (cm/s)	12.4±2.3	13.6±2.3	**0.027**
Tricuspid E/e' ratio	5.3±1.5	4.9±1.4	0.278
RA Vmax index (ml/m^2)	19.4±5.5	19.5±5.9	0.943
RA reservoir strain (%)	49.3±10.7	59.6±9.9	**0.000**
RA contractile strain (%)	22.9±5.8	25.3±5.7	0.082
RA conduit strain (%)	26.8±8.1	34.3±7.3	**0.000**
RA stiffness	0.11±0.04	0.08±0.02	**0.001**

Statistically significant p-values are formatted in bold ($p<0.05$)

6.2.2 Echocardiographic predictors of functional capacity of SSc patients

6MWD covered by the SSc patients was 391 ± 95 m. Univariate and multivariate predictors of the 6MWD are reported in **Table 7**.

Table 7. Predictors of the 6MWD in SSc patients: univariate and multivariate regression analyses

Variables	**Associations with 6-minute walking distance (m)**			
	Univariate analysis		**Multivariate analysis**	
	r	**p**	**β**	**p**
Age (years)	-0.452	**0.000**		
RV wall thickness (mm)	-0.369	**0.002**	-0.289	**0.030**
TAPSE (mm)	0.367	**0.002**		
Tricuspid e' (cm/s)	0.407	**0.001**		
Tricuspid E/e' ratio	-0.320	**0.008**		
RA reservoir strain (%)	0.273	**0.024**		
RA conduit strain (%)	0.327	**0.006**		
RA stiffness	-0.401	**0.001**	-0.418	**0.002**

Statistically significant p-values are formatted in bold ($p<0.05$)

In stepwise multiple linear regression analysis RV wall thickness and RA stiffness became independent predictors of 6MWD (multiple r = 0.506; p = 0.001; F = 7.754). VIF values for all variables were below 2.5. Main predictors of the 6MWD in SSc patients are reported in **Figure 4**.

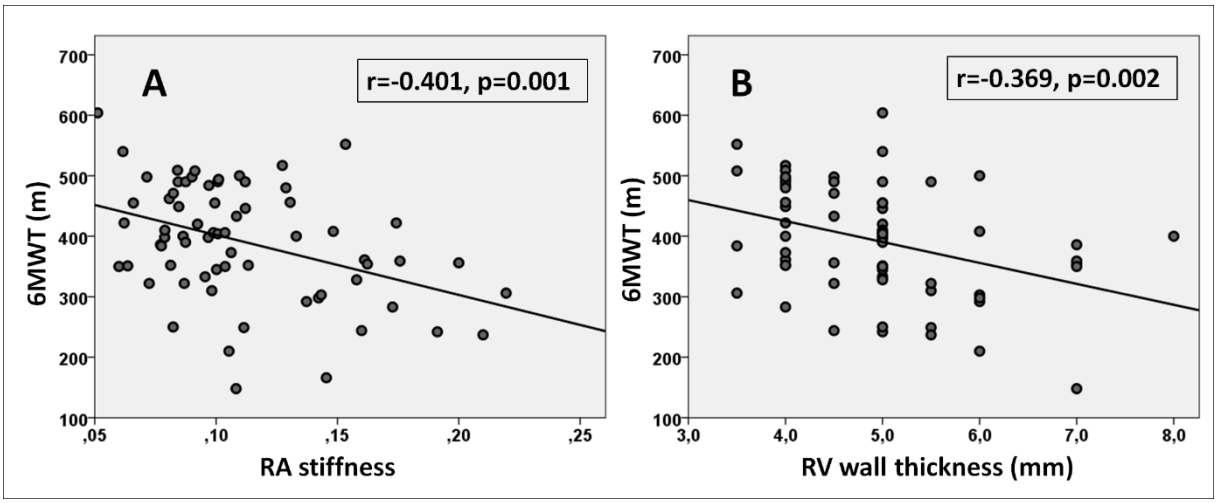

***Figure 4**. Main predictors of the 6MWD in patients with SSc are RA stiffness (A) and RV wall thickness (B).*

6MWD < 300 m was covered by 11 patients. Using ROC analysis, RA stiffness ≥ 0.107 and RV wall thickness ≥ 5.2 mm were the best predictors of the 6MWD < 300 m. ROC curves demonstrating the predictive power of these parameters are presented in **Figure 5.**

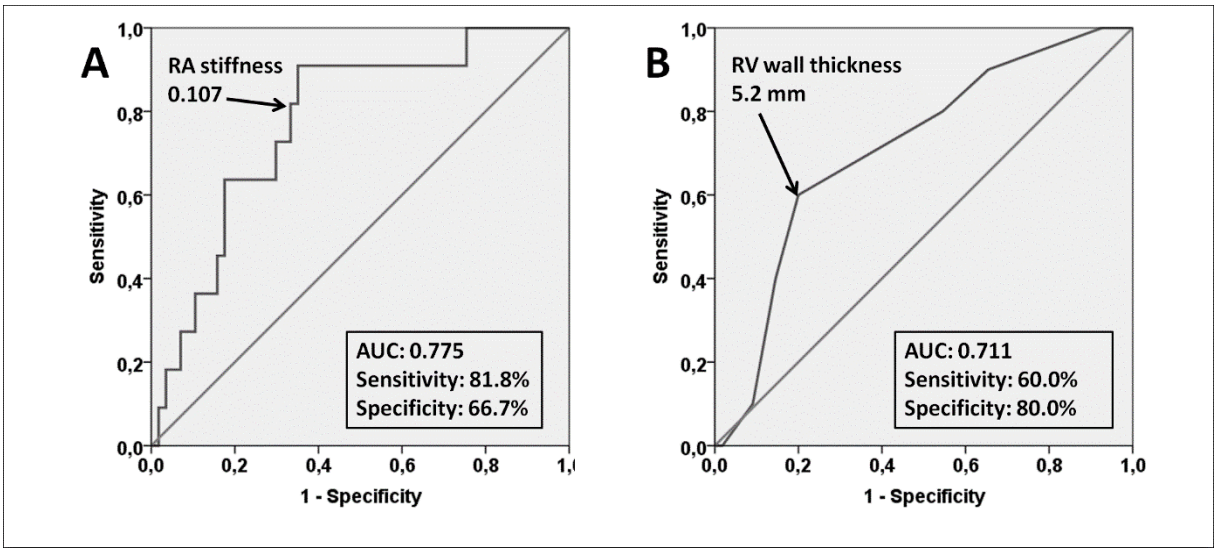

***Figure 5**. ROC curves demonstrating the sensitivity and specificity of RA stiffness (A) and RV wall thickness (B) in predicting poor functional capacity (6MWD < 300 m)*

6.2.3 Associations of outcome

During the follow-up period of 1721 ± 344 days (4.7 ± 0.9 years), 6 patients (8.6%) died. No patient was lost to follow-up.

Among all clinical and laboratory parameters, known coronary artery disease and NT-proBNP levels showed significant correlation with outcome whereas correlations with 6MWD and DLCO showed borderline significance. LV EF did not, but the grade of LV diastolic dysfunction showed significant association with all-cause mortality in univariate Cox regression analyses.

In addition to the PASP, parameters of the RV longitudinal systolic function (TAPSE and tricuspid S) and RV filling pressure (tricuspid E/e') became significant predictors of mortality. RA Vmax index showed significant association with outcome, whereas RA reservoir and conduit strain did not. Regarding contractile strain, the association showed borderline significance. RA stiffness, in contrast, became significant predictor of mortality in univariate analysis. Results of the univariate Cox regression analyses are reported in **Table 8**.

Table 8. Univariate Cox regression analysis of associations with all-cause mortality in patients with SSc

Variable	**HR (95% CI)**	**p**
Clinical characteristics		
Age (years)	1.029 (0.951-1.113)	0.472
BSA (m^2)	0.278 (0.003-28.131)	0.587
Female gender (y/n)	0.502 (0.059-4.298)	0.529
Disease duration (years)	1.049 (0.935-1.177)	0.415
Limited cutaneous form (y/n)	0.350 (0.063-1.940)	0.229
Modified Rodnan skin score	1.047 (0.957-1.146)	0.314
Anti-Centromere Antibody positivity (y/n)	1.490 (0.273-8.140)	0.645
Anti-Topoisomerase I Antibody positivity (y/n)	2.136 (0.427-10.676)	0.355
Coronary artery disease (y/n)	10.170 (1.171-88.354)	**0.035**
Systemic arterial hypertension (y/n)	1.082 (0.215-5.442	0.923
Angiotensin convertase enzyme inhibitor use (y/n)	0.844 (0.169-4.216)	0.837
Calcium channel blocker use (y/n)	5.244 (0.612-44.952)	0.131
Loop diuretics use (y/n)	1.469 (0.269-8.024)	0.657
Mineralocorticoid receptor antagonist use (y/n)	2.939 (0.593-14.569)	0.187
New York Heart Association functional class	2.380 (0.714-7.938)	0.158
6MWD (m)	0.993 (0.985-1.001)	*0.079*
Modified Borg dyspnoea index	1.171 (0.763-1.798)	0.469
Erythrocyte sedimentation rate (mm/h)	0.996 (0.945-1.050)	0.885
C-reactive protein (mg/l)	0.979 (0.824-1.163)	0.809
Creatinine (µmol/l)	0.999 (0.963-1.037)	0.969
NT-proBNP (pg/ml)	2.447 (1.299-4.609)	**0.006**
Troponin-T (ng/l)	1.070 (1.024-1.118)	**0.003**
Forced vital capacity (%)	0.972 (0.911-1.036)	0.382
Diffusing capacity of carbon monoxide (%)	0.956 (0.912-1.002)	*0.061*
Echocardiographic characteristics		
LV ejection fraction (%)	1.007 (0.840-1.206)	0.942
Grade of LV diastolic dysfunction	6.751 (1.428-31.909)	**0.016**
Grade of tricuspid regurgitation	3.113 (1.330-7.283)	**0.009**

Variable	HR (95% CI)	p
PASP (mmHg)	1.130 (1.003-1.272)	**0.044**
RV basal diameter index (mm/m^2)	1.167 (0.862-1.579)	0.318
RV mid-cavity diameter index (mm/m^2)	1.154 (0.792-1.682)	0.455
RV longitudinal diameter index (mm/m^2)	1.111 (0.897-1.376)	0.334
IVC (mm)	1.026 (0.812-1.295)	0.832
Collapsibility index (%)	1.053 (0.961-1.153)	0.272
RV wall thickness (mm)	0.953 (0.436-2.080)	0.903
RVFAC (%)	0.976 (0.867-1.099)	0.689
TAPSE (mm)	0.638 (0.445-0.914)	**0.014**
Tricuspid E (cm/s)	1.039 (0.969-1.114)	0.282
Tricuspid A (cm/s)	1.049 (0.976-1.127)	0.192
Tricuspid e' (cm/s)	0.735 (0.492-1.100)	0.134
Tricuspid a' (cm/s)	0.676 (0.439-1.043	*0.077*
Tricuspid S (cm/s)	0.548 (0.355-0.848)	**0.007**
Tricuspid E/e'	2.002 (1.220-3.285)	**0.006**
RA size and function		
RA Vmax index (ml/m^2)	1.202 (1.061-1.362)	**0.004**
RA reservoir strain (%)	0.952 (0.874-1.036)	0.253
RA contractile strain (%)	0.839 (0.690-1.020)	*0.079*
RA conduit strain (%)	0.978 (0.877-1.091)	0.690
RA stiffness	3.185 (1.544-6.570)	**0.002**

Statistically significant p-values ($p < 0.05$) are formatted in bold. $0.05 \leq p < 0.1$ values are formatted in italics.

When added to tricuspid S in sequential Cox model, RA stiffness significantly improved the diagnostic performance of the model ($\Delta chi^2 = 3.950$; $p = 0.047$) and remained independent predictor of the outcome (HR 2.460 (1.005-6.021); p=0.049). In contrast, RA Vmax index and RA contractile strain did not show incremental prognostic value over tricuspid S in the chi^2 model **(Table 9).**

Table 9. Models of sequential Cox regression analysis for predicting outcome in SSc. *C-statistics represents the overall performance of the predictive model. Δchi² reflects the incremental prognostic value of the RA variables over tricuspid S, when added to the model.*

		Model 1	**Model 2**	**Model 3**
C-statistics	0.721	0.737	0.820	0.849
Δchi²		2.376; p=0.123	2.536; p=0.111	3.950; **p=0.047**
Variables in model	**HR (95%CI) p-value**	**HR (95%CI) p-value**	**HR (95%CI) p-value**	**HR (95%CI) p-value**
Tricuspid S (cm/s)	0.548 (0.355-0.848); **p=0.007**	0.687 (0.421-1.122); p=0.134	0.599 (0.399-0.901); **p=0.014**	0.768 (0.464-1.271); p=0.304
RA Vmax index (ml/m²)		1.114 (0.967-1.283); p=0.135		
RA contractile strain (%)			0.867 (0.716-1.049); p=0.141	
RA stiffness				2.460 (1.005-6.021); **p=0.049**

Statistically significant p-values (p < 0.05) are formatted in bold.

6.2.4 Discriminative ability of RA stiffness

To demonstrate the performance of RA stiffness in predicting all-cause mortality, ROC curve was created, with an AUC of 0.859. The optimal cut-off point for predicting all-cause mortality was 0.156. Patients with RA stiffness equal or above this cut-off value had significantly higher risk for death (log-rank p < 0.001). ROC curve and Kaplan–Meier cumulative survival curve demonstrating the predictive power of the RA stiffness are presented in **Figure 6**.

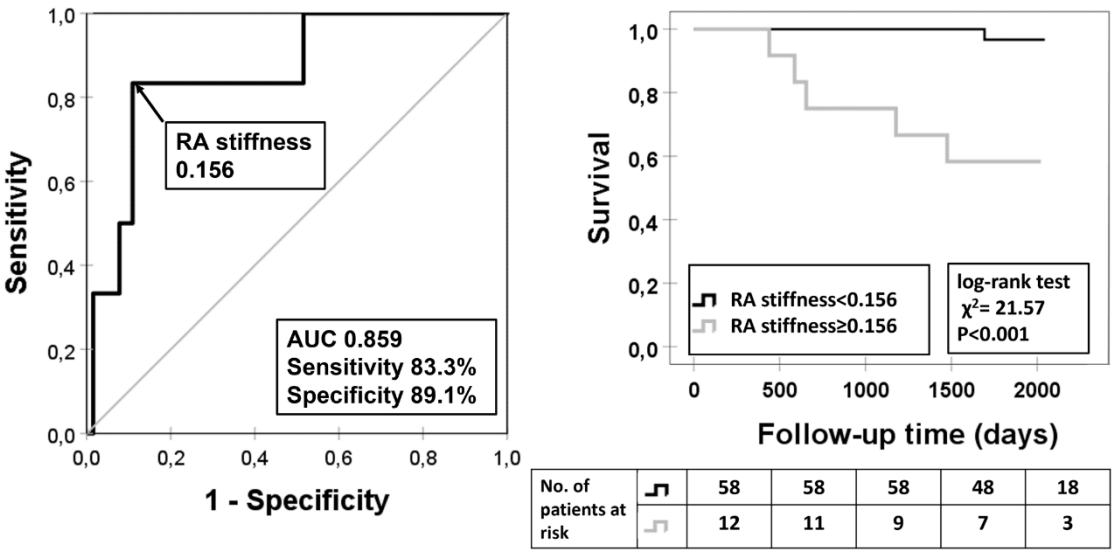

Figure 6. *ROC curve and Kaplan–Meier survival curve demonstrating the performance of RA stiffness in predicting all-cause mortality (χ^2: chi^2)*

Clinical and echocardiographic characteristics of the study cohort stratified by the cut-off RA stiffness value are shown in **Table 10** and **Table 11**. Patients with elevated RA stiffness were significantly older and their walking distance was significantly shorter compared with the other subgroup. Significantly higher NT-proBNP levels whereas significantly lower DLCO values were found in these patients. Anti-topoisomerase I antibody positivity was also more common in this subgroup.

Table 10. Clinical characteristics of the study population stratified by the RA stiffness cut-off

Variable		**RA stiffness < 0.156 (n=58)**	**RA stiffness ≥ 0.156 (n=12)**	**p**
Age (years)		56±12	64± 7	**0.030**
BSA (m^2)		1.76±0.20	1.74±0.14	0.781
Female gender n (%)		52 (90)	11 (92)	0.833
Disease duration (years)		6.8±5.0	8.8±8.7	0.456
Limited cutaneous form n (%)		27 (46.5)	5 (42)	0.757
Modified Rodnan skin score		10.8±7.5	14.3±10.1	0.187
Follow-up time (days)		1768±234	1491±623	0.155
Death n (%)		1 (2)	5 (42)	**<0.001**
Anti-Centromere Antibody n (%)		14 (24)	4 (33)	0.577
Anti-Topoisomerase I Antibody n (%)		14 (24)	6 (50)	**0.042**
Coronary artery disease n (%)		1 (2)	1 (8.5)	0.211
Systemic arterial hypertension n (%)		30 (52)	6 (50)	0.913
Angiotensin convertase enzyme inhibitors n (%)		29 (50)	4 (33)	0.378
Calcium channel blockers n (%)		28 (48)	8 (67)	0.246
Loop diuretics n (%)		24 (41)	7 (58)	0.282
Mineralocorticoid receptor antagonists n (%)		14 (24)	4 (33)	0.507
New York Heart Association functional class n (%)	I	19 (33)	1 (8.5)	**0.014**
	II	28 (48)	4 (33)	
	III	11 (19)	7 (58.5)	
6MWD (m)		405±95	323±61	**0.006**
Modified Borg dyspnoea index		1.6±1.6	2.1±1.8	0.286
Erythrocyte sedimentation rate (mm/h)		20.9±15.8	26.6±17.3	0.269
C-reactive protein (mg/l)		3.3±5.4	4.9±5.9	0.357
Creatinine (µmol/l)		70.8±24.7	70.0± 18.4	0.919
NT-proBNP (pg/ml)		164.4±136.4	325.6±217.6	**0.007**
Troponin-T (ng/l)		9.3±7.9	19.5±15.6	0.090
Forced vital capacity (%)		101.4±15.4	96.1±12.4	0.265
Diffusing capacity of carbon monoxide (%)		67.2±13.9	51.4±14.8	**0.001**

Statistically significant p-values (p<0.05) are formatted in bold.

LV EF values were similar in the two subgroups. Patients with higher RA stiffness exhibited worse LV diastolic function, though this difference has borderline significance. Global RV systolic function (RVFAC) was preserved in both subgroups. Parameters reflecting the RV longitudinal systolic function (TAPSE, tricuspid S), however, were significantly lower in patients with RA stiffness above the cut-off. Significantly lower tricuspid e' and higher tricuspid E/e' values were also found in these patients. PASP was significantly higher in this subgroup, but still within the normal range.

Table 11. Echocardiographic characteristics of the study population stratified by the RA stiffness cut-off

Variable		**RA stiffness <0.156 (n=58)**	**RA stiffness ≥0.156 (n=12)**	**p**
LV ejection fraction (%)		60.7±4.7	60.8±3.8	0.949
LV diastolic function n (%)	Normal	20 (34.5)	0	0.052
	Impaired relaxation	27 (46.5)	8 (66.6)	
	Pseudonormal	11 (19)	4 (33.3)	
Grade of tricuspid regurgitation n (%)	Mild	53 (91)	10 (84)	0.445
	Moderate	4 (7)	1 (8)	
	Severe	1 (2)	1 (8)	
PASP (mmHg)		25.1±5.0	30.2±6.8	**0.008**
RV basal diameter index (mm/m^2)		18.3±2.6	19.1±1.5	0.287
RV mid-cavity diameter index (mm/m^2)		13.4±2.2	13.9±1.4	0.512
RV longitudinal diameter index (mm/m^2)		31.8±3.7	31.2±3.2	0.606
IVC (mm)		14.3±3.5	12.3±4.7	0.119
Collapsibility index (%)		55.6±11.8	55.9±9.6	0.910
RV wall thickness (mm)		5.0±1.0	5.0±1.1	0.894
RVFAC (%)		47.9±6.0	46.0±11.4	0.426
TAPSE (mm)		21.6±2.3	18.8±3.0	**0.001**
Tricuspid E (cm/s)		46.7±9.7	51.4±5.2	0.101
Tricuspid A (cm/s)		38.0±8.0	46.6±9.2	**0.002**
Tricuspid e' (cm/s)		10.1±2.4	6.9±1.2	**<0.001**
Tricuspid a' (cm/s)		13.5±2.5	12.0±2.4	0.074
Tricuspid S (cm/s)		12.8±2.1	10.4±2.2	**0.001**

Variable	RA stiffness <0.156 (n=58)	RA stiffness ≥0.156 (n=12)	p
Tricuspid E/e'	4.8±1.1	7.6±1.2	**<0.001**
RA size and function			
RA Vmax index (mL/m^2)	18.8±4.8	22.6±7.8	0.171
RA reservoir strain (%)	50.5±10.2	43.6±11.4	**0.041**
RA contractile strain (%)	23.0±5.1	22.5±8.4	0.770
RA conduit strain (%)	27.6±7.5	22.9±10.0	0.066
RA stiffness	0.098±0.024	0.180±0.021	**<0.001**

Statistically significant p-values (p<0.05) are formatted in bold.

6.2.5 Incremental prognostic value of RA stiffness

When evaluated by comparing groups above and below the cut-off value (10 cm/s for tricuspid S and 0.156 for RA stiffness) for each parameter, patients with high tricuspid S AND low RA stiffness (n=55) showed the lowest mortality rate (1 event (1.8%)). Compared with this reference group, patients with low tricuspid S OR high RA stiffness (n=10) had significantly higher mortality rate (2 events (20%); log-rank p=0.008) whereas the highest mortality rate was observed in patients with low tricuspid S AND elevated RA stiffness (n=5, 3 events (60%), log-rank p<0.001) (**Figure 7**).

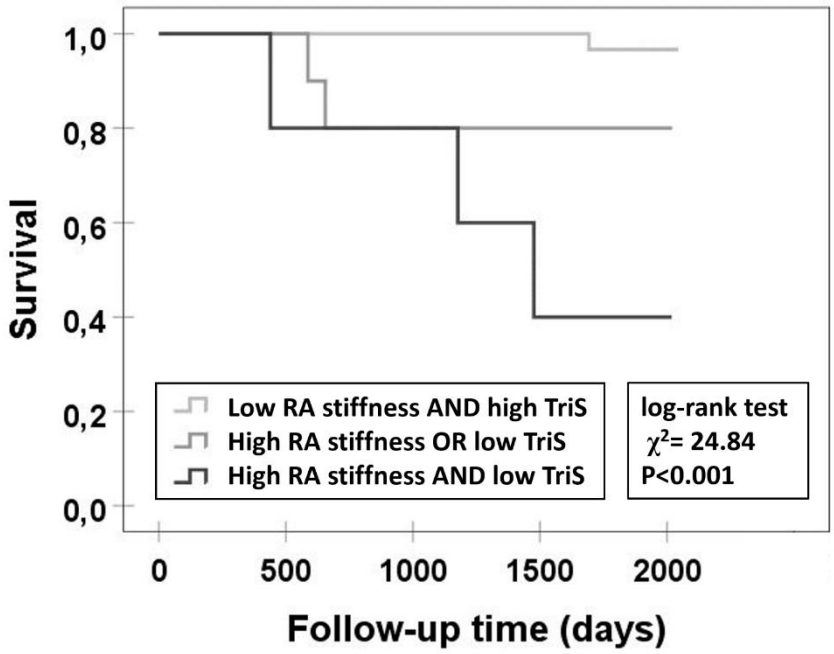

No. of patients at risk						
	⎍	55	55	55	47	18
	⎍	10	10	8	6	1
	⎍	5	4	4	2	2

Figure 7. *Kaplan–Meier survival curve demonstrating the incremental prognostic value of RA stiffness when added to tricuspid S (TriS) in predicting all-cause mortality. The cohort was stratified by tricuspid S and RA stiffness profile of the patients. (χ^2: chi^2)*

7 Discussion

7.1 Correlation between echocardiographic parameters of LV and RV diastolic function and the functional capacity of the patients in COPD

Dyspnoea and reduced functional capacity are common consequences of COPD. The aetiology of reduced exercise tolerance is multifactorial thus parameters of the resting pulmonary function like FEV1 are poor predictors of the functional capacity [4, 5] , as it was proved also in our study (see **Figure 2**). Dynamic lung hyperinflation is an important contributory factor that can be targeted for treatment [5, 6]. Depression, skeletal muscle weakness or PH as well as alterations of the cardiac function may also serve as limiting factor to reduced functional capacity [7, 8]. Our hypothesis was that LV and RV diastolic dysfunction is a contributing factor to exercise intolerance in this disease.

LV EF was preserved or mildly reduced in our COPD population. Mitral annular S values, however, were significantly decreased as compared to healthy subjects. This subclinical impairment of the LV systolic function commonly occurs in patients with impaired LV diastolic function as the evidence of the interdependence between contraction and relaxation [218].

Many mechanisms may explain the presence of LV diastolic dysfunction in patients with COPD. Significant reduction of the LV diastolic diameter and consequential impairment of LV filling was reported in pulmonary hyperinflation [219]. Abnormal patterns of LV diastolic filling have been also described in patients with COPD and elevated pulmonary pressure, due to ventricular interdependence [45]. In addition, hypoxemia and systemic inflammation may directly impair LV myocardial function [220]. Cardiovascular comorbidities, such as systemic hypertension or ischaemic heart disease, are common in COPD [221, 222], which may be also responsible for the LV diastolic dysfunction.

COPD on CT scan was associated with reduced pulmonary vein cross-sectional area. Smith et al. therefore suggested that impaired LV filling in COPD may be predominantly due to the reduced LV preload from upstream pulmonary causes rather than intrinsic diastolic dysfunction [223]. In fact, the mitral inflow pattern (E/A) is dependent on loading conditions. Mitral annular TDI parameters, however, are able to reveal the intrinsic relaxation

abnormalities of the LV myocardium [224]. This technique is useful for the assessment of the LV diastolic function in COPD patients as well [10, 11, 225]. The results of these recent studies are not completely comparable, as different approaches were used to estimate the frequency of the LV diastolic dysfunction. Nevertheless, these works have concordantly proved that LV diastolic dysfunction is common in COPD. In accordance with these previous findings, mild or moderate form of LV diastolic dysfunction was found in 74% of our COPD patients. In addition to the manifest diastolic and subclinical systolic RV dysfunction, LV diastolic dysfunction may be also responsible for the large number of heart failure cases in our population.

Lopez-Sanchez et al. [11] reported significant correlation between E/A ratio and the functional capacity of the patients while in the work of Cuttica et al. [10] mitral E/e' and the degree of diastolic dysfunction were predictors of the 6MWD in univariate analysis. In our population, LA area index was the only parameter in the left heart, which showed significant correlation with 6MWD. Whereas mitral E/e' reflects the momentary value of the LV filling pressure, LA area is considered as a reliable indicator of the cumulative effects of the elevated LV filling pressure over time [162] and may predict abnormal elevation of LV filling pressure during exercise in patients with normal resting LV filling pressure [226]. These facts may serve as explanation for the superiority of LA size over E/e' in the prediction of the functional capacity of the patients.

RVFAC was preserved in our COPD population, whereas TAPSE and tricuspid S, the parameters reflecting RV longitudinal systolic function, were significantly decreased as compared to healthy subjects, suggesting subclinical impairment of RV systolic function. These results are in line with the data of Hilde at al. who reported the decrease of the RV longitudinal strain in a COPD population without PH [138].

Prolonged RV MPI as well as significantly decreased tricuspid e' and tricuspid e'/a' were found as the signs of RV diastolic dysfunction. Enlarged RA area suggested chronic or intermittent elevation of the RV filling pressure [227]. Besides, the more dilated IVC and lower collapsibility index were the signs of the elevated RA pressure in our patients.

Cuttica et al. have already demonstrated that structural changes in the right heart are associated with reduced functional capacity in patients with COPD. In their study, RA size and RV wall thickness were independent predictors of 6MWD. Tricuspid annular TDI parameters, however, were not investigated in their work [10]. In our study a more comprehensive analysis of this topic was performed applying 2D, spectral Doppler and TDI techniques both in the left and right heart. Tricuspid e'/a', RA area index and collapsibility index were proved to be independent predictors of 6MWD in our study, providing further evidence, that RV diastolic function and filling pressure have major impact on the functional capacity in patients with COPD.

HFpEF may be accompanied by RV dysfunction. In this setting, impaired RV function is related to both primary myocardial involvement and elevated RV afterload [228]. LV diastolic dysfunction and elevated LV filling pressure were common in our COPD population. This fact suggests that RV dysfunction of our patients is not necessarily related to COPD, but may be the consequence of the LV disease. On the other hand, all independent echocardiographic predictors of the 6MWD represented the right heart. It does not support the primary role of the left heart disease in the reduced functional capacity of our COPD patients.

PH is a well-known comorbidity in advanced COPD. In patients with severe COPD, waiting for lung volume reduction surgery or lung transplantation, PH and consequential RV dysfunction was present in the half of the patients [39]. In unselected COPD patients with moderate to severe disease, incidence of the resting PH is much lower. Subclinical systolic and manifest diastolic dysfunction of the RV, however, is already present in patients without resting PH [138, 229], as it was proved also in our study. The possible explanation for this phenomenon is the subclinically elevated PVR which may be unmasked by exercise, when the pulmonary circulation no longer has the capacity to adapt, and the pulmonary pressure increases parallel with the increasing CO [230]. Similarly, Kovacs et al. reported that borderline resting PAP is associated with decreased exercise capacity in patients with SSc. In their work, 6MWD showed significant negative correlation with PVR measured at peak exercise [27].

Figure 8 demonstrates the hypothesized changes in the typical parameters of the RV systolic and diastolic function parallel with the progression of the pulmonary vascular disease in patients with COPD. As the consequence of the transient pressure overload, RV diastolic dysfunction and enlarged RA is present already in patients without resting PH whereas the manifest RV systolic dysfunction develops later during the course of the disease, in patients with permanent RV pressure overload.

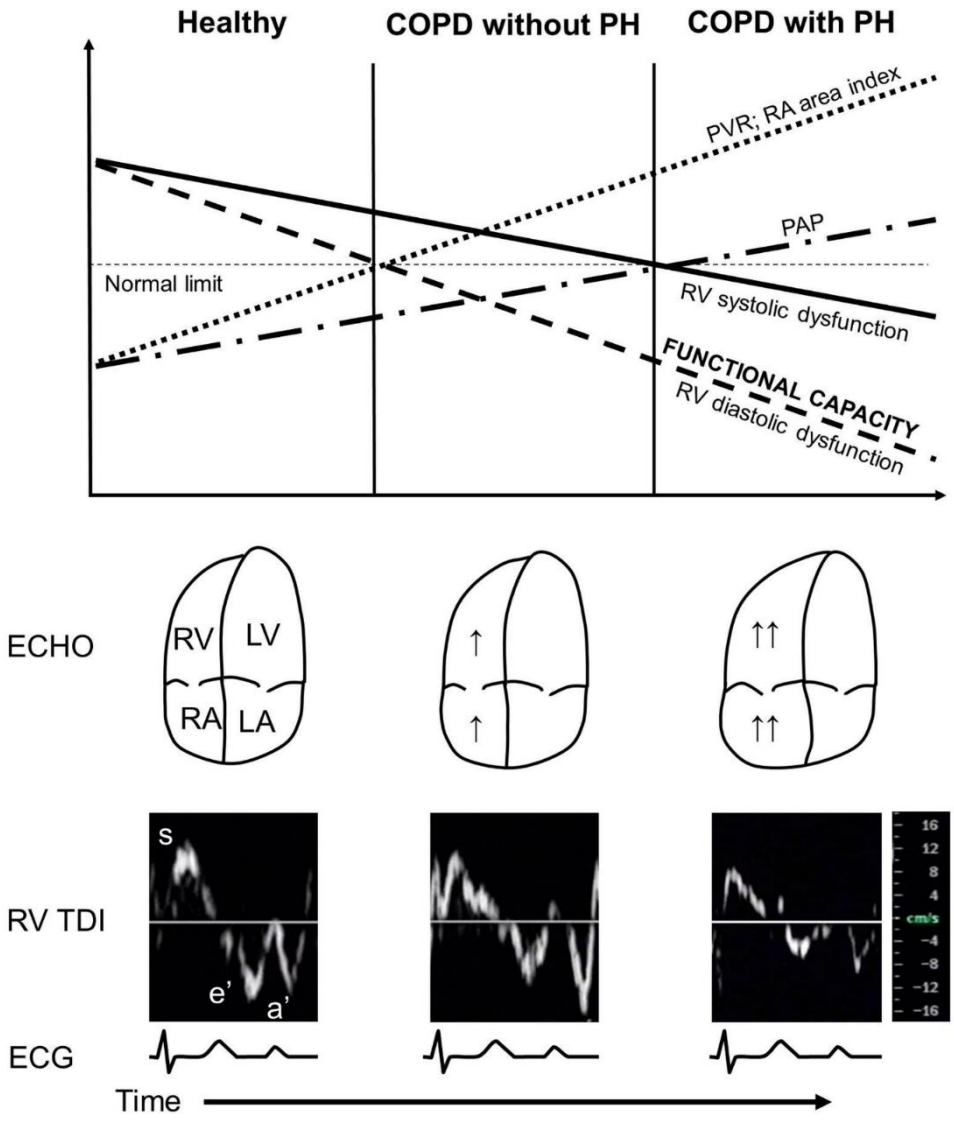

Figure 8. *Schematic diagram demonstrating the hypothesized changes in the typical echocardiographic and hemodynamic parameters parallel with the course of the disease in patients with COPD.*

7.1.1 Limitations of the study

Various limitations of our study are to be acknowledged. Data about the extent of the dynamic lung hyperinflation may provide further insight into the pulmonary function of the patients. This, however, was not investigated in our patients.

The number of patients with resting PH was low in our COPD population and the elevation of the pulmonary pressure was mild in most of these cases. In addition, few patients with GOLD stage IV disease participated in the study. A higher proportion of patients with considerable PH and/or more advanced lung disease may also alter our results.

Our patients did not undergo RHC, therefore PASP was estimated noninvasively. Thus, no data are available about the PVR of the patients. Due to the lack of invasive measurements, LV and RV filling pressures were also estimated by Doppler methods. Unfortunately, these parameters are less reliable in the evaluation of filling dynamics than the invasive measurements.

7.2 Significance of RA size and mechanics in SSc: correlation with functional capacity and prognostic value

LV diastolic dysfunction is frequent in SSc [13, 68] and is often accompanied by impaired LA function [16, 17, 231]. RV dysfunction was traditionally attributed to the development of PAH or pulmonary fibrosis [18]. Subclinical RV dysfunction, however, was also proved in SSc patients without the resting elevation of the pulmonary pressure, by using tissue Doppler or speckle tracking measurements [19-22]. By the help of this technique, impaired RA function has been recently reported in SSc [20]. Recent data suggest that RA size and mechanics correlate well with the functional capacity of the patients in conditions with known right heart involvement, such as in idiopathic PAH or COPD [23, 232]. Thus, we aimed to investigate the abnormalities of the RA function as compared with healthy subjects and to assess the potential correlations between RA mechanics and the functional capacity in SSc patients, by using 2D speckle tracking technique.

LV diastolic dysfunction is associated with increased risk of mortality [13, 69, 233]. Prognostic value of the increased LA volume was also reported [13]. Speckle tracking-derived LV global longitudinal [234] and circumferential strain [235] – both representing subclinically impaired LV systolic function – showed significant associations with the outcome in this condition. Besides, both tricuspid S [235] and TAPSE [234] showed significant, independent association with the adverse outcome. Prognostic value of the impaired RA function was not known in this disease. Recent studies suggested, however, that RA size and mechanics are associated with unfavourable prognosis in patients with idiopathic or CTD associated PAH [203, 236]. In addition, Jain et al. proved, that RA reservoir and conduit strain are independent predictors of mortality in left heart failure with both preserved and reduced EF [205]. Thus, we hypothesized that RA size and mechanics may have prognostic role even in SSc patients without manifest PAH.

In SSc there are few data about RA size and function. Lindqvist et al. found enlarged RA area in SSc patients with normal RV end-diastolic diameters and without manifest PH [22]. Similarly, D'Andrea et al. reported significant enlargement of the RA area compared with healthy subjects [237], while Durmus et al. found RA area index values similar to those in the healthy persons [20]. In the latter two studies RA function was also investigated, by the help of 2D speckle tracking technique. Significantly decreased segmental strain values were reported by D'Andrea et al. in SSc patients, especially in those with pulmonary fibrosis [237]. Durmus et al. found decreased RA reservoir and conduit strain values compared to a healthy control population. Contractile strain was not investigated in their study [20]. Our findings are in line with the results of Durmus et al.: although RA volume values were similar in our SSc patients and in the healthy group, we found significantly decreased reservoir and conduit strain values in the SSc group. Contractile strain values did not differ between SSc group and healthy persons in our study.

We applied another parameter of the atrial performance, RA stiffness, which has never been investigated in SSc before. The role of this parameter was first reported in the left heart: it was proven to be an accurate index to distinguish HFpEF patients from those with asymptomatic diastolic dysfunction [206]. Less is known, however, about the use of the atrial

stiffness in the right heart. Teixeira et al. demonstrated increased RA stiffness in patients with left heart failure [209]. In our study, RA stiffness turned out to be significantly elevated in the SSc population, compared with healthy subjects.

In treatment-naive patients with idiopathic PAH Saha et al. demonstrated significant correlation between RA reservoir strain and 6MWD [23]. Similarly, as it was reported in the first part of this thesis, RA area index was proved to be an independent predictor of the 6MWD in patients with COPD [232]. Our results are in line with these previous findings, suggesting that speckle tracking-derived RA stiffness has a strong influence on the functional capacity of the SSc patients.

Karna et al. demonstrated the increased RV thickness as the single most important predictor of the prolonged RV MPI among SSc patients [238]. Lindqvist et al. reported altered RV diastolic function in SSc patients, with an increase in RV wall thickness as early markers of RV dysfunction, probably in response to intermittent P(A)H [22]. Although we could not prove significantly increased RV wall thickness in our population compared with healthy subjects, RV wall thickness became independent predictor of the functional capacity in SSc patients. Our data suggest, however, that for utilizing its predictive capabilities, RV wall thickness should be measured by 0.1 mm increments. Unfortunately, the accuracy of the echocardiographic measurements is limited at this level, making this parameter clinically less useful.

In univariate Cox regression analysis RA Vmax index and RA stiffness showed significant association with 5-year all-cause mortality, whereas, regarding RA contractile strain, this association had borderline significance. When added to tricuspid S in sequential Cox model, RA stiffness significantly improved the diagnostic performance of the model and remained independent predictor of the outcome. Our data support the strong prognostic value of RA stiffness in SSc patients without manifest PAH.

In SSc, RV myocardial dysfunction may be considered as the sign of the primary myocardial involvement of the disease [145]. On the other hand, in SSc patients with ILD or subclinical pulmonary vascular disease, the subclinical elevation of the PVR may be unmasked by exercise, when pulmonary circulation no longer has the capacity to adapt, and the pulmonary

pressure increases parallel with the increasing cardiac output [239]. This exercise induced, intermittent pressure overload may also lead to ultrastructural changes in the right heart [22, 145]. In addition, independently from the aetiology, LV diastolic dysfunction is often associated with impaired mechanics of the right heart. This phenomenon is thought to be explained by the exercise-induced elevation of LV filling pressure and the consequential elevation of PAP [240]. (**Figure 9**)

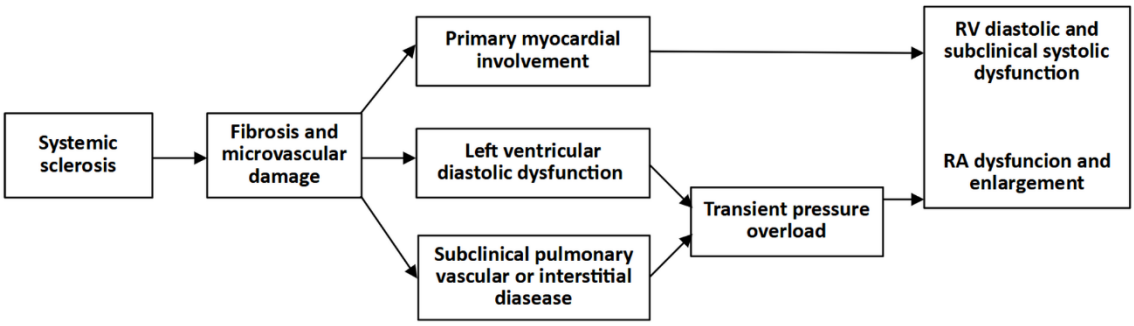

Figure 9. *Mechanisms involved in the development of RA dysfunction and enlargement in SSc patients without manifest PAH*

D'Andrea et al. reported significant correlation between RA lateral segmental strain and PASP during effort, suggesting, that in SSc patients with exercise PH the intermittent pressure overload may lead to ultrastructural changes in the RA wall [237]. Besides, it has been demonstrated that LA reservoir strain correlated significantly with the extent of LA wall fibrosis as assessed by cardiac MRI and with LA interstitial fibrosis in patients with mitral valve disease in pathological specimens [241, 242]. Although similar histopathologic evidence is not available in the right heart, impaired RA function and elevated RA stiffness may represent the consequence the intermittent pressure overload due to stress induced elevation of PAP in SSc. This functional alteration reduces the capacity of the atrium to help maintain CO during exercise.

RA stiffness is a complex parameter reflecting atrial mechanics and RV filling pressure simultaneously. This may explain its superiority over the RA volume and strain parameters.

When stratified by RA stiffness cut-off, our data may support all the potential mechanisms demonstrated in **Figure 9**: High risk patient with RA stiffness above the cut-off exhibited significantly higher PASP (but still within the normal range) and significantly lower DLCO values. Besides, there was a clear tendency suggesting worse LV diastolic function in the high-risk subgroup, though the difference was not statistically significant. Diagnostic and prognostic utility of the well-known cardiac biomarkers, NT-proBNP and troponin-T, has already been proved in SSc [243-245]. Patient with RA stiffness above the cut-off showed significantly higher NT-proBNP values. Troponin-T level was also higher in this subgroup, albeit the differences were not statistically significant. Anti-Topoisomerase I antibody positivity was also significantly more common in the high-risk subgroup. The potential clinical significance of this antibody level has been reported in evaluating disease severity and prognosis in SSc [246, 247].

7.2.1 Limitations of the study

Our data should be interpreted in the context of their limitations. First, the statistical power of our analysis is limited by the relatively low number of participants and events. Our results require further validation in a larger SSc population. For obtaining RA strain values, we used a software that was developed for LV strain analysis because a dedicated software for atrial strain estimation was not available. RV strain may better reflect the subclinical impairment of the RV systolic function than our traditional and TDI parameters. Nevertheless, in the lack of appropriate analytical software, RV strain analysis was not performed in our study. Our patients did not undergo RHC, therefore PASP was estimated noninvasively, and no data were available about the PVR of the patients. Due to the lack of invasive measurements, RV filling pressures were also estimated by Doppler methods. It is important to note that the non-invasive approach used for the estimation of the RA stiffness has not been invasively validated in the right heart yet.

8 Conclusion

In our work we proved that RV diastolic function and filling pressure have strong influence on the functional capacity in patients with COPD. Similarly, our results suggest that speckle tracking-derived RA stiffness is increased in SSc compared with healthy subjects and shows strong correlation with the functional capacity of the patients. Besides, RA stiffness is significantly associated with all-cause mortality in SSc patients without PAH independent of and incremental to the RV longitudinal systolic function.

A possible explanation to these results is the pathological increase of PAP on exercise, leading to transient pressure overload of the right heart, which in turn results in decreased functional capacity as well as a latent functional impairment of RV and RA, which may be identified with the modern, sensitive echocardiographic techniques applied in our studies.

Our results suggest that these relatively simple, resting echocardiographic parameters may be useful in screening high risk populations and identifying patients with potential exercise PH and worse prognosis.

9 Novel findings

- Echocardiographic parameters of the RV diastolic function and filling pressure show strong correlation with the functional capacity of COPD patients.
- Right atrial reservoir and conduit strain are impaired, whereas RA stiffness is increased in SSc compared with healthy subjects.
- Right atrial stiffness is one of the main determinants of the functional capacity in SSc patients.
- Right atrial stiffness is associated with all-cause mortality in SSc patients without PAH independent of and incremental to the RV longitudinal systolic function.

10 References

1. Humbert, M., et al., *Pathology and pathobiology of pulmonary hypertension: state of the art and research perspectives.* European Respiratory Journal, 2019. **53**(1): p. 1801887.
2. Global initiative for chronic obstructive lung disease, *Global strategy for the diagnosis, management, and prevention of Chronic Obstructive Pulmonary Disease (2023 Report).* Available from: https://goldcopd.org [Accessed 03.03.2023]
3. Gredic, M., et al., *Pulmonary hypertension in chronic obstructive pulmonary disease.* British Journal of Pharmacology, 2021. **178**(1): p. 132-151.
4. Bauerle, O., C.A. Chrusch, and M. Younes, *Mechanisms by Which COPD Affects Exercise Tolerance.* American Journal of Respiratory and Critical Care Medicine, 1998. **157**(1): p. 57-68.
5. Marin, J.M., et al., *Inspiratory Capacity, Dynamic Hyperinflation, Breathlessness, and Exercise Performance during the 6-Minute-Walk Test in Chronic Obstructive Pulmonary Disease.* American Journal of Respiratory and Critical Care Medicine, 2001. **163**(6): p. 1395-1399.
6. Laveneziana, P., et al., *New physiological insights into dyspnea and exercise intolerance in chronic obstructive pulmonary disease patients.* Expert Review of Respiratory Medicine, 2012. **6**(6): p. 651-662.
7. Nici, L., *Mechanisms and measures of exercise intolerance in chronic obstructive pulmonary disease.* Clinics in Chest Medicine, 2000. **21**(4): p. 693-704.
8. Barnes, P.J., *Chronic Obstructive Pulmonary Disease: Effects beyond the Lungs.* PLoS Medicine, 2010. **7**(3): p. e1000220.
9. Hoeper, M.M., et al., *Diagnosis, Assessment, and Treatment of Non-Pulmonary Arterial Hypertension Pulmonary Hypertension.* Journal of the American College of Cardiology, 2009. **54**(1 Suppl): p. S85-S96.
10. Cuttica, M.J., et al., *Right Heart Structural Changes Are Independently Associated with Exercise Capacity in Non-Severe COPD.* PLoS ONE, 2011. **6**(12): p. e29069.
11. Lopez-Sanchez, M., et al., *High Prevalence of Left Ventricle Diastolic Dysfunction in Severe COPD Associated with A Low Exercise Capacity: A Cross-Sectional Study.* PLoS One, 2013. **8**(6): p. e68034.
12. Komócsi, A., et al., *The impact of cardiopulmonary manifestations on the mortality of SSC: A systematic review and meta-analysis of observational studies.* Rheumatology (Oxford), 2012. **51**(6): p. 1027-1036.
13. Faludi, R., et al., *Five-year follow-up of left ventricular diastolic function in systemic sclerosis patients: determinants of mortality and disease progression.* Seminars in Arthritis and Rheumatism, 2014. **44**(2): p. 220-227.
14. Allanore, Y., et al., *Prevalence and factors associated with left ventricular dysfunction in the EULAR Scleroderma Trial and Research group (EUSTAR) database of patients with systemic sclerosis.* Annals of the Rheumatic Diseases 2010. **69**(1): p. 218-221.
15. Ataş, H., et al., *Evaluation of left atrial volume and function in systemic sclerosis patients using speckle tracking and real-time three-dimensional echocardiography.* The Anatolian Journal of Cardiology, 2016. **16**(5): p. 316-22.
16. Agoston, G., et al., *Left atrial dysfunction detected by speckle tracking in patients with systemic sclerosis.* Cardiovascular Ultrasound, 2014. **12**(1): p. 30.
17. Porpáczy, A., et al., *Impairment of Left Atrial Mechanics Is an Early Sign of Myocardial Involvement in Systemic Sclerosis.* Journal of Cardiac Failure, 2018. **24**(4): p. 234-242.

18. Yiu, K.H., et al., *Impact of pulmonary fibrosis and elevated pulmonary pressures on right ventricular function in patients with systemic sclerosis.* Rheumatology, 2015. **55**(3): p. kev342.
19. Faludi, R., et al., *Isolated diastolic dysfunction of right ventricle: Stress-induced pulmonary hypertension.* European Respiratory Journal, 2008. **31**(2): p. 475-476.
20. Durmus, E., et al., *Right ventricular and atrial functions in systemic sclerosis patients without pulmonary hypertension: Speckle-tracking echocardiographic study* Herz, 2015. **40**(4): p. 709-715.
21. Mukherjee, M., et al., *Unique Abnormalities in Right Ventricular Longitudinal Strain in Systemic Sclerosis Patients.* Circulation: Cardiovascular Imaging, 2016. **9**(6): p. e003792.
22. Lindqvist, P., et al., *Disturbed right ventricular diastolic function in patients with systemic sclerosis: A Doppler tissue imaging study.* Chest, 2005. **128**(2): p. 755-763.
23. Saha, S.K., et al., *Association of right atrial mechanics with hemodynamics and physical capacity in patients with idiopathic pulmonary arterial hypertension: Insight from a single-center cohort in Northern Sweden.* Echocardiography, 2016. **33**(1): p. 46-56.
24. Humbert, M., et al., *2022 ESC/ERS Guidelines for the diagnosis and treatment of pulmonary hypertension.* European Heart Journal, 2022. **43**(38): p. 3618-3731.
25. Galiè, N., et al., *2015 ESC/ERS Guidelines for the diagnosis and treatment of pulmonary hypertension.* European Heart Journal, 2016. **37**(1): p. 67-119.
26. Kovacs, G., et al., *Pulmonary arterial pressure during rest and exercise in healthy subjects: A systematic review.* European Respiratory Journal, 2009. **34**(4): p. 888-894.
27. Kovacs, G., et al., *Borderline Pulmonary Arterial Pressure Is Associated with Decreased Exercise Capacity in Scleroderma.* American Journal of Respiratory and Critical Care Medicine, 2009. **180**(9): p. 881-886.
28. Bae, S., et al., *Baseline characteristics and follow-up in patients with normal haemodynamics versus borderline mean pulmonary arterial pressure in systemic sclerosis: Results from the PHAROS registry.* Annals of the Rheumatic Diseases, 2012. **71**(8): p. 1335-1342.
29. Valerio, C.J., et al., *Borderline Mean Pulmonary Artery Pressure in Patients With Systemic Sclerosis: Transpulmonary Gradient Predicts Risk of Developing Pulmonary Hypertension.* Arthritis and Rheumatism, 2013. **65**(4): p. 1074-1084.
30. Stamm, A., et al., *Exercise pulmonary haemodynamics predict outcome in patients with systemic sclerosis.* European Respiratory Journal, 2016. **48**(6): p. 1658-1667.
31. Guth, S., et al., *Exercise right heart catheterisation before and after pulmonary endarterectomy in patients with chronic thromboembolic disease.* European Respiratory Journal, 2018. **52**(3): p. 1800458.
32. Taboada, D., et al., *Outcome of pulmonary endarterectomy in symptomatic chronic thromboembolic disease.* European Respiratory Journal, 2014. **44**(6): p. 1635-1645.
33. Hoeper, M.M., et al., *A global view of pulmonary hypertension.* The Lancet Respiratory Medicine, 2016. **4**(4): p. 306-322.
34. Hamada, K., et al., *Significance of pulmonary arterial pressure and diffusion capacity of the lung as prognosticator in patients with idiopathic pulmonary fibrosis.* Chest, 2007. **131**(3): p. 650-656.
35. Douschan, P., et al., *Mild elevation of pulmonary arterial pressure as a predictor of mortality.* American Journal of Respiratory and Critical Care Medicine, 2018. **197**(4): p. 509-516.
36. Maron, B.A., et al., *Association of Borderline Pulmonary Hypertension With Mortality and Hospitalization in a Large Patient Cohort: Insights From the Veterans Affairs Clinical Assessment, Reporting, and Tracking Program.* Circulation, 2016. **133**(13): p. 1240-1248.
37. Assad, T.R., et al., *Prognostic effect and longitudinal hemodynamic assessment of borderline pulmonary hypertension.* JAMA Cardiology, 2017. **2**(12): p. 1361-1368.

38. Simonneau, G., et al., *Haemodynamic definitions and updated clinical classification of pulmonary hypertension.* European Respiratory Journal, 2019. **53**(1): p. 1801913.
39. Thabut, G., et al., *Pulmonary Hemodynamics in Advanced COPD Candidates for Lung Volume Reduction Surgery or Lung Transplantation.* Chest, 2005. **127**(5): p. 1531-1536.
40. Andersen, K.H., et al., *Prevalence, predictors, and survival in pulmonary hypertension related to end-stage chronic obstructive pulmonary disease.* Journal of Heart and Lung Transplantation, 2012. **31**(4): p. 373-380.
41. Sims, M.W., et al., *Impact of Pulmonary Artery Pressure on Exercise Function in Severe COPD.* Chest, 2009. **136**(2): p. 412-419.
42. Scharf, S.M., et al., *Hemodynamic characterization of patients with severe emphysema.* American Journal of Respiratory and Critical Care Medicine, 2002. **166**(3): p. 314-322.
43. Chaouat, A., et al., *Severe Pulmonary Hypertension and Chronic Obstructive Pulmonary Disease.* American Journal of Respiratory and Critical Care Medicine, 2005. **172**(2): p. 189-194.
44. Nathan, S.D., et al., *Pulmonary hypertension in chronic lung disease and hypoxia.* European Respiratory Journal, 2020. **53**(1): p. 1801914.
45. Funk, G.-C., et al., *Left Ventricular Diastolic Dysfunction in Patients With COPD in the Presence and Absence of Elevated Pulmonary Arterial Pressure.* Chest, 2008. **133**(6): p. 1354-1359.
46. Kim, V., et al., *Risk Factors for Venous Thromboembolism in Chronic Obstructive Pulmonary Disease.* Chronic Obstructive Pulmonary Diseases: Journal of the COPD Foundation, 2014. **1**(2): p. 239-249.
47. Morgan, A., et al., *COPD disease severity and the risk of venous thromboembolic events: a matched case–control study.* International Journal of Chronic Obstructive Pulmonary Disease, 2016. **11**: p. 899-908.
48. Aleva, F.E., et al., *Prevalence and Localization of Pulmonary Embolism in Unexplained Acute Exacerbations of COPD.* Chest, 2017. **151**(3): p. 544-554.
49. Kovacs, G., et al., *PULMONARY PERSPECTIVE Pulmonary Vascular Involvement in Chronic Obstructive Pulmonary Disease Is There a Pulmonary Vascular Phenotype?* American Journal of Respiratory and Critical Care Medicine, 2018. **198**(8): p. 1000-1011.
50. Weitzenblum, E., et al., *Prognostic value of pulmonary artery pressure in chronic obstructive pulmonary disease.* Thorax, 1981. **36**(10): p. 752-758.
51. Kessler, R., et al., *"Natural history" of pulmonary hypertension in a series of 131 patients with chronic obstructive lung disease.* American Journal of Respiratory and Critical Care Medicine, 2001. **164**(2): p. 219-224.
52. Oswald-Mammosser, M., et al., *Prognostic Factors in COPD Patients Receiving Long-term Oxygen Therapy.* Chest, 1995. **107**(5): p. 1193-1198.
53. Burrows, B., et al., *Patterns of cardiovascular dysfunction in chronic obstructive lung disease.* The New England Journal of Medicine, 1972. **286**(17): p. 912-8.
54. Kessler, R., et al., *Predictive Factors of Hospitalization for Acute Exacerbation in a Series of 64 Patients with Chronic Obstructive Pulmonary Disease.* American Journal of Respiratory and Critical Care Medicine, 1999. **159**(1): p. 158-164.
55. Iyer, A.S., et al., *CT Scan-Measured Pulmonary Artery to Aorta Ratio and Echocardiography for Detecting Pulmonary Hypertension in Severe COPD.* Chest, 2014. **145**(4): p. 824-832.
56. Wells, J.M., et al., *Pulmonary Arterial Enlargement and Acute Exacerbations of COPD.* The New England Journal of Medicine, 2012. **367**(10): p. 913-921.
57. Humbert, M., et al., *Pulmonary Arterial Hypertension in France.* American Journal of Respiratory and Critical Care Medicine, 2006. **173**(9): p. 1023-1030.

58. Condliffe, R., et al., *Connective tissue disease-associated pulmonary arterial hypertension in the modern treatment era.* American Journal of Respiratory and Critical Care Medicine, 2009. **179**(2): p. 151-157.
59. Hao, Y.-J., et al., *Connective tissue disease-associated pulmonary arterial hypertension in Chinese patients.* European Respiratory Journal, 2014. **44**(4): p. 963-972.
60. Mukerjee, D., *Echocardiography and pulmonary function as screening tests for pulmonary arterial hypertension in systemic sclerosis.* Rheumatology, 2004. **43**(4): p. 461-466.
61. Avouac, J., et al., *Prevalence of Pulmonary Hypertension in Systemic Sclerosis in European Caucasians and Metaanalysis of 5 Studies.* The Journal of Rheumatology, 2010. **37**(11): p. 2290-2298.
62. Humbert, M., et al., *Screening for pulmonary arterial hypertension in patients with systemic sclerosis: Clinical characteristics at diagnosis and long-term survival.* Arthritis and Rheumatism, 2011. **63**(11): p. 3522-3530.
63. Hachulla, E., et al., *The three-year incidence of pulmonary arterial hypertension associated with systemic sclerosis in a multicenter nationwide longitudinal study in France.* Arthritis and Rheumatism, 2009. **60**(6): p. 1831-1839.
64. Ruiz-Irastorza, G., et al., *Pulmonary hypertension in systemic lupus erythematosus: prevalence, predictors and diagnostic strategy.* Autoimmunity Reviews, 2013. **12**(3): p. 410-415.
65. Yang, X., et al., *Prevalence of pulmonary arterial hypertension in patients with connective tissue diseases: a systematic review of the literature.* Clinical Rheumatology, 2013. **32**(10): p. 1519-1531.
66. Wu, C.-H., et al., *Connective Tissue Disease-Associated Pulmonary Arterial Hypertension in Southern Taiwan: A Single-Center 10-Year Longitudinal Observation Cohort.* Healthcare (Basel), 2021. **9**(5): p. 615.
67. Haque, A., et al., *Pulmonary hypertension phenotypes in patients with systemic sclerosis.* European Respiratory Review, 2021. **30**(161): p. 210053.
68. Kahan, A. and Y. Allanore, *Primary myocardial involvement in systemic sclerosis.* Rheumatology, 2006. **45**(Suppl 4): p. iv14-iv17.
69. Hinchcliff, M., et al., *Prevalence, prognosis, and factors associated with left ventricular diastolic dysfunction in systemic sclerosis.* Clinical and Experimental Rheumatology, 2012. **30**(2 Suppl 71): p. S30-S37.
70. Fernández-Codina, A., et al., *Cardiac involvement in systemic sclerosis: differences between clinical subsets and influence on survival.* Rheumatology International, 2017. **37**(1): p. 75-84.
71. Oliveira, M.F., et al., *Prevalence and prognostic significance of heart failure with preserved ejection fraction in systemic sclerosis.* Future Cardiology, 2022. **18**(1): p. 17-25.
72. Launay, D., et al., *Pulmonary hypertension in systemic sclerosis: different phenotypes.* European Respiratory Review, 2017. **26**(145): p. 170056.
73. Hinchcliff, M., et al., *Pulmonary Hypertension Assessment and Recognition of Outcomes in Scleroderma (PHAROS): Baseline Characteristics and Description of Study Population.* The Journal of Rheumatology, 2011. **38**(10): p. 2172-2179.
74. Coghlan, J.G., et al., *Evidence-based detection of pulmonary arterial hypertension in systemic sclerosis: the DETECT study.* Annals of the Rheumatic Diseases, 2014. **73**(7): p. 1340-1349.
75. Bourji, K.I., et al., *Poor survival in patients with scleroderma and pulmonary hypertension due to heart failure with preserved ejection fraction.* Pulmonary Circulation, 2017. **7**(2): p. 409-420.
76. Fox, B.D., et al., *High prevalence of occult left heart disease in scleroderma-pulmonary hypertension.* European Respiratory Journal, 2013. **42**(4): p. 1083-1091.

77. Hyldgaard, C., et al., *Interstitial Lung Disease in Connective Tissue Diseases: Survival Patterns in a Population-Based Cohort.* Journal of Clinical Medicine, 2021. **10**(21): p. 4830.
78. Xiong, A., et al., *Increased risk of mortality in systemic sclerosis-associated pulmonary hypertension: a systemic review and meta-analysis.* Advances in Rheumatology, 2022. **62**(1): p. 10.
79. Vonk, M.C., E. Vandecasteele, and A.P. Dijk, *Pulmonary hypertension in connective tissue diseases, new evidence and challenges.* European Journal of Clinical Investigation, 2021. **51**(4): p. e13453.
80. Chung, L., et al., *Unique predictors of mortality in patients with pulmonary arterial hypertension associated with systemic sclerosis in the REVEAL registry.* Chest, 2014. **146**(6): p. 1494-1504.
81. Lefèvre, G., et al., *Survival and Prognostic Factors in Systemic Sclerosis-Associated Pulmonary Hypertension: A Systematic Review and Meta-Analysis.* Arthritis and Rheumatism, 2013. **65**(9): p. 2412-2423.
82. Khanna, D., et al., *Recommendations for screening and detection of connective tissue disease-associated pulmonary arterial hypertension.* Arthritis and Rheumatism, 2013. **65**(12): p. 3194-3201.
83. Hachulla, E., et al., *Early detection of pulmonary arterial hypertension in systemic sclerosis: A French nationwide prospective multicenter study.* Arthritis and Rheumatism, 2005. **52**(12): p. 3792-3800.
84. Frost, A., et al., *Diagnosis of pulmonary hypertension.* European Respiratory Journal, 2019. **53**(1): p. 1801904.
85. Galie, N., et al., *Guidelines on diagnosis and treatment of pulmonary arterial hypertension. The Task Force on Diagnosis and Treatment of Pulmonary Arterial Hypertension of the European Society of Cardiology.* European Heart Journal, 2004. **25**(24): p. 2243-78.
86. Hoeper, M.M., *Definition, classification, and epidemiology of pulmonary arterial hypertension.* Seminars in Respiratory and Critical Care Medicine, 2009. **30**(4): p. 369-375.
87. Galie, N., et al., *Guidelines for the diagnosis and treatment of pulmonary hypertension: The Task Force for the Diagnosis and Treatment of Pulmonary Hypertension of the European Society of Cardiology (ESC) and the European Respiratory Society (ERS), endorsed by the International Society of Heart and Lung Transplantation (ISHLT).* European Heart Journal, 2009. **30**(20): p. 2493-2537.
88. Naeije, R., et al., *Exercise-induced pulmonary hypertension: Physiological basis and methodological concerns.* American Journal of Respiratory and Critical Care Medicine, 2013. **187**(6): p. 576-583.
89. Kovacs, G. and H. Olschewski, *Advancing into the details of pulmonary haemodynamics during exercise.* European Respiratory Journal, 2018. **52**(3): p. 1801578.
90. Herve, P., et al., *Criteria for diagnosis of exercise pulmonary hypertension.* European Respiratory Journal, 2015. **46**(3): p. 728-737.
91. Ho, J.E., et al., *Exercise Pulmonary Hypertension Predicts Clinical Outcomes in Patients With Dyspnea on Effort.* Journal of the American College of Cardiology, 2020. **75**(1): p. 17-26.
92. Eisman, A.S., et al., *Pulmonary Capillary Wedge Pressure Patterns During Exercise Predict Exercise Capacity and Incident Heart Failure.* Circulation: Heart Failure, 2018. **11**(5): p. e004750.
93. Zeder, K., et al., *Diagnostic, prognostic and differential-diagnostic relevance of pulmonary hemodynamics during exercise - a systematic review.* European Respiratory Journal, 2022. **60**(4): p. 2103181.

94. Cherneva, R.V., S.V. Denchev, and Z.V. Cherneva, *Cardio-pulmonary-exercise testing, stress-induced right ventricular diastolic dysfunction and exercise capacity in non-severe chronic obstructive pulmonary disease.* Pulmonology, 2021. **27**(3): p. 194-207.
95. Christensen, C.C., *Relationship between exercise desaturation and pulmonary haemodynamics in COPD patients.* European Respiratory Journal, 2004. **24**(4): p. 580-586.
96. Skjørten, I., et al., *Exercise capacity in COPD patients with exercise-induced pulmonary hypertension.* International Journal of COPD, 2018. **13**: p. 3599-3610.
97. Portillo, K., et al., *Pulmonary hemodynamic profile in chronic obstructive pulmonary disease.* International Journal of COPD, 2015. **10**: p. 1313-1320.
98. Hilde, J.M., et al., *Haemodynamic responses to exercise in patients with COPD.* European Respiratory Journal, 2013. **41**(5): p. 1031-1041.
99. Hager, W.D., et al., *Exercise during cardiac catheterization distinguishes between pulmonary and left ventricular causes of dyspnea in systemic sclerosis patients.* Clinical Respiratory Journal, 2013. **7**(3): p. 227-236.
100. Saggar, R.R., et al., *Exercise-induced pulmonary hypertension associated with systemic sclerosis: Four distinct entities.* Arthritis Care and Research, 2010. **62**(12): p. 3741-3750.
101. Miyanaga, S., et al., *Predictors of exercise-induced pulmonary hypertension in patients with connective tissue disease.* Heart and Vessels, 2019. **34**(9): p. 1509-1518.
102. Quinn, K.A., et al., *Exercise Echocardiography Predicts Future Development of Pulmonary Hypertension in a High-risk Cohort of Patients with Systemic Sclerosis.* The Journal of Rheumatology, 2020. **47**(5): p. 708-713.
103. Zeder, K., et al., *Exercise Pulmonary Resistances Predict Long-Term Survival in Systemic Sclerosis.* Chest, 2021. **159**(2): p. 781-790.
104. Dean, N.C., et al., *Oxygen may improve dyspnea and endurance in patients with chronic obstructive pulmonary disease and only mild hypoxemia.* American Review of Respiratory Disease, 1992. **146**(4): p. 941-5.
105. Himelman, R.B., et al., *Noninvasive evaluation of pulmonary artery pressure during exercise by saline-enhanced Doppler echocardiography in chronic pulmonary disease.* Circulation, 1989. **79**(4): p. 863-871.
106. Sadaniantz, A., A. Katz, and W.-C. Wu, *Miscellaneous Use of Exercise Echocardiography in Patients with Chronic Pulmonary Disease or Congenital Heart Defect.* Echocardiography, 2004. **21**(5): p. 477-484.
107. Cherneva, R.V., et al., *Stress echocardiography for left ventricular diastolic dysfunction detection in patients with non-severe chronic obstructive pulmonary disease: a cross-sectional study.* Croatian Medical Journal, 2019. **60**(5): p. 449-457.
108. Cherneva, R., S. Denchev, and Z. Cherneva, *The 'right way' to the left chamber in non-severe COPD: Echocardiographic predictors for stress-induced left ventricular diastolic dysfunction.* Archives of the Turkish Society of Cardiology, 2020. **48**(4): p. 380-391.
109. Alkotob, M.L., et al., *Reduced exercise capacity and stress-induced pulmonary hypertension in patients with scleroderma.* Chest, 2006. **130**(1): p. 176-181.
110. Steen, V., et al., *Exercise-induced pulmonary arterial hypertension in patients with systemic sclerosis.* Chest, 2008. **134**(1): p. 146-151.
111. Baptista, R., et al., *Exercise-Induced Pulmonary Hypertension in Scleroderma Patients: A Common Finding but with Elusive Pathophysiology.* Echocardiography, 2013. **30**(4): p. 378-384.
112. Gargani, L., et al., *Clinical and echocardiographic correlations of exercise-induced pulmonary hypertension in systemic sclerosis: A multicenter study.* American Heart Journal, 2013. **165**(2): p. 200-207.

113. Voilliot, D., et al., *Determinants of exercise-induced pulmonary arterial hypertension in systemic sclerosis.* International Journal of Cardiology, 2014. **173**: p. 373-379.
114. Ojima, S., et al., *Significant Clinical Indexes of Exercise-Induced Pulmonary Hypertension in Patients With Connective Tissue Disease.* Circulation reports, 2019. **1**(12): p. 610-616.
115. Baptista, R., et al., *Exercise echocardiography for the assessment of pulmonary hypertension in systemic sclerosis: A systematic review.* Arthritis Research and Therapy, 2016. **18**(1): p. 153.
116. Kusunose, K., et al., *Prediction of future overt pulmonary hypertension by 6-min walk stress echocardiography in patients with connective tissue disease.* Journal of the American College of Cardiology, 2015. **66**(4): p. 376-384.
117. Greiner, S., et al., *Reliability of noninvasive assessment of systolic pulmonary artery pressure by doppler echocardiography compared to right heart catheterization: Analysis in a large patient population.* Journal of the American Heart Association, 2014. **3**(4): p. e001103.
118. Cordina, R.L., et al., *State-of-the-Art Review: Echocardiography in Pulmonary Hypertension.* Heart Lung and Circulation, 2019. **28**(9): p. 1351-1364.
119. Fisher, M.R., et al., *Accuracy of Doppler Echocardiography in the Hemodynamic Assessment of Pulmonary Hypertension.* American Journal of Respiratory and Critical Care Medicine, 2009. **179**(7): p. 615-621.
120. Nathan, S.D., et al., *Right ventricular systolic pressure by echocardiography as a predictor of pulmonary hypertension in idiopathic pulmonary fibrosis.* Respiratory Medicine, 2008. **102**(9): p. 1305-1310.
121. Rudski, L.G., et al., *Guidelines for the echocardiographic assessment of the right heart in adults: a report from the American Society of Echocardiography endorsed by the European Association of Echocardiography, a registered branch of the European Society of Cardiology, and the Canadian Society of Echocardiography.* Journal of the American Society of Echocardiography, 2010. **23**(7): p. 685-688.
122. Karas, M.G. and J.R. Kizer, *Echocardiographic assessment of the right ventricle and associated hemodynamics.* Progress in Cardiovascular Diseases, 2012. **55**(2): p. 144-160.
123. Wang, Z., et al., *[Association between echocardiography derived right ventricular function parameters with cardiac magnetic resonance derived right ventricular ejection fraction and 6-minute walk distance in pulmonary hypertension patients].* Zhonghua Xin Xue Guan Bing Za Zhi, 2014. **42**(9): p. 748-52.
124. Li, Y.D., et al., *Relationship between echocardiographic and cardiac magnetic resonance imaging-derived measures of right ventricular function in patients with chronic thromboembolic pulmonary hypertension.* Thrombosis Research, 2015. **135**(4): p. 602-6.
125. Ghio, S., et al., *Prognostic relevance of the echocardiographic assessment of right ventricular function in patients with idiopathic pulmonary arterial hypertension.* International Journal of Cardiology, 2010. **140**(3): p. 272-8.
126. Ameloot, K., et al., *Clinical value of echocardiographic doppler-derived right ventricular dp/dt in patients with pulmonary arterial hypertension.* European Heart Journal Cardiovascular Imaging, 2014. **15**(12): p. 1411-1419.
127. Badagliacca, R., et al., *Echocardiography Combined With Cardiopulmonary Exercise Testing for the Prediction of Outcome in Idiopathic Pulmonary Arterial Hypertension.* Chest, 2016. **150**(6): p. 1313-1322.
128. Forfia, P.R., et al., *Tricuspid annular displacement predicts survival in pulmonary hypertension.* American Journal of Respiratory and Critical Care Medicine, 2006. **174**(9): p. 1034-41.
129. Brierre, G., et al., *New echocardiographic prognostic factors for mortality in pulmonary arterial hypertension †.* European Journal of Echocardiography, 2010. **11**(6): p. 516-522.

130. Saito, C., et al., *Prognostic impact of right ventricular function affected by pulmonary hypertension in hospitalized heart failure patients.* Journal of Cardiology, 2022. **79**(3): p. 376-384.
131. Gorter, T.M., et al., *Right ventricular dysfunction in heart failure with preserved ejection fraction: a systematic review and meta-analysis.* European Journal of Heart Failure, 2016. **18**(12): p. 1472-1487.
132. Prins, K.W., et al., *Clinical Determinants and Prognostic Implications of Right Ventricular Dysfunction in Pulmonary Hypertension Caused by Chronic Lung Disease.* Journal of the American Heart Association, 2019. **8**(2): p. e011464.
133. Burgess, M.I., et al., *Comparison of echocardiographic markers of right ventricular function in determining prognosis in chronic pulmonary disease.* Journal of the American Society of Echocardiography, 2002. **15**(6): p. 633-639.
134. Moceri, P., et al., *Echocardiographic predictors of outcome in Eisenmenger syndrome.* Circulation, 2012. **126**(12): p. 1461-1468.
135. Manca, P., et al., *The right ventricular involvement in dilated cardiomyopathy: prevalence and prognostic implications of the often-neglected child.* Heart Failure Reviews, 2022. **27**(5): p. 1795-1805.
136. Ruan, Q. and S.F. Nagueh, *Clinical application of tissue Doppler imaging in patients with idiopathic pulmonary hypertension.* Chest, 2007. **131**(2): p. 395-401.
137. D'Andrea, A., et al., *Right Ventricular Structure and Function in Idiopathic Pulmonary Fibrosis with or without Pulmonary Hypertension.* Echocardiography, 2016. **33**(1): p. 57-65.
138. Hilde, J.M., et al., *Right ventricular dysfunction and remodeling in chronic obstructive pulmonary disease without pulmonary hypertension.* Journal of the American College of Cardiology, 2013. **62**(12): p. 1103-1111.
139. Fukuda, Y., et al., *Utility of combining assessment of right ventricular function and right atrial remodeling as a prognostic factor for patients with pulmonary hypertension.* The International Journal of Cardiovascular Imaging, 2014. **30**(7): p. 1269-1277.
140. Nagueh, S.F., et al., *Recommendations for the Evaluation of Left Ventricular Diastolic Function by Echocardiography: An Update from the American Society of Echocardiography and the European Association of Cardiovascular Imaging.* Journal of the American Society of Echocardiography, 2016. **29**(4): p. 277-314.
141. Zaidi, A., et al., *Echocardiographic assessment of the right heart in adults: a practical guideline from the British Society of Echocardiography.* Echo Research & Practice, 2020. **7**(1): p. G19-G41.
142. Kosmala, W., et al., *Right Ventricular Dysfunction in Asymptomatic Diabetic Patients.* Diabetes Care, 2004. **27**(11): p. 2736-2738.
143. Kosar, F., et al., *Usefulness of Pulsed-Wave Tissue Doppler Echocardiography for the Assessment of the Left and Right Ventricular Function in Patients with Clinical Hypothyroidism.* Echocardiography, 2006. **23**(6): p. 471-477.
144. Al-Biltagi, M., et al., *Tissue Doppler, speckling tracking and four-dimensional echocardiographic assessment of right ventricular function in children with dilated cardiomyopathy.* World Journal of Clinical Pediatrics, 2022. **11**(1): p. 71-84.
145. Meune, C., et al., *A right ventricular diastolic impairment is common in systemic sclerosis and is associated with other target-organ damage.* Seminars in Arthritis and Rheumatism, 2016. **45**(4): p. 439-445.
146. Agoston-Coldea, L., et al., *Right atrium volume index in patients with secondary pulmonary hypertension due to chronic obstructive pulmonary disease.* Acta Cardiologica Sinica, 2015. **31**(4): p. 325-336.

147. Seyfeli, E., et al., *Right ventricular diastolic abnormalities in rheumatoid arthritis and its relationship with left ventricular and pulmonary involvement. A tissue Doppler echocardiographic study.* The International Journal of Cardiovascular Imaging, 2006. **22**(6): p. 745-754.
148. Ozdemirel, T.S., et al., *Effects of right ventricular dysfunction on exercise capacity and quality of life and associations with serum NT-proBNP levels in COPD: an observational study.* The Anatolian Journal of Cardiology, 2014. **14**(4): p. 370-347.
149. Huez, S., et al., *Isolated right ventricular dysfunction in systemic sclerosis: Latent pulmonary hypertension?* European Respiratory Journal, 2007. **30**(5): p. 928-936.
150. Mor-Avi, V., et al., *Current and evolving echocardiographic techniques for the quantitative evaluation of cardiac mechanics: ASE/EAE consensus statement on methodology and indications endorsed by the Japanese Society of Echocardiography.* European Journal of Echocardiography, 2011. **12**(3): p. 167-205.
151. Li, Y., et al., *Right ventricular regional and global systolic function is diminished in patients with pulmonary arterial hypertension: a 2-dimensional ultrasound speckle tracking echocardiography study.* The International Journal of Cardiovascular Imaging, 2013. **29**(3): p. 545-551.
152. Fukuda, Y., et al., *Utility of Right Ventricular Free Wall Speckle-Tracking Strain for Evaluation of Right Ventricular Performance in Patients with Pulmonary Hypertension.* Journal of the American Society of Echocardiography, 2011. **24**(10): p. 1101-1108.
153. Morris, D.A., et al., *Normal range and usefulness of right ventricular systolic strain to detect subtle right ventricular systolic abnormalities in patients with heart failure: a multicentre study.* European Heart Journal – Cardiovascular Imaging, 2017. **18**(2): p. 212-223.
154. Rice, J.L., et al., *Speckle Tracking Echocardiography to Evaluate for Pulmonary Hypertension in Chronic Obstructive Pulmonary Disease.* COPD: Journal of Chronic Obstructive Pulmonary Disease, 2016. **13**(5): p. 595-600.
155. Sachdev, A., et al., *Right ventricular strain for prediction of survival in patients with pulmonary arterial hypertension.* Chest, 2011. **139**(6): p. 1299-1309.
156. Gavazzoni, M., et al., *Prognostic value of right ventricular free wall longitudinal strain in a large cohort of outpatients with left-side heart disease.* European Heart Journal - Cardiovascular Imaging, 2020. **21**(9): p. 1013-1021.
157. Tadic, M., et al., *Right ventricular strain in heart failure: Clinical perspective.* Archives of Cardiovascular Diseases, 2017. **110**(10): p. 562-571.
158. Fine, N.M., et al., *Outcome Prediction by Quantitative Right Ventricular Function Assessment in 575 Subjects Evaluated for Pulmonary Hypertension.* Circulation: Cardiovascular Imaging, 2013. **6**(5): p. 711-721.
159. Hardegree, E.L., et al., *Role of Serial Quantitative Assessment of Right Ventricular Function by Strain in Pulmonary Arterial Hypertension.* The American Journal of Cardiology, 2013. **111**(1): p. 143-148.
160. Kanar, B.G., et al., *Right Ventricular Functional Improvement after Pulmonary Rehabilitation Program in Patients with COPD Determined by Speckle Tracking Echocardiography.* Arquivos Brasileiros de Cardiologia, 2018. **111**(3): p. 375-381.
161. Hoit, B.D., *Left atrial size and function: Role in prognosis.* Journal of the American College of Cardiology, 2014. **63**(6): p. 493-505.
162. Douglas, P.S., *The left atrium: a biomarker of chronic diastolic dysfunction and cardiovascular disease risk.* Journal of the American College of Cardiology, 2003. **42**(7): p. 1206-1207.
163. Tadic, M., *The right atrium, a forgotten cardiac chamber: An updated review of multimodality imaging.* Journal of Clinical Ultrasound, 2015. **43**(6): p. 335-345.

164. Gaynor, S.L., et al., *Reservoir and conduit function of right atrium: impact on right ventricular filling and cardiac output.* American Journal of Physiology-Heart and Circulatory Physiology, 2005. **288**(5): p. H2140-5.
165. Rai, A.B.S., et al., *Speckle tracking echocardiography of the right atrium: The neglected chamber.* Clinical Cardiology, 2015. **38**(11): p. 692-697.
166. Alenezi, F., S. Rajagopal, and S. Kutty, *Assessing right atrial function in pulmonary hypertension: window to the soul of the right heart?* American Journal of Physiology-Heart and Circulatory Physiology, 2020. **318**(1): p. H154-H155.
167. Gaynor, S.L., et al., *Right atrial and ventricular adaptation to chronic right ventricular pressure overload.* Circulation, 2005. **112**(9 Suppl): p. 212-218.
168. Lang, R.M., et al., *Recommendations for cardiac chamber quantification by echocardiography in adults: an update from the American Society of Echocardiography and the European Association of Cardiovascular Imaging.* Journal of the American Society of Echocardiography, 2015. **28**(1): p. 1-39 e14.
169. Ebtia, M., et al., *Best method for right atrial volume assessment by two-dimensional echocardiography: Validation with magnetic resonance imaging.* Echocardiography, 2015. **32**(5): p. 734-739.
170. Takahashi, A., et al., *Quantitative evaluation of right atrial volume and right atrial emptying fraction by 320-slice computed tomography compared with three-dimensional echocardiography.* International Journal of Cardiology, 2011. **146**(1): p. 96-99.
171. Moreno, J., et al., *Right atrial indexed volume in healthy adult population: Reference values for two-dimensional and three-dimensional echocardiographic measurements.* Echocardiography, 2013. **30**(6): p. 667-671.
172. Peluso, D., et al., *Right atrial size and function assessed with three-dimensional and speckle-tracking echocardiography in 200 healthy volunteers.* European Heart Journal Cardiovascular Imaging, 2013. **14**(11): p. 1106-1114.
173. Müller, H., et al., *Measurement of right atrial volumes: Comparison of a semi-automatic algorithm of real-time 3D echocardiography with cardiac magnetic resonance imaging.* International Journal of Cardiology, 2016. **202**: p. 621-623.
174. Keller, A.M., A.S. Gopal, and D.L. King, *Left and Right Atrial Volume by Freehand Three-dimensional Echocardiography: In Vivo Validation Using Magnetic Resonance Imaging.* European Journal of Echocardiography, 2000. **1**(1): p. 55-65.
175. Almodares, Q., et al., *Larger right atrium than left atrium is associated with all-cause mortality in elderly patients with heart failure.* Echocardiography, 2017. **34**(5): p. 662-667.
176. Chow, V., et al., *Right atrial to left atrial area ratio on early echocardiography predicts long-term survival after acute pulmonary embolism.* Cardiovascular Ultrasound, 2013. **11**: p. 17.
177. Limongelli, G., et al., *Clinical and genetic characterization of patients with hypertrophic cardiomyopathy and right atrial enlargement.* Journal of Cardiovascular Medicine, 2017. **18**(4): p. 249-254.
178. Marra, A.M., et al., *Change of right heart size and function by long-term therapy with riociguat in patients with pulmonary arterial hypertension and chronic thromboembolic pulmonary hypertension.* International Journal of Cardiology, 2015. **195**: p. 19-26.
179. Kelly, N.F.A., et al., *The Relative Atrial Index (RAI)-A Novel, Simple, Reliable, and Robust Transthoracic Echocardiographic Indicator of Atrial Defects.* Journal of the American Society of Echocardiography, 2010. **23**(3): p. 275-281.
180. Altes, A., et al., *Impact of Increased Right Atrial Size on Long-Term Mortality in Patients With Heart Failure Receiving Cardiac Resynchronization Therapy.* American Journal of Cardiology, 2019. **123**(6): p. 936-941.

181. Sallach, J.A., et al., *Right Atrial Volume Index in Chronic Systolic Heart Failure and Prognosis.* JACC: Cardiovascular Imaging, 2009. **2**(5): p. 527-534.
182. Ivanov, A., et al., *Right atrial volume by cardiovascular magnetic resonance predicts mortality in patients with heart failure with reduced ejection fraction.* PLoS ONE, 2017. **12**(4): p. e0173245.
183. Proplesch, M., et al., *Right atrial structure and function in patients with hypertension and with chronic heart failure.* Echocardiography, 2018. **35**(7): p. 905-914.
184. Darahim, K., *Usefulness of right atrial volume index in predicting outcome in chronic systolic heart failure.* Journal of the Saudi Heart Association, 2014. **26**(2): p. 73-79.
185. Mysore, M.M., et al., *Right atrial to left atrial volume index ratio is associated with increased mortality in patients with pulmonary hypertension.* Echocardiography, 2018. **35**(11): p. 1729-1735.
186. Bredfelt, A., et al., *Increased right atrial volume measured with cardiac magnetic resonance is associated with worse clinical outcome in patients with pre-capillary pulmonary hypertension.* ESC Heart Failure, 2018. **5**(5): p. 864-875.
187. Querejeta Roca, G., et al., *Right Atrial Function in Pulmonary Arterial Hypertension.* Circulation: Cardiovascular Imaging, 2015. **8**(11): p. e003521.
188. Stefanadis, C., *A clinical appraisal of left atrial function.* European Heart Journal, 2001. **22**(1): p. 22-36.
189. Boyd, A.C. and L. Thomas, *Left atrial volumes : two-dimensional , three- dimensional , cardiac magnetic resonance and computed tomography measurements.* Current Opinion in Cardiology, 2014. **29**(5): p. 408-416.
190. Willens, H.J., et al., *Effects of age and pulmonary arterial hypertension on the different phases of right atrial function.* International Journal of Cardiovascular Imaging, 2008. **24**(7): p. 703-710.
191. Soulat-Dufour, L., et al., *Normal Values of Right Atrial Size and Function According to Age, Sex, and Ethnicity: Results of the World Alliance Societies of Echocardiography Study.* Journal of the American Society of Echocardiography, 2021. **34**(3): p. 286-300.
192. Aune, E., et al., *Normal reference ranges for left and right atrial volume indexes and ejection fractions obtained with real-time three-dimensional echocardiography.* European Journal of Echocardiography, 2009. **10**(6): p. 738-44.
193. Darsaklis, K., et al., *Right atrial emptying fraction non-invasively predicts mortality in pulmonary hypertension.* International Journal of Cardiovascular Imaging, 2016. **32**(7): p. 1121-1130.
194. Brunner, N.W., et al., *Prognostic Utility of Right Atrial Emptying Fractions in Pulmonary Arterial Hypertension.* Pulmonary Circulation, 2015. **5**(3): p. 473-480.
195. Deng, Y., et al., *Right Atrial Evaluation in Patients with Pulmonary Hypertension: A Real-time 3-Dimensional Transthoracic Echocardiographic Study.* Journal of Ultrasound in Medicine, 2016. **35**(1): p. 49-61.
196. Meng, X., et al., *Three-dimensional echocardiography to evaluate right atrial volume and phasic function in pulmonary hypertension.* Echocardiography, 2018. **35**(2): p. 153-161.
197. Kanar, B.G., et al., *Evaluation of right atrial volumes and functions by real-time three-dimensional echocardiography in patients after acute inferior myocardial infarction.* Echocardiography, 2018. **35**(11): p. 1806-1811.
198. Padeletti, M., et al., *Right atrial speckle tracking analysis as a novel noninvasive method for pulmonary hemodynamics assessment in patients with chronic systolic heart failure.* Echocardiography, 2011. **28**(6): p. 658-664.

199. Bhave, N.M., et al., *Right atrial strain is predictive of clinical outcomes and invasive hemodynamic data in group 1 pulmonary arterial hypertension.* The International Journal of Cardiovascular Imaging, 2017. **33**(6): p. 847-855.
200. Fukuda, Y., et al., *Comprehensive Functional Assessment of Right-Sided Heart Using Speckle Tracking Strain for Patients with Pulmonary Hypertension.* Echocardiography, 2016. **33**(7): p. 1001-1008.
201. Sakata, K., et al., *Evaluation of right atrial function using right atrial speckle tracking analysis in patients with pulmonary artery hypertension.* Journal of Echocardiography, 2016. **14**(1): p. 30-38.
202. D'Alto, M., et al., *Right atrial function and prognosis in idiopathic pulmonary arterial hypertension.* International Journal of Cardiology, 2017. **248**: p. 320-325.
203. Bai, Y., et al., *Right atrial function for the prediction of prognosis in connective tissue disease-associated pulmonary arterial hypertension: a study with two-dimensional speckle tracking.* International Journal of Cardiovascular Imaging, 2019. **35**(9): p. 1637-1649.
204. Haghighi, Z.O., et al., *Quantitative assessment of right atrial function by strain and strain rate imaging in patients with heart failure.* Acta Cardiologica, 2011. **66**(6): p. 737-742.
205. Jain, S., et al., *Right Atrial Phasic Function in Heart Failure With Preserved and Reduced Ejection Fraction.* JACC: Cardiovascular Imaging, 2019. **12**(8 Pt 1): p. 1460-1470.
206. Kurt, M., et al., *Left atrial function in diastolic heart failure.* Circulation: Cardiovascular Imaging, 2009. **2**(1): p. 10-15.
207. Porpáczy, A., et al., *Left atrial stiffness is superior to volume and strain parameters in predicting elevated NT-proBNP levels in systemic sclerosis patients.* International Journal of Cardiovascular Imaging, 2019. **35**(10): p. 1795-1802.
208. Zhao, Y., et al., *Left atrial stiffness index as a marker of early target organ damage in hypertension.* Hypertension Research, 2021. **44**(3): p. 299-309.
209. Teixeira, R.R.r., et al., *The relationship between tricuspid regurgitation severity and right atrial mechanics: a speckle tracking echocardiography study.* International Journal of Cardiovascular Imaging, 2015. **31**(6): p. 1125-1135.
210. Vestbo, J., et al., *Global strategy for the diagnosis, management, and prevention of chronic obstructive pulmonary disease: GOLD executive summary.* American Journal of Respiratory and Critical Care Medicine, 2013. **187**(4): p. 347-365.
211. Lang, R.M., et al., *Recommendations for chamber quantification: a report from the American Society of Echocardiography's Guidelines and Standards Committee and the Chamber Quantification Writing Group, developed in conjunction with the European Association of Echocardiography, a branch of the European Society of Cardiology.* Journal of the American Society of Echocardiography, 2005. **18**(12): p. 1440-1463.
212. Nagueh, S.F., et al., *Recommendations for the evaluation of left ventricular diastolic function by echocardiography.* Journal of the American Society of Echocardiography, 2009. **22**(2): p. 107-133.
213. ATS Committee on Proficiency Standards for Clinical Pulmonary Function Laboratories, *ATS statement: guidelines for the six-minute walk test*. American Journal of Respiratory and Critical Care Medicine, 2002. **166**(1): p. 111-117.
214. van den Hoogen, F., et al., *2013 classification criteria for systemic sclerosis: an American college of rheumatology/European league against rheumatism collaborative initiative.* Annals of the Rheumatic Diseases, 2013. **72**(11): p. 1747-1755.
215. Schwaiger, J.P., D. Khanna, and J. Gerry Coghlan, *Screening patients with scleroderma for pulmonary arterial hypertension and implications for other at-risk populations.* European Respiratory Review, 2013. **22**(130): p. 515-525.

216. Badano, L.P., et al., *Standardization of left atrial, right ventricular, and right atrial deformation imaging using two-dimensional speckle tracking echocardiography: A consensus document of the EACVI/ASE/Industry Task Force to standardize deformation imaging.* European Heart Journal Cardiovascular Imaging, 2018. **19**(6): p. 591-600.
217. Cameli, M., et al., *Left atrial strain: a new parameter for assessment of left ventricular filling pressure.* Heart Failure Reviews, 2016. **21**(1): p. 65-76.
218. Vinereanu, D., et al., *"Pure" diastolic dysfunction is associated with long-axis systolic dysfunction. Implications for the diagnosis and classification of heart failure.* European Journal of Heart Failure, 2005. **7**(5): p. 820-828.
219. Watz, H., et al., *Decreasing cardiac chamber sizes and associated heart dysfunction in COPD: role of hyperinflation.* Chest, 2010. **138**(1): p. 32-38.
220. Hannink, J.D., et al., *Heart failure and COPD: partners in crime?* Respirology, 2010. **15**(6): p. 895-901.
221. Falk, J.A., et al., *Cardiac disease in chronic obstructive pulmonary disease.* Proceedings of the. American Thoracic Society, 2008. **5**(4): p. 543-548.
222. Sin, D.D., et al., *Mortality in COPD: Role of comorbidities.* European Respiratory Journal, 2006. **28**(6): p. 1245-1257.
223. Smith, B.M., et al., *Impaired left ventricular filling in COPD and emphysema: is it the heart or the lungs? The Multi-Ethnic Study of Atherosclerosis COPD Study.* Chest, 2013. **144**(4): p. 1143-1151.
224. Sohn, D.W., et al., *Assessment of mitral annulus velocity by Doppler tissue imaging in the evaluation of left ventricular diastolic function.* Journal of the American College of Cardiology, 1997. **30**(2): p. 474-480.
225. Schoos, M.M., et al., *Echocardiographic predictors of exercise capacity and mortality in chronic obstructive pulmonary disease.* BMC Cardiovascular Disorders, 2013. **13**: p. 84.
226. Hammoudi, N., et al., *Left atrial volume predicts abnormal exercise left ventricular filling pressure.* European Journal of Heart Failure, 2014. **16**(10): p. 1089-1095.
227. Do, D.H., et al., *Right atrial size relates to right ventricular end-diastolic pressure in an adult population with congenital heart disease.* Echocardiography, 2011. **28**(1): p. 109-116.
228. Melenovsky, V., et al., *Right heart dysfunction in heart failure with preserved ejection fraction.* European Heart Journal, 2014. **35**(48): p. 3452-3462.
229. Sabit, R., et al., *Sub-clinical left and right ventricular dysfunction in patients with COPD.* Respiratory Medicine, 2010. **104**(8): p. 1171-1178.
230. Rubin, L.J., *Cor pulmonale revisited.* Journal of the American College of Cardiology, 2013. **62**(12): p. 1112-1113.
231. Ataş, H., et al., *Evaluation of left atrial volume and function in systemic sclerosis patients using speckle tracking and real-time three-dimensional echocardiography.* The Anatolian Journal of Cardiology, 2015. **16**(5): p. 316-322.
232. Faludi, R., et al., *Diastolic Dysfunction Is a Contributing Factor to Exercise Intolerance in COPD.* COPD: Journal of Chronic Obstructive Pulmonary Disease, 2016. **13**(3): p. 345-351.
233. Tennoe, A.H., et al., *Left Ventricular Diastolic Dysfunction Predicts Mortality in Patients With Systemic Sclerosis.* Journal of the American College of Cardiology, 2018. **72**(15): p. 1804-1813.
234. Tennøe, A.H., et al., *Systolic Dysfunction in Systemic Sclerosis: Prevalence and Prognostic Implications.* ACR Open Rheumatology, 2019. **1**(4): p. 258-266.
235. Saito, M., et al., *Mechanics and prognostic value of left and right ventricular dysfunction in patients with systemic sclerosis.* European Heart Journal Cardiovascular Imaging, 2018. **19**(6): p. 660-667.

236. Hasselberg, N.E., et al., *The Prognostic Value of Right Atrial Strain Imaging in Patients with Precapillary Pulmonary Hypertension.* Journal of the American Society of Echocardiography, 2021. **34**(8): p. 851-861.e1.
237. D'Andrea, A., et al., *Right atrial morphology and function in patients with systemic sclerosis compared to healthy controls: a two-dimensional strain study.* Clinical Rheumatology, 2016. **35**(7): p. 1733-1742.
238. Karna, S.K., M.K. Rohit, and A. Wanchu, *Right ventricular thickness as predictor of global myocardial performance in systemic sclerosis: A Doppler tissue imaging study.* Indian Heart Journal, 2015. **67**(6): p. 521-528.
239. Lewis, G.D., et al., *Pulmonary vascular hemodynamic response to exercise in cardiopulmonary diseases.* Circulation, 2013. **128**(13): p. 1470-1479.
240. Brand, A., et al., *Right heart function in impaired left ventricular diastolic function: 2D speckle tracking echocardiography–based and Doppler tissue imaging–based analysis of right atrial and ventricular function.* Echocardiography, 2018. **35**(1): p. 47-55.
241. Kuppahally, S.S., et al., *Left atrial strain and strain rate in patients with paroxysmal and persistent atrial fibrillation: Relationship to left atrial structural remodeling detected by delayed-enhancement MRI.* Circulation: Cardiovascular Imaging, 2010. **3**(3): p. 231-239.
242. Her, A.-Y., et al., *Prediction of left atrial fibrosis with speckle tracking echocardiography in mitral valve disease: a comparative study with histopathology.* Korean Circulation Journal, 2012. **42**(5): p. 311-318.
243. Allanore, Y., et al., *N-terminal pro-brain natriuretic peptide is a strong predictor of mortality in systemic sclerosis.* International Journal of Cardiology, 2016. **223**: p. 385-389.
244. Költő, G., et al., *Prognostic value of N-terminal natriuretic peptides in systemic sclerosis: a single centre study.* Clinical and Experimental Rheumatology, 2014. **32**(6 Suppl 86): p. S-75-81.
245. Paik, J.J., et al., *Troponin elevation independently associates with mortality in systemic sclerosis.* Clinical and Experimental Rheumatology, 2022. **40**(10): p. 1933-1940.
246. Sato, S., et al., *Clinical significance of anti-topoisomerase I antibody levels determined by ELISA in systemic sclerosis.* Rheumatology, 2001. **40**(10): p. 1135-1140.
247. van Leeuwen, N.M., et al., *Association Between Centromere- and Topoisomerase-specific Immune Responses and the Degree of Microangiopathy in Systemic Sclerosis.* The Journal of Rheumatology, 2021. **48**(3): p. 402-409.

11 Publications of the author

Original papers and letters

In connection with the topic of the thesis

Nógrádi, Á.; Varga, Z.; Hajdu, M.; Czirják, L.; Komócsi, A.; Faludi, R. Prognostic value of right atrial stiffness in systemic sclerosis. CLINICAL AND EXPERIMENTAL RHEUMATOLOGY 40: 10 pp. 1977-1985. (2022)
Q1 IF≈ 4.862

Nógrádi, Á.; Porpáczy, A.; Porcsa, L.; Minier, T.; Czirják, L.; Komócsi, A.; Faludi, R. Relation of Right Atrial Mechanics to Functional Capacity in Patients With Systemic Sclerosis. AMERICAN JOURNAL OF CARDIOLOGY 122: 7 pp. 1249-1254. (2018)
Q1 IF 2.843

Faludi, R.; Hajdu, M.; Vértes, V.; **Nógrádi, Á.;** Varga, N.; Illés, M.B.; Sárosi, V.; Alexy, G.; Komócsi, A. Diastolic Dysfunction Is a Contributing Factor to Exercise Intolerance in COPD. COPD-JOURNAL OF CHRONIC OBSTRUCTIVE PULMONARY DISEASE 13: 3 pp. 345-351. (2016)
Q1 IF 2.576

Nógrádi, Á.; Faludi, R. A jobb pitvari méret és funkció noninvazív vizsgálatának módszerei és jelentőségük. CARDIOLOGIA HUNGARICA 50: 1 pp. 54-59. (2020).

Not in connection with the topic of the thesis

Vértes, V.; Porpáczy, A.; **Nógrádi, Á.;** Tőkés-Füzesi, M.; Hajdu, M.; Czirják, L.; Komócsi, A.; Faludi, R. Galectin-3 and sST2: associations to the echocardiographic markers of the myocardial mechanics in systemic sclerosis – a pilot study. CARDIOVASCULAR ULTRASOUND 20 : 1 Paper: 1. (2022)
Q2 IF 2.263

Ezer, P.; Kálmán, E.; **Nógrádi, Á.;** Vértes, V.; Cziráki, A.; Faludi, R. Chloroquin indukálta cardiomyopathia avagy a „pszeudo-Fabry-kór" fatális lefolyású esete. CARDIOLOGIA HUNGARICA 52: 1 pp. 38-44. (2022)

Hajdu, M.; Krämer, K.; Vértes, V.; **Nógrádi, Á.;** Varga, N.; Illés, M.B.; Sárosi, V.; Faludi, R. Krónikus obstruktív tüdőbetegségben a bal kamra diasztolés funkciózavara gyakori és rossz prognózissal társul. CARDIOLOGIA HUNGARICA 50 pp. 410-416. (2020)

Porpáczy, A.; **Nógrádi, Á.;** Vértes, V.; Tőkés-Füzesi, M.; Czirják, L.; Komócsi, A.; Faludi, R. Left atrial stiffness is superior to volume and strain parameters in predicting elevated NT-proBNP levels in systemic sclerosis patients. INTERNATIONAL JOURNAL OF CARDIOVASCULAR IMAGING 35: 10 pp. 1795-1802. (2019)
Q2 IF 1.969

Vértes, V.; **Nógrádi, Á.;** Porpáczy, A.; Minier, T.; Czirják, L.; Komócsi, A.; Faludi, R. A bal kamrai globális longitudinális strain károsodott szisztémás szklerózisban és korrelál a betegek funkcionális kapacitásával. CARDIOLOGIA HUNGARICA 49: 1 pp. 12-16. (2019)

Porpáczy, A.; **Nógrádi, Á.;** Kehl, D.; Strenner, M.; Minier, T.; Czirják, L.; Komócsi, A; Faludi, R. Impairment of the Left Atrial Mechanics is an Early Sign of the Myocardial Involvement in Systemic Sclerosis. JOURNAL OF CARDIAC FAILURE 24: 4 pp. 234-242. (2018)
Q1 IF 3.967

Cumulative impact factor: 18.480

Independent citations: 56

Citable abstracts

In connection with the topic of the thesis

Nógrádi , Á.; Varga, Zs.; Szebényi, D.; Porpáczy, A.; Vértes, V.; Czirják, L.; Komócsi, A.; Faludi, R. Prognostic role of right ventricular and atrial mechanics in systemic sclerosis. In: Kajos, Luca Fanni; Bali, Cintia; Preisz, Zsolt; Polgár, Petra; Glázer-Kniesz, Adrienn; Tislér, Ádám; Szabó, Rebeka (szerk.) 10th Jubilee Interdisciplinary Doctoral Conference: Book of Abstracts. Pécsi Tudományegyetem Doktorandusz Önkormányzat p. 25. (2021)

Nógrádi, Á.; Varga, Z.; Szebényi, D.; Porpáczy, A.; Vértes, V.; Czirják, L; Komócsi, A.; Faludi, R. Prognostic role of right ventricular and atrial mechanics in systemic sclerosis. EUROPEAN HEART JOURNAL 41: Suppl. 2 p. 106. (2020)

Nógrádi, Á.; Varga, Zs.; Szebényi, D.; Porpáczy, A.; Vértes, V.; Czirják, L.; Komócsi, A.; Faludi, R. A jobb kamra és pitvar funkcióját jellemző echokardiográfiás paraméterek prognosztikus szerepe sclerodermás populációban. CARDIOLOGIA HUNGARICA 50: Suppl. D pp. 158-159. (2020)

Nógrádi, Á.; Porpáczy, A.; Molnár, F.; Minier, T.; Czirják, L.; Komócsi, A.; Faludi, R. A speckle tracking alapú jobb pitvari strain paraméterek jól korrelálnak a fázisos pitvari volumen indexekkel systemás sclerosisos betegekben. CARDIOLOGIA HUNGARICA 48: Suppl. C p. C23 (2018)

Nógrádi, Á; Porpáczy, A.; Molnár, F.; Minier, T.; Czirják, L.; Komócsi, A.; Faludi, R. Speckle tracking derived right atrial strain parameters show strong correlation with phasic volume indices in systemic sclerosis patients. EUROPEAN HEART JOURNAL 38: Suppl. pp. 1092-1093. (2017)

Nógrádi, Á.; Porpáczy, A.; Molnár, F.; Minier, T.; Czirják, L.; Komócsi, A. Faludi, R. A jobb pitvari stiffness a funkcionális kapacitás meghatározója systemás sclerosisos betegekben. CARDIOLOGIA HUNGARICA 47: Suppl. C p. C3. (2017)

Nógrádi, Á.; Porcsa, L.; Minier, T.; Czirják, L.; Komócsi, A.; Faludi, R. Determinants of the right atrial mechanics in systemic sclerosis (P1436) EUROPEAN HEART JOURNAL 37: 1. Suppl. p. 258. (2016)

Nógrádi, Á.; Porpáczy, A.; Porcsa, L.; Minier, T.; Czirják, L.; Komócsi, A.; Faludi, R. Echocardiographic determinants of the functional capacity in systemic sclerosis: role of the right heart. EUROPEAN HEART JOURNAL-CARDIOVASCULAR IMAGING 17: Suppl. 2 p. ii279. (2016)

Nógrádi, Á.; Porcsa, L.; Minier, T.; Czirják, L.; Komócsi, A.; Faludi, R. A jobb pitvari funkció meghatározó tényezői szisztémás szklerózisos betegekben. CARDIOLOGIA HUNGARICA 46: Suppl. F p. 4. (2016)

Not in connection with the topic of the thesis

Vértes, V.; Porpáczy, A.; **Nógrádi, Á.;** Hajdu, M.; Czirják, L.; Komócsi, A.; Faludi, R. Echocardiographic markers of the myocardial involvement are related to the physical functioning dimension of SF-36 health survey in systemic sclerosis. EUROPEAN JOURNAL OF HEART FAILURE 24 pp. 76-77. (2022)

Vértes, V.; Tőkés-Fuzesi, M.; Porpáczy, A.; **Nógrádi, Á.;** Czirják, L.; Komócsi, A.; Faludi, R. Circulating biomarkers of cardiac fibrosis: do they correlate with the echocardiographic parameters of the myocardial mechanics in systemic sclerosis? EUROPEAN HEART JOURNAL-CARDIOVASCULAR IMAGING 22: Suppl. 1 p. i149 (2021)

Vértes, V.; Nochta, A.; Porpáczy, A.; **Nógrádi, Á.;** Czirják, L.; Komócsi, A.; Faludi, R. A szívizom érintettséget tükröző echokardiográfiás paraméterek korrelációt mutatnak az SF-36 életminőség kérdőív „fizikai funkció" pontszámával szklerodermás betegekben = Echocardiographic markers of the myocardial involvement are related to the physical functioning dimension of SF-36 health survey in systemic sclerosis. CARDIOLOGIA HUNGARICA 51: Suppl. B pp. B224-B225. (2021)

Kengyelné, Fődi E.; **Nógrádi, Á.;** Tóth, L.; Simor, T.; Faludi, R. Progresszív szívbetegség a benignusnak látszó palpitációs panaszok mögött: esetismertetés. CARDIOLOGIA HUNGARICA 50: Suppl. D pp. 203-204. (2020)

Vértes, V.; Tőkés-Füzesi, M.; Porpáczy, A.; **Nógrádi, Á.;** Czirják, L.; Komócsi, A.; Faludi, R. A szívizom fibrózis keringő biomarkerei mutatnak-e összefüggést a miokardiális funkciót jellemző echokardiográfiás paraméterekkel szisztémás szklerózisban? CARDIOLOGIA HUNGARICA 50: Suppl. D p. 159. (2020)

Porpáczy, A.; **Nógrádi, Á.;** Vértes, V.; Tőkés-Füzesi, M.; Czirják, L.; Komócsi, A.; Faludi, R. A bal pitvari stiffness hatékonyabb az emelkedett NT-proBNP szint azonosításában szisztémás szklerózisban szenvedő betegekben, mint a volumen és strain paraméterek. CARDIOLOGIA HUNGARICA 49: Suppl. B pp. B116-B117. (2019)

Hepp, T.; Zsigmond, Á.; Kis, E.; Maláti, É.; Pere, T.; Szukits, S; Tóth, L.; Faludi, R.; **Nógrádi, Á.;** Cziráki, A. et al. Mitrális műbillentyű endocarditis diagnózisa 3D renderelt szív CT képekkel alátámasztva CARDIOLOGIA HUNGARICA 48: Suppl. C p. C47 (2018)

Vértes, V.; Porcsa, L.; Strenner, M.; **Nógrádi, Á.;** Porpáczy, A.; Minier, T.; Czirják, L.; Komócsi, A.; Faludi, R. A galectin-3 szérum szintje korrelál a bal kamrai globális longitudinális strain értékekkel systemás sclerosisban. CARDIOLOGIA HUNGARICA 48: Suppl. C p. C24 (2018)

Porpáczy, A.; **Nógrádi, Á.;** Varga N.; Minier, T.; Czirják, L. ; Komócsi, A.; Faludi, R. Left atrial stiffness is a robust predictor of the elevated NT-proBNP levels in systemic sclerosis patients with preserved left ventricular ejection fraction. EUROPEAN HEART JOURNAL 38: Suppl. 1 p. 422 Paper: P2076 (2017)

Porpáczy, A.; **Nógrádi, Á.;** Strenner, M.; Minier, T.; Czirják, L.; Komócsi, A. ; Faludi, R. A bal pitvari stiffness meghatározói systemás sclerosisos betegekben CARDIOLOGIA HUNGARICA 47: Suppl. C p. C66. (2017)

Vértes, V.; Porcsa, L. ; Strenner M.; **Nógrádi, Á.;** Porpáczy, A.; Minier, T. ; Czirják, L.; Komócsi, A.; Faludi, R. Galectin-3 levels correlate with left ventricular global longitudinal strain in systemic

sclerosis patients. EUROPEAN HEART JOURNAL-CARDIOVASCULAR IMAGING 18: Suppl. 3 p. iii112-iii113. (2017)

Vértes, V.; Porcsa, L. ; Strenner, M.; **Nógrádi, Á. ;** Porpáczy, A.; Minier, T.; Czirják, L.; Komócsi, A.; Faludi, R. A galectin-3 szérumszintje korrelál a bal kamrai globális longitudinális strain értékekkel systemás sclerosisban. In: Bódog, Ferenc; Csiszár, Beáta; Hegyi, Dávid; Pónusz, Róbert (szerk.) DKK17-Doktoranduszok a Klinikai Kutatásokban absztraktkötet. Pécs, Magyarország: Pécsi Tudományegyetem Doktorandusz Önkormányzat (2017): p. 12.

Vértes, V.; **Nógrádi, Á.;** Porpáczy, A.; Minier, T.; Czirják, L.; Komócsi, A.; Faludi, R. A globális longitudinális strain alkalmas a subklinikus bal kamrai funkciózavar kimutatására systemás sclerosisban. CARDIOLOGIA HUNGARICA 47: Suppl. C p. C4. (2017)

Porpáczy, A.; **Nógrádi, Á**.; Strenner, M.; Minier, T.; Czirják; A.; Komócsi, A.; Faludi, R. Determinants of the left atrial stiffness in systemic sclerosis. EUROPEAN HEART JOURNAL-CARDIOVASCULAR IMAGING 17: Suppl. 2 p. ii243. (2016)

Porpáczy, A; **Nógrádi, Á.;** Strenner, M. ; Minier, T.; Czirják, L.; Komócsi, A.; Faludi, R. Left ventricular diastolic function is a determinant of the left atrial mechanics in systemic sclerosis. EUROPEAN HEART JOURNAL 37: S1 p. 261. Paper: P1446 . (2016)

Porpáczy, A.; **Nógrádi, Á.;** Strenner, M.; Minier, T.; Czirják, L.; Komócsi, A.; Faludi, R. A bal pitvari funkció összefüggést mutat a bal kamrai diasztolés funkcióval szisztémás szklerózisos betegekben. CARDIOLOGIA HUNGARICA 46: Suppl. F pp. 4-5. (2016)

Vértes, V.; **Nógrádi, Á.;** Porpáczy, A.; Minier, T.; Czirják, L.; Komócsi, A.; Faludi, R. Global longitudinal strain is a suitable tool to unmask the subclinical left ventricular dysfunction in patients with systemic sclerosis. EUROPEAN HEART JOURNAL-CARDIOVASCULAR IMAGING 17: Suppl. 2 p. ii177. (2016)

Nógrádi, Á.; Kónyi, A.; Cziráki, A.; Szabados, S.; Faludi, R. Iszkémiás DCM-es beteg eredményes kezelése külső ellenpulzációs pumpával. CARDIOLOGIA HUNGARICA 45: Suppl. D p. D62 (2015)

Nógrádi, Á.; Faludi, R.; Cziráki, A.; Szabados, S. Mellkasi irradiatio késői cardialis szövődményei. CARDIOLOGIA HUNGARICA 44: Suppl. E p. E5. (2014)

Nógrádi , Á.; Faludi, R.; Fődi, E.; Szűcs, A.; Tóth, A.; Szabados, S.; Simor, T. Trouble never comes alone- case of left ventricular noncompaction complicated by bicuspid aortic valve. EUROPEAN JOURNAL OF HEART FAILURE 11: S1 p. S78 (2012)

Nógrádi, Á.; Faludi, R.; Fődi, E.; Szűcs, A.; Tóth, A.; Szabados, S.; Simor, T. A baj nem jár egyedül... - Noncompact cardiomyopathia bicuspidalis aorta billentyűvel szövődött esete. CARDIOLOGIA HUNGARICA 42: Suppl. A p. A109 (2012)

12 Acknowledgments

I would like to express my gratitude to all who supported me throughout my research and work on this doctoral thesis.

First of all, my heartfelt thanks to my supervisor, Dr. Réka Faludi, for her guidance, teaching and her unfailing support. Her dedication and high standards have been a formative example to me throughout my clinical and scientific career. Without her, this work could not have been realized.

I would like to express my thanks to Prof. Dr. Attila Cziráki, the present Chair of the Heart Institute as well as Prof. Dr. Lajos Papp and Prof. Dr. Sándor Szabados, previous Chairs of the Heart Institute for providing the opportunity for my clinical work and to do my research and write my thesis.

The longstanding collaboration with Prof. Dr. László Czirják and Dr. Tünde Minier from the Rheumatology and Immunology Department provided the opportunity to recruit the systemic sclerosis patients and to collect the clinical data on their disease. I would like to express my gratitude to them.

I am deeply grateful to the community of colleagues, doctors, nurses and assistants in the Heart Institute who accompanied, assisted and supported me throughout my working and research career.

Last but not least, the love and encouragement of my husband and my family was an invaluable help. Without their support this work would not have been possible.

COPD: Journal of Chronic Obstructive Pulmonary Disease

ISSN: 1541-2555 (Print) 1541-2563 (Online) Journal homepage: https://www.tandfonline.com/loi/icop20

Diastolic Dysfunction Is a Contributing Factor to Exercise Intolerance in COPD

Réka Faludi, Máté Hajdu, Vivien Vértes, Ágnes Nógrádi, Noémi Varga, Miklós Balázs Illés, Veronika Sárosi, György Alexy & András Komócsi

To cite this article: Réka Faludi, Máté Hajdu, Vivien Vértes, Ágnes Nógrádi, Noémi Varga, Miklós Balázs Illés, Veronika Sárosi, György Alexy & András Komócsi (2016) Diastolic Dysfunction Is a Contributing Factor to Exercise Intolerance in COPD, COPD: Journal of Chronic Obstructive Pulmonary Disease, 13:3, 345-351, DOI: 10.3109/15412555.2015.1084614

To link to this article: https://doi.org/10.3109/15412555.2015.1084614

COPD: JOURNAL OF CHRONIC OBSTRUCTIVE PULMONARY DISEASE
2016, VOL. 13, NO. 3, 345–351
http://dx.doi.org/10.3109/15412555.2015.1084614

Taylor & Francis
Taylor & Francis Group

ORIGINAL RESEARCH

Diastolic Dysfunction Is a Contributing Factor to Exercise Intolerance in COPD

Réka Faludi[a], Máté Hajdu[a], Vivien Vértes[a], Ágnes Nógrádi[a], Noémi Varga[a], Miklós Balázs Illés[b], Veronika Sárosi[b], György Alexy[c], and András Komócsi[a]

[a]Heart Institute, University of Pécs, Pécs, Hungary; [b]Department of Pulmonology, 1st Department of Internal Medicine, University of Pécs, Pécs, Hungary; [c]Department of Pulmonology, Unified Health Institutions, Pécs, Hungary

ABSTRACT

Right ventricular (RV) systolic failure is rare in patients with COPD, but they often develop RV diastolic dysfunction. Left ventricular (LV) diastolic dysfunction is also common in this population. Nevertheless, data are scarce regarding the effect of diastolic dysfunction on the functional capacity in patients with COPD. We investigated the correlation between echocardiographic parameters of RV and LV diastolic function and the exercise capacity in COPD, by using conventional echocardiographic methods and tissue Doppler imaging. 65 patients with COPD (61 ± 9 years) in stages GOLD II-IV were investigated. Functional capacity was measured with 6-minute walk test (6MWT). Right (RA) and left atrial (LA) area index were measured; collapsibility index inferior vena cava was calculated. Parameters of the mitral and tricuspid inflow (E, A) as well as annular systolic (S), early- (e′) and late- (a′) diastolic myocardial longitudinal velocities were measured. E/A, E/e′ and e′/a′ ratios were calculated. 6MWT distance was 330 ± 76 m. LV diastolic dysfunction was found in 48 (74%) patients. LV and RV filling pressures were elevated in 28 (43%) and in 29 (45%) patients, respectively. In the left heart, LA area index showed significant correlation with the functional capacity ($r = -0.319$; $p = 0.011$). In stepwise multiple linear regression analysis tricuspid e′/a′ ($r = 0.611$; $p = 0.000$), collapsibility index ($r = 0.505$; $p = 0.000$), RA area index ($r = -0.445$; $p = 0.000$) and body surface area ($r = 0.314$; $p = 0.011$) were independent predictors of 6MWT distance. Right ventricular diastolic function and filling pressure have strong influence on the functional capacity in patients with COPD.

KEYWORDS

6-minute walk test; echocardiography; functional capacity; right atrial area; tissue Doppler imaging

Introduction

Chronic obstructive pulmonary disease (COPD) is a growing global epidemic, which is forecasted to be the third leading cause of death by 2020 (1,2). Beside its impact on mortality, COPD represents large health care burden and it is important cause of disability (3). Dyspnoea and reduced functional capacity are common consequences of COPD. The aetiology of reduced exercise tolerance is multifactorial thus parameters of the resting pulmonary function such as forced expiratory volume (FEV_1) are poor predictors of the functional capacity (4,5). Dynamic lung hyperinflation is an important contributory factor that can be targeted for treatment (5,6). Depression, skeletal muscle weakness or pulmonary hypertension as well as alterations of the cardiac function may also serve as limiting factor to reduced functional capacity (7,8).

Right ventricular systolic failure with low cardiac output is rare in patients with COPD, but they often develop right ventricular diastolic dysfunction with stress induced or resting elevation of filling pressures (9,10). Left ventricular diastolic dysfunction is also reported to be common in the COPD population (11–14). Nevertheless, data are scarce regarding the effect of the right and left ventricular diastolic dysfunction on the functional capacity in COPD.

Thus we aimed to investigate the relation between the echocardiographic parameters of the right and left ventricular diastolic function and the exercise capacity in patients with COPD. In addition to the conventional echocardiographic methods tissue Doppler imaging technique (TDI) was used offering a more sensitive assessment both of systolic and diastolic function.

Methods

Study population

Eighty outpatients with stable COPD of varying severity were consecutively screened for this study. Diagnosis and pulmonological management of the COPD were based on GOLD strategy document (15). In patients with borderline FEV_1/FVC (below 0.70 but above the lower limit of normal) the diagnosis of COPD was based on the clinical symptoms (dyspnea, chronic cough and/or sputum production) and a history of exposure to risk factors for the disease. All patients underwent spirometry within one month before the inclusion. They had to be free of exacerbations for the two months before inclusion. Patients with moderate-to-severe left ventricular (LV) systolic dysfunction (ejection fraction <45%), atrial fibrillation, neuromuscular disorders affecting exercise capacity, significant left sided valvular abnormalities or prosthetic valves were excluded. Detailed medical history was obtained. Significant ischemic heart disease was defined as coronary artery stenosis >50% proved by invasive measurements or as history of previous myocardial

CONTACT Réka Faludi faludi.reka@pte.hu Heart Institute, University of Pécs, H-7624, Pécs, Ifjúság u. 13, H-7624 Hungary, phone: +3672536000, fax: +3672536388

infarction. Heart failure was diagnosed when the patient was regularly treated with loop diuretics and/or at any symptoms of heart failure.

Data of 34 healthy volunteers without any cardiac disease were used as control. The study complied with the Declaration of Helsinki. The institutional ethics committee approved the study. All subjects had given written informed consent prior to inclusion.

Echocardiography

Echocardiography was performed using Philips CX50 ultrasound system (Philips Healthcare, Best, The Netherlands). Studies were performed by a single cardiologist blinded to all other data. 2D and M-mode echocardiographic data collected for analysis included: LV ejection fraction; LV mass corrected for body surface area (LVM index); maximal left and right atrial areas, corrected for body surface area (LA and RA area index); basal, mid-cavity, and longitudinal dimensions of the right ventricle (RV); tricuspid annular plane systolic excursion (TAPSE); RV fractional area change (RVFAC); maximal and minimal diameters of the inferior vena cava (IVC); collapsibility index (the percent decrease in the diameter during inspiration); RV wall thickness (16, 17).

The following Doppler data were collected: spectral Doppler based myocardial performance (Tei) index, mitral and tricuspid E/A, calculated RV systolic pressure, myocardial systolic (S), early- (e′) and late- (a′) diastolic velocities at the lateral and septal mitral annulus and at the lateral tricuspid annulus, mitral and tricuspid E/e′ and e′/a′ ratios. Doppler measurements were obtained during end-expiratory apnoea (16). LV diastolic dysfunction was identified if mitral lateral e′ < 10 cm/s and septal e′ < 8 cm/s. Elevated LV filling pressure was defined as mean E/e′ ≥ 9 (18). Elevated RV filling pressure was diagnosed if tricuspid E/e′ > 6 (16).

Six-minute walk test

Functional capacity of the patients was measured with 6 minute walk test (6MWT), at the day of the echocardiography. Borg dyspnoea index (0–10) was used for subjective assessment of shortness of breath during the exercise (19).

Statistical analysis

Categorical data were expressed as frequencies and percentages; continuous data were expressed as the mean ± SD. Intraclass correlation coefficient was calculated to assess intraobserver reliability. Comparisons of data between two groups were performed using independent-sample *t*-tests for continuous variables and chi square tests for categorical variables. Comparisons of data between more groups were performed using ANOVA with LSD post hoc test. Univariate predictors of 6MWT distance were assessed using linear regression analysis. A *p*-value of < 0.05 was considered significant.

Multiple stepwise linear regression analysis was performed by entering those variables that were considered significant ($p < 0.05$) on univariate analysis. In this method the variable with the smallest probability of its *F*-statistic ($p \leq 0.05$) is entered into the model first. This process continues to add variables to the model until there are no variables left that have *F* statistics that meet the criteria. As this process progresses, the *F* statistics for variables already in the model may change. If the significance level of these *F* statistics exceeds the criterion (if $p \geq 0.1$), then these variables are removed from the model. Variance Inflation Factor (VIF) values above 2.5 were considered to have potential multicollinearity. IBM SPSS 22 statistical software was used.

Results

Of a total of 80 patients with COPD, 65 were eligible for the study. Fifteen patients were excluded due to atrial fibrillation (4 patients), poor acoustic window (2), severe sinus tachycardia (1), moderate-to-severe left-sided valve disease (1 aortic stenosis, 1 mitral regurgitation), severely reduced LV systolic function (1 patient with dilated cardiomyopathy, 1 patient with previous myocardial infarction), and severe pericardial constriction (1). Three patients (all in GOLD stage IV) did not attempt to perform 6MWT because of their weak physical condition.

Systemic hypertension, heart failure and diabetes were common in our COPD population. In 1 case percutaneous coronary intervention was performed while 4 patients underwent coronary artery bypass surgery. In 3 cases prior myocardial infarction was reported, but coronary intervention was not feasible. Clinical and echocardiographic data of the 65 patients are reported in Table 1.

Thirty-five patients were in GOLD stage II, 27 patients in GOLD stage III, and 3 patients in GOLD stage IV. Borg dyspnoea index was significantly higher in GOLD III patients compared with GOLD II. On the other hand, no significant difference was found between the 6MWT distances covered by the patients in GOLD stage II and III (Figure 1).

Spectral Doppler and TDI measurements were feasible in all patients. Intraclass correlation coefficients were 0.988 and 0.981 for mitral and tricuspid E, respectively. Intraclass correlation coefficients for e′, a′ and S were 0.984, 0.984 and 0.917 on mitral lateral annulus; 0.983, 0.978 and 0.977 on mitral septal annulus as well as 0.970, 0.982 and 0.986 on tricuspid annulus.

Comparison of COPD population with healthy controls

Our patients and healthy controls were matched in age and gender distribution (Table 1). Body surface area was significantly larger in patients with COPD, but the difference was clinically not remarkable. LV ejection fraction was preserved (≥ 55%) in 59 (91%), while mildly reduced (45–54%) in 6 (9%) patients. LVM index was significantly higher in patients with COPD. Both lateral and septal myocardial early diastolic velocities (e′) were significantly lower, while mean E/e′ was significantly higher in the COPD population. LV diastolic dysfunction was found in 48 (74%), while LV filling pressure was elevated in 28 (43%) patients. (Grade I and grade II diastolic dysfunction in 20 (31%) and in 28 (43%) patients, respectively.)

Assessment of the tricuspid regurgitation's velocity was feasible in 41 (63%) patients. RV systolic pressure was significantly higher in patients with COPD. Pulmonary hypertension (RV systolic pressure ≥ 35 mmHg) was found in 9 (14%) patients.

Table 1. Baseline characteristics of the COPD population and comparison with healthy subjects.

	COPD patients ($n = 65$)	Healthy volunteers ($n = 34$)	P
Clinical data			
Age (years)	60.8 ± 9.0	58.0 ± 8.3	0.092
Male sex (%)	39 (60%)	18 (53%)	0.500
Body surface area (m^2)	1.9 ± 0.3	1.8 ± 0.2	**0.023**
FEV_1% predicted	54.6 ± 14.8		
FEV_1/FVC (%)	57.2 ± 10.5		
Pack-years of smoking	33.5 ± 26.2		
Echocardiography			
LV ejection fraction (%)	60.2 ± 4.8	61.9 ± 3.3	**0.044**
LVM index (g/m^2)	106.5 ± 25.3	95.0 ± 14.0	**0.003**
LA area index (cm^2/m^2)	8.9 ± 1.5	8.5 ± 1.0	0.065
Mitral E/A	0.9 ± 0.2	1.3 ± 0.3	**0.000**
Lateral S (cm/s)	9.5 ± 1.9	10.8 ± 2.0	**0.000**
Lateral e′ (cm/s)	8.7 ± 1.9	11.1 ± 3.1	**0.000**
Lateral a′ (cm/s)	11.2 ± 2.1	11.0 ± 2.3	0.744
Septal S (cm/s)	8.2 ± 1.4	9.2 ± 1.4	**0.001**
Septal e′ (cm/s)	7. 0 ± 1.4	9.0 ± 2.1	**0.000**
Septal a′ (cm/s)	9.6 ± 1.6	9.6 ± 1.8	0.982
Mean LV E/e′	8.8 ± 2.1	6.4 ± 1.4	**0.000**
RV basal diameter index (mm/m^2)	16.2 ± 2.0	14.3 ± 2.1	**0.000**
RV mid-cavity diameter index (mm/m^2)	11.5 ± 1.5	11.2 ± 1.6	0.301
RV longitudinal diameter index (mm/m^2)	28.5 ± 3.1	27.4 ± 4.3	0.121
RVFAC (%)	49.1 ± 7.4	51.2 ± 5.9	0.092
TAPSE (mm)	20.8 ± 2.5	25. 1 ± 3.5	**0.000**
Myocardial performance index	0.43 ± 0.19	0.31 ± 0.04	**0.000**
RA area index (cm^2/m^2)	8.3 ± 1.5	7.2 ± 1.3	**0.000**
RV wall thickness (mm)	6.0 ± 1.3	3.6 ± 1.0	**0.000**
RV systolic pressure (mmHg)	27.9 ± 6.5	22.7 ± 3.0	**0.000**
IVC (mm)	13.3 ± 3.1	9.5 ± 2.2	**0.000**
Collapsibility index (%)	59.1 ± 14.4	64.4 ± 9.0	**0.018**
Tricuspid E/A	1.1 ± 0.2	1.4 ± 0.2	**0.000**
Tricuspid S (cm/s)	12.6 ± 2.0	13.9 ± 2.1	**0.001**
Tricuspid e′ (cm/s)	7.9 ± 1.3	11.4 ± 2.3	**0.000**
Tricuspid a′ (cm/s)	13.4 ± 2.2	13.0 ± 4.3	0.618
Tricuspid e′/a′	0.6 ± 0.1	0.9 ± 0.3	**0.000**
Tricuspid E/e′	6.0 ± 1.8	3.8 ± 1.3	**0.000**
Co-morbidities			
Ischemic heart disease (%)	9 (12%)		
Systemic hypertension (%)	51 (78%)		
Diabetes (%)	18 (28%)		
Heart failure (%)	51 (78%)		
Medication			
ACE inhibitors (%)	32 (49%)		
Beta-blockers (%)	29 (45%)		
Spironolactone (%)	3 (5%)		
Other diuretics (%)	27 (42%)		

Statistically significant p-values are formatted in bold ($p < 0.05$).

RV wall thickness, RA area and RV basal diameter were significantly increased in patients with COPD. IVC was dilated, while collapsibility index was significantly lower in the COPD group. TAPSE and myocardial longitudinal systolic velocity (tricuspid S) were significantly lower in our patients as compared with controls. RV systolic dysfunction was rare in the COPD population: RVFAC < 35%, TAPSE < 16 mm and tricuspid S < 10 cm/s were found in 1 (1.5%), 3 (5%) and 7 (11%) patients, respectively. Myocardial performance index was prolonged (> 0.4) in 31 (47%) patients. Tricuspid e′ and tricuspid e′/a′ were significantly decreased in the COPD population. RV filling pressure was elevated in 29 (45%) patients.

Determinants of functional capacity in patients with COPD

Among all clinical parameters, 6MWT distance showed significant negative correlation with age and significant positive correlation with body surface area. FEV_1% and FEV_1/FVC did not show significant correlation with 6MWT distance, but were significant predictors of Borg dyspnoea index (FEV_1%: r = -0.474; $p = 0.000$ and FEV_1/FVC: r = -0.374; $p = 0.002$). Among all echocardiographic parameters, significant negative correlation was found between LA area index and 6MWT distance. Other parameters of LV systolic and diastolic function did not show correlation with the functional capacity. A number of parameters representing RV size, RV diastolic function and filling pressure were proven to be significant predictors of 6MWT. No correlation was found between 6MWT results and the echocardiographic parameters of RV systolic function.

Univariate and multivariate predictors of the 6MWT distance are reported in Table 2. In stepwise multiple linear regression analysis tricuspid e′/a′, body surface area, RA area index and collapsibility index were independent predictors of 6MWT distance (multiple r = 0.764; $p = 0.000$; $F = 19.269$) (Figure 2). VIF values for all variables were below 2.5.

Discussion

Multiple mechanisms lead to the restriction of functional capacity in COPD. Our hypothesis was that left and right ventricular diastolic dysfunction is a contributing factor to exercise intolerance in this disease.

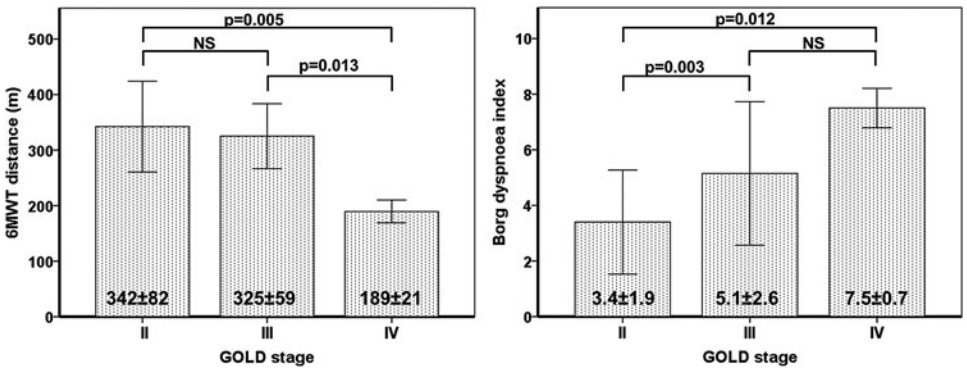

Figure 1. 6MWT and Borg dyspnoea index results in different GOLD stages (Mean ± SD; ANOVA with LSD post hoc test).

Table 2. Predictors of the 6MWT distance (m) in patients with COPD: univariate and multivariate regression analyses (Unstandardized (B) and standardized (β) regression coefficients).

	Univariate analysis			Multivariate analysis		
	B	r	p	B	β	P
Age (years)	− 2.297	− 0.273	**0.029**			
Body surface area (m^2)	91.399	0.314	**0.011**	96.914	0.359	**0.000**
LA area index (cm^2/m^2)	− 15.515	− 0.319	**0.011**			
RV basal diameter index (mm/m^2)	− 10.627	− 0.290	**0.021**			
RV longitudinal diameter index (mm/m^2)	− 6.357	− 0.271	**0.031**			
RA area index (cm^2/m^2)	− 22.522	− 0.445	**0.000**	− 15.606	− 0.304	**0.001**
Collapsibility index (%)	2.677	0.505	**0.000**	1.384	0.270	**0.005**
Tricuspid a′ (cm/s)	− 17.858	− 0.525	**0.000**			
Tricuspid e′/a′	355.493	0.611	**0.000**	213.688	0.377	**0.000**

Statistically significant *p*-values are formatted in bold ($p < 0.05$).

LV systolic and diastolic function: correlation with 6MWT distance

LV ejection fraction was preserved or mildly reduced in our COPD population. Mitral annular S values, however, were significantly decreased as compared to healthy subjects. This subclinical impairment of the LV systolic function commonly occurs in patients with impaired LV diastolic function as the evidence of the interdependence between contraction and relaxation (20).

More mechanisms may explain the presence of LV diastolic dysfunction in patients with COPD. Significant reduction of the LV diastolic diameter and consequential impairment of LV filling was reported in pulmonary hyperinflation (21). Abnormal patterns of LV diastolic filling have been also described in patients with COPD and elevated pulmonary pressure, due to ventricular interdependence (22). In addition, hypoxemia and systemic inflammation may directly impair LV myocardial function (23). Cardiovascular comorbidities, such as systemic hypertension or ischaemic heart disease, are common in COPD (24, 25), which may be also responsible for the LV diastolic dysfunction.

COPD on CT scan was associated with reduced pulmonary vein cross-sectional area. These findings suggest that impaired LV filling in COPD may be predominantly due to reduced LV preload from upstream pulmonary causes rather than intrinsic diastolic dysfunction (26). The mitral inflow pattern (E/A) is in fact dependent on loading conditions. Mitral annular TDI parameters, however, are able to verify the presence of relaxation abnormalities by reflecting the intrinsic features of the LV myocardium (27). In patients with COPD this new technique was used for the assessment of the diastolic function only in few recent studies (12–14).

These results are not completely comparable, since different approaches were used to estimate the frequency of the diastolic dysfunction. Nevertheless, these works have concordantly proved that LV diastolic dysfunction is common in COPD. We applied the recent ASE/EACVI recommendation for the evaluation of the left ventricular diastolic function (18). Mild

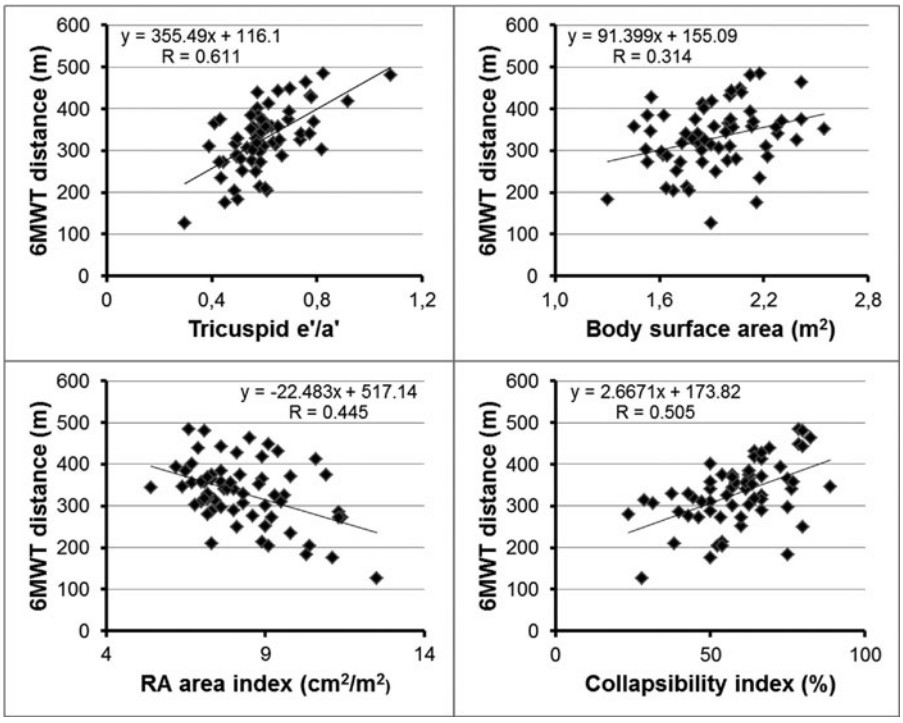

Figure 2. Main predictors of the 6MWT distance in patients with COPD.

or moderate form of left ventricular diastolic dysfunction was found in 74% of our COPD patients, what is in accordance with the previous findings (12–14). In addition to the manifest diastolic and subclinical systolic RV dysfunction, LV diastolic dysfunction may be also responsible for the large number of heart failure cases in our population.

Lopez-Sanchez et al. (13) reported significant correlation between E/A ratio and the functional capacity of the patients while in the work of Cuttica et al. (14) E/e′ and the degree of diastolic dysfunction were predictors of the 6MWT distance in univariate analysis. In our population, LA area index was the only parameter in the left heart, which showed significant correlation with 6MWT distance. Although E/e′ reflects the momentary value of the LV filling pressure, LA size is considered as a reliable indicator of the cumulative effects of the elevated LV filling pressure over time (28) and also predicts abnormal elevation of LV filling pressure during exercise in patients with normal resting LV filling pressure (29). These facts may serve as explanation for the superiority of LA size over E/e′ in the prediction of the functional capacity of the patients.

RV systolic and diastolic function: correlations with 6MWT distance

RVFAC was preserved in our COPD population, while TAPSE and tricuspid S, the parameters of RV longitudinal systolic function, were significantly decreased as compared to healthy subjects, suggesting subclinical impairment of RV systolic function. These results are in line with the data of Hilde at al., who reported the decrease of the RV longitudinal strain in a COPD population without pulmonary hypertension (30).

Prolonged myocardial performance index as well as significantly decreased tricuspid e′ and tricuspid e′/a′ were found as the signs of RV diastolic dysfunction. Enlarged RA suggested chronic or intermittent elevation of the RV filling pressure (31), while the dilated IVC and lower collapsibility index were the signs of the elevated RA pressure in our patients.

Cuttica et al. have already demonstrated that structural changes in the right heart are associated with reduced functional capacity in patients with COPD. In their study, RA size and RV wall thickness were independent predictors of 6MWT distance. Tricuspid annular TDI parameters, however, were not included in their work (14). In our study an even more comprehensive analysis of this topic was performed investigating all the available echocardiographic (2D, spectral Doppler and TDI) parameters of the left and right heart. With this approach we provided further evidence suggesting that right ventricular diastolic function and filling pressure have a major impact on the functional capacity in patients with COPD.

Aetiology of RV dysfunction in patients with COPD

Heart failure with preserved ejection fraction may be accompanied by RV dysfunction. In these cases impaired RV function is related to both primary myocardial impairment and elevated RV afterload (32). LV diastolic dysfunction and elevated LV filling pressure were common in our COPD population. This fact suggests that RV dysfunction of our patients is not necessarily related to COPD, but may be the consequence of the LV

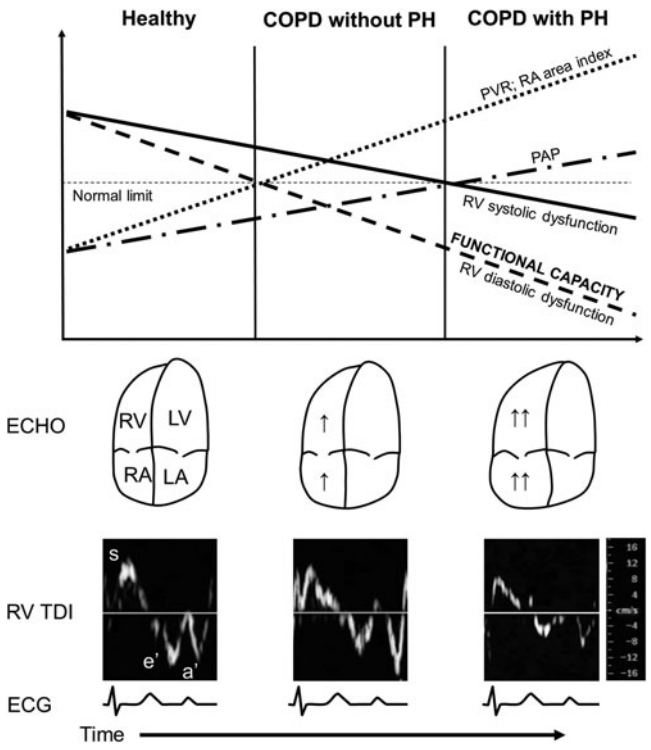

Figure 3. Schematic diagram demonstrating the hypothesized changes in the typical echocardiographic and hemodynamic parameters parallel with the course of the disease in patients with COPD.

disease. On the other hand, all independent echocardiographic predictors of the 6MWT distance represented the right heart. It does not support the primary role of the left heart disease in the reduced functional capacity of the patients with COPD.

Pulmonary hypertension is a well-known comorbidity in advanced COPD. In patients with severe COPD waiting for lung volume reduction surgery or lung transplantation, pulmonary hypertension and consequential RV dysfunction was present in the half of the patients (33). In unselected COPD patients with moderate-to-severe disease the incidence of the resting pulmonary hypertension is much lower. Subclinical systolic and manifest diastolic dysfunction of the RV, however, is already present in patients without pulmonary hypertension (30,34). The possible explanation for this phenomenon is the elevated pulmonary vascular resistance, which may be unmasked by exercise, when the pulmonary circulation no longer has the capacity to adapt and the pulmonary pressure increases parallel with the increasing cardiac output (35). Kovacs et al. reported that borderline resting pulmonary arterial pressure is associated with decreased exercise capacity in patients with systemic sclerosis. In their work, 6MWT distance showed significant negative correlation with pulmonary vascular resistance measured at peak exercise (36). Figure 3 demonstrates the hypothesized changes in the typical parameters of the RV systolic and diastolic function parallel with the progression of the pulmonary vascular disease in patients with COPD.

Limitations of the study

Some limitations of our study are to be acknowledged. The extent of the dynamic lung hyperinflation was not investigated

in our patients. This may be the cause that not any measures of respiratory function show significant correlation with the 6MWT distance in our study.

The number of patients with resting pulmonary hypertension was low in our COPD population and the elevation of the pulmonary pressure was mild in the majority of these cases. In addition, few patients with GOLD stage IV disease participated in the study. A higher proportion of patients with considerable pulmonary hypertension or more advanced lung disease may also alter our results.

Our patients did not undergo right heart catheterization, therefore the pulmonary arterial pressure was estimated non-invasively, and no data were available about the pulmonary vascular resistance of the patients. Due to the lack of invasive measurements, left and right ventricular filling pressures were also estimated by Doppler methods. Unfortunately, these parameters are less reliable in the evaluation of filling dynamics than the invasive measurements.

Conclusion

The mechanism of the exercise intolerance is complex in COPD, thus it is difficult to identify the true contributors. Nevertheless, our study suggests that RV diastolic function and filling pressure have strong influence on the functional capacity in patients with COPD.

Funding

This research was supported by the European Union and the State of Hungary, co-financed by the European Social Fund in the framework of TÁMOP 4.2.4. A/2-11-1-2012-0001 "National Excellence Program" to R.F.

Declaration of interest

The authors report no conflicts of interest. The authors alone are responsible for the content and writing of the paper.

References

1. Mathers CD, Boerma T, Ma Fat D. Global and regional causes of death. Br Med Bull 2009; 92:7–32.
2. Murray CJ, Lopez AD. Alternative projections of mortality and disability by cause 1990–2020: Global Burden of Disease Study. Lancet 1997; 349(9064):1498–1504.
3. Chapman KR, Mannino DM, Soriano JB, Vermeire PA, Buist AS, Thun MJ, et al. Epidemiology and costs of chronic obstructive pulmonary disease. Eur Respir J 2006; 27(1):188–207.
4. Bauerle O, Chrusch CA, Younes M. Mechanisms by which COPD affects exercise tolerance. Am J Respir Crit Care Med 1998; 157(1):57–68.
5. Marin JM, Carrizo SJ, Gascon M, Sanchez A, Gallego B, Celli BR. Inspiratory capacity, dynamic hyperinflation, breathlessness, and exercise performance during the 6-minute-walk test in chronic obstructive pulmonary disease. Am J Respir Crit Care Med 2001; 163(6):1395–1399.
6. Laveneziana P, Guenette JA, Webb KA, O'Donnell DE. New physiological insights into dyspnea and exercise intolerance in chronic obstructive pulmonary disease patients. Expert Rev Respir Med 2012; 6(6):651–662.
7. Nici L. Mechanisms and measures of exercise intolerance in chronic obstructive pulmonary disease. Clin Chest Med 2000; 21(4):693–704.
8. Barnes PJ. Chronic obstructive pulmonary disease: effects beyond the lungs. PLoS Med 2010; 343(3):269–280.
9. Hoeper MM, Barbera JA, Channick RN, Hassoun PM, Lang IM, Manes A, et al. Diagnosis, assessment, and treatment of non-pulmonary arterial hypertension pulmonary hypertension. J Am Coll Cardiol 2009; 54(1 Suppl):S85–96.
10. Scharf SM, Iqbal M, Keller C, Criner G, Lee S, Fessler HE, et al. Hemodynamic characterization of patients with severe emphysema. Am J Respir Crit Care Med 2002; 166(3):314–322.
11. Freixa X, Portillo K, Pare C, Garcia-Aymerich J, Gomez FP, Benet M, et al. Echocardiographic abnormalities in patients with COPD at their first hospital admission. The Eur Respir J 2013; 41(4):784–791.
12. Schoos MM, Dalsgaard M, Kjaergaard J, Moesby D, Jensen SG, Steffensen I, et al. Echocardiographic predictors of exercise capacity and mortality in chronic obstructive pulmonary disease. BMC Cardiovasc Disord 2013; 13:84.
13. Lopez-Sanchez M, Munoz-Esquerre M, Huertas D, Gonzalez-Costello J, Ribas J, Manresa F, et al. High prevalence of left ventricle diastolic dysfunction in severe COPD associated with a low exercise capacity: A cross-sectional study. PLoS One 2013; 8(6):e68034.
14. Cuttica MJ, Shah SJ, Rosenberg SR, Orr R, Beussink L, Dematte JE, et al. Right heart structural changes are independently associated with exercise capacity in non-severe COPD. PLoS One 2011; 6(12):e29069.
15. Vestbo J, Hurd SS, Agusti AG, Jones PW, Vogelmeier C, Anzueto A, et al. Global strategy for the diagnosis, management, and prevention of chronic obstructive pulmonary disease: GOLD executive summary. Am J Respir Crit Care Med 2013; 187(4):347–365.
16. Rudski LG, Lai WW, Afilalo J, Hua L, Handschumacher MD, Chandrasekaran K, et al. Guidelines for the echocardiographic assessment of the right heart in adults. J Am Soc Echocardiogr 2010; 23(7):685–713.
17. Lang RM, Bierig M, Devereux RB, Flachskampf FA, Foster E, Pellikka PA, et al. Recommendations for chamber quantification. J Am Soc Echocardiogr 2005; 18(12):1440–1463.
18. Nagueh SF, Appleton CP, Gillebert TC, Marino PN, Oh JK, Smiseth OA, et al. Recommendations for the evaluation of left ventricular diastolic function by echocardiography. J Am Soc Echocardiogr 2009; 22(2):107–133.
19. ATS statement: guidelines for the six-minute walk test. Am J Respir Crit Care Med 2002; 166(1):111–117.
20. Vinereanu D, Nicolaides E, Tweddel AC, Fraser AG. "Pure" diastolic dysfunction is associated with long-axis systolic dysfunction. Implications for the diagnosis and classification of heart failure. Eur J Heart Fail 2005; 7(5):820–828.
21. Watz H, Waschki B, Meyer T, Kretschmar G, Kirsten A, Claussen M, et al. Decreasing cardiac chamber sizes and associated heart dysfunction in COPD: role of hyperinflation. Chest 2010; 138(1):32–38.
22. Funk GC, Lang I, Schenk P, Valipour A, Hartl S, Burghuber OC. Left ventricular diastolic dysfunction in patients with COPD in the presence and absence of elevated pulmonary arterial pressure. Chest 2008; 133(6):1354–1359.
23. Hannink JD, van Helvoort HA, Dekhuijzen PN, Heijdra YF. Heart failure and COPD: partners in crime? Respirology 2010; 15(6):895–901.
24. Falk JA, Kadiev S, Criner GJ, Scharf SM, Minai OA, Diaz P. Cardiac disease in chronic obstructive pulmonary disease. Proc Am Thorac Soc 2008; 5(4):543–548.
25. Sin DD, Anthonisen NR, Soriano JB, Agusti AG. Mortality in COPD: Role of comorbidities. Eur Respir J 2006; 28(6):1245–1257.
26. Smith BM, Prince MR, Hoffman EA, Bluemke DA, Liu CY, Rabinowitz D, et al. Impaired left ventricular filling in COPD and emphysema: Is it the heart or the lungs? The Multi-Ethnic Study of Atherosclerosis COPD Study. Chest 2013; 144(4):1143–1151.
27. Sohn DW, Chai IH, Lee DJ, Kim HC, Kim HS, Oh BH, et al. Assessment of mitral annulus velocity by Doppler tissue imaging in the evaluation of left ventricular diastolic function. J Am Coll Cardiol 1997; 30(2):474–480.
28. Douglas PS. The left atrium: a biomarker of chronic diastolic dysfunction and cardiovascular disease risk. J Am Coll Cardiol 2003; 42(7):1206–1207.
29. Hammoudi N, Achkar M, Laveau F, Boubrit L, Djebbar M, Allali Y, et al. Left atrial volume predicts abnormal exercise left ventricular filling pressure. Eur J Heart Fail 2014; 16(10):1089–1095.

30. Hilde JM, Skjorten I, Grotta OJ, Hansteen V, Melsom MN, Hisdal J, et al. Right ventricular dysfunction and remodeling in chronic obstructive pulmonary disease without pulmonary hypertension. J Am Coll Cardiol 2013; 62(12):1103–1111.
31. Do DH, Therrien J, Marelli A, Martucci G, Afilalo J, Sebag IA. Right atrial size relates to right ventricular end-diastolic pressure in an adult population with congenital heart disease. Echocardiography 2011; 28(1):109–116.
32. Melenovsky V, Hwang SJ, Lin G, Redfield MM, Borlaug BA. Right heart dysfunction in heart failure with preserved ejection fraction. Eur Heart J 2014; 35(48):3452–3462.
33. Thabut G, Dauriat G, Stern JB, Logeart D, Levy A, Marrash-Chahla R, et al. Pulmonary hemodynamics in advanced COPD candidates for lung volume reduction surgery or lung transplantation. Chest 2005; 127(5):1531–1536.
34. Sabit R, Bolton CE, Fraser AG, Edwards JM, Edwards PH, Ionescu AA, et al. Sub-clinical left and right ventricular dysfunction in patients with COPD. Respir Med 2010; 104(8):1171–1178.
35. Rubin LJ. Cor pulmonale revisited. J Am Coll Cardiol 2013; 62(12):1112–1113.
36. Kovacs G, Maier R, Aberer E, Brodmann M, Scheidl S, Troster N, et al. Borderline pulmonary arterial pressure is associated with decreased exercise capacity in scleroderma. Am J Respir Crit Care Med 2009; 180(9):881–886.

Relation of Right Atrial Mechanics to Functional Capacity in Patients With Systemic Sclerosis

Ágnes Nógrádi, MD[a], Adél Porpáczy, MD[a], Lili Porcsa[a], Tünde Minier, MD, PhD[b], László Czirják, MD, DSc[b], András Komócsi, MD, DSc[a], and Réka Faludi, MD, PhD[a,*]

Cardiac involvement in systemic sclerosis (SSc) implies a worse prognosis. Little is known about the right atrial (RA) mechanics in this disease, but recent data suggest that it correlates well with the functional capacity of the patients in conditions with known right heart involvement. Thus we aimed to investigate the abnormalities of the RA function as compared with healthy subjects and to assess the potential correlations between RA mechanics and the functional capacity in SSc patients using 2D speckle tracking technique. A total of 70 SSc patients (age: 57 ± 12 years) were investigated. Functional capacity was measured with 6-minute walk test (6MWT). Echocardiographic parameters of the right ventricular (RV) systolic function (TAPSE, RVFAC), parameters of the tricuspid inflow (E, A), and tricuspid annular systolic (S), early- (e') and late- (a') diastolic myocardial velocities were measured. RV wall thickness was obtained. RA reservoir (ε_R), conduit (ε_{CD}), and contractile (ε_{CT}) strain were measured. RA stiffness was calculated as ratio of E/e' to ε_R. Echocardiographic data were compared with an age- and gender-matched group of 25 healthy volunteers. RA ε_R (49.3 ± 10.7 vs 59.6 ± 9.9%, p = 0.000) and ε_{CD} (26.8 ± 8.1 vs 34.3 ± 7.3%, p = 0.000) were significantly lower in SSc patients. No significant difference was found in ε_{CT} (22.9 ± 5.8 vs 25.3 ± 5.7%, p = 0.082). RA stiffness was significantly increased in SSc patients (0.11 ± 0.04 vs 0.08 ± 0.02, p = 0.001). 6MWT distance was 391 ± 95 m. In stepwise multiple linear regression analysis RV wall thickness (r = −0.289, p = 0.030) and RA stiffness (r = −0.418, p = 0.002) became independent predictors of 6MWT distance. In conclusion, RA ε_R and ε_{CD} are impaired, while RA stiffness is increased in SSc compared with healthy subjects. Speckle tracking-derived RA stiffness is turned out to be one of the main determinants of the functional capacity in SSc patients. **(Am J Cardiol 2018;122:1249−1254)**

Systemic sclerosis (SSc) is a systemic connective tissue disease characterized by inflammation and fibrosis of various organs. Cardiac involvement is common in SSc and implies a worse prognosis.[1] Left ventricular diastolic dysfunction is frequent[2,3] and is often accompanied by impaired left atrial function.[4−6] Right ventricular (RV) dysfunction was traditionally attributed to the development of pulmonary arterial hypertension (PAH) or pulmonary fibrosis.[7] Subclinical RV dysfunction, however, was also proved in SSc patients without the resting elevation of the pulmonary pressure, by using tissue Doppler or speckle tracking measurements.[8−11] Speckle tracking-derived strain imaging also allows us to assess the phasic function of the atria.[12] By the help of this new technique, impaired right atrial (RA) function has been recently reported in SSc.[9] Atrial stiffness—a tissue Doppler and speckle tracking-derived parameter—represents the change in pressure required to increase the volume of the atrium in a given measure.[13,14] Recent data suggest that RA size and mechanics correlate well with the functional capacity of the patients in conditions with known right heart involvement, such as in idiopathic PAH or chronic obstructive pulmonary disease.[15,16] Thus we aimed to investigate the abnormalities of the RA function as compared with healthy subjects and assess the potential correlations between RA mechanics and the functional capacity in SSc patients, by using 2D speckle tracking technique.

Methods

A total of 80 consecutive patients diagnosed with SSc in the tertiary center of the Department of Rheumatology and Immunology, University of Pécs were recruited into our prospective study. All enrolled cases complied with the updated ACR/EULAR classification criteria.[17] Patients with atrial fibrillation, significant left-sided valvular disease as well as with significant peripheral artery disease, cognitive issues, neuromuscular, or musculoskeletal problems were excluded from the study. Right heart catheterization was initiated in the presence of echocardiographic abnormalities suggestive of PAH.[18] Patients with invasively verified PAH (mean pulmonary artery pressure ≥25 mm Hg and pulmonary capillary wedge pressure ≤15 mm Hg) were excluded from the study. An age and gender matched group of 25 healthy

[a]Heart Institute, Medical School, University of Pécs, Pécs, Hungary; and [b]Department of Rheumatology and Immunology, Medical School, University of Pécs, Pécs, Hungary. Manuscript received February 27, 2018; revised manuscript received and accepted June 14, 2018.

See page 1256 for disclosure information.

*Corresponding author: Tel: +3672536000; fax: +3672536388.

E-mail address: faludi.reka@pte.hu (R. Faludi).

0002-9149/

https://doi.org/10.1016/j.amjcard.2018.06.021

volunteers without any signs or symptoms of cardiac disease was used as control.

The study complied with the Declaration of Helsinki. The institutional ethics committee approved the study. All subjects had given written informed consent before inclusion.

Echocardiography was performed using Philips Epiq 7G ultrasound system (Philips Healthtech, Best, The Netherlands) by a single investigator. 2D and M-mode echocardiographic data collected for analysis included: left ventricular ejection fraction measured by Simpson's method; basal, midcavity, and longitudinal dimensions of the RV corrected for body surface area; tricuspid annular plane systolic excursion (TAPSE); RV fractional area change (RVFAC); maximal and minimal diameters of the inferior vena cava (IVC); collapsibility index of IVC (the percent decrease in the diameter during inspiration). RV wall thickness was measured at end-diastole, in a zoomed subcostal view, by 0.5 mm increments. The following Doppler data were collected: tricuspid E/A, pulmonary artery systolic pressure (assessed as a sum of the pressure difference across the tricuspid valve and an estimate of mean RA pressure (5 to 15 mmHg) using the diameter and collapsibility index of the IVC); myocardial systolic (S), early- (e'), and late- (a') diastolic velocities measured at the lateral tricuspid annulus; tricuspid E/e' ratio. Doppler measurements were obtained from ≥3 consecutive beats during end-expiratory apnea. Elevated RV filling pressure was diagnosed if tricuspid E/e' > 6.[19]

For atrial speckle tracking analysis, RA−focused apical 4-chamber view movies were obtained. Care was taken to obtain true apical images using standard anatomic landmarks to avoid foreshortening (a situation where the ultrasound plane is not appropriate and RA is not opened up to its fullest size). A total 3 consecutive heart cycles were recorded digitally and processed by a single investigator blinded to standard echocardiographic and clinical data of the patients. The beginning of the QRS was predefined by the software (QLab 10.5, Philips Healthtech, Andover, Massachusetts) as reference point. The first positive peak of the curve was measured at the end of the reservoir phase, just before tricuspid valve opening (reservoir strain, ε_R). This was followed by a plateau and a second late peak at the onset of the P wave on the electrocardiogram (contractile strain, ε_{CT}). The conduit strain (ε_{CD}) was defined as the difference between the reservoir and the contractile strain (Figure 1).[12,20] Maximal RA volume was assessed by the same software and corrected for body surface area (RA Vmax index). RA stiffness was calculated as ratio of tricuspid E/e' to ε_R.[13,14,21]

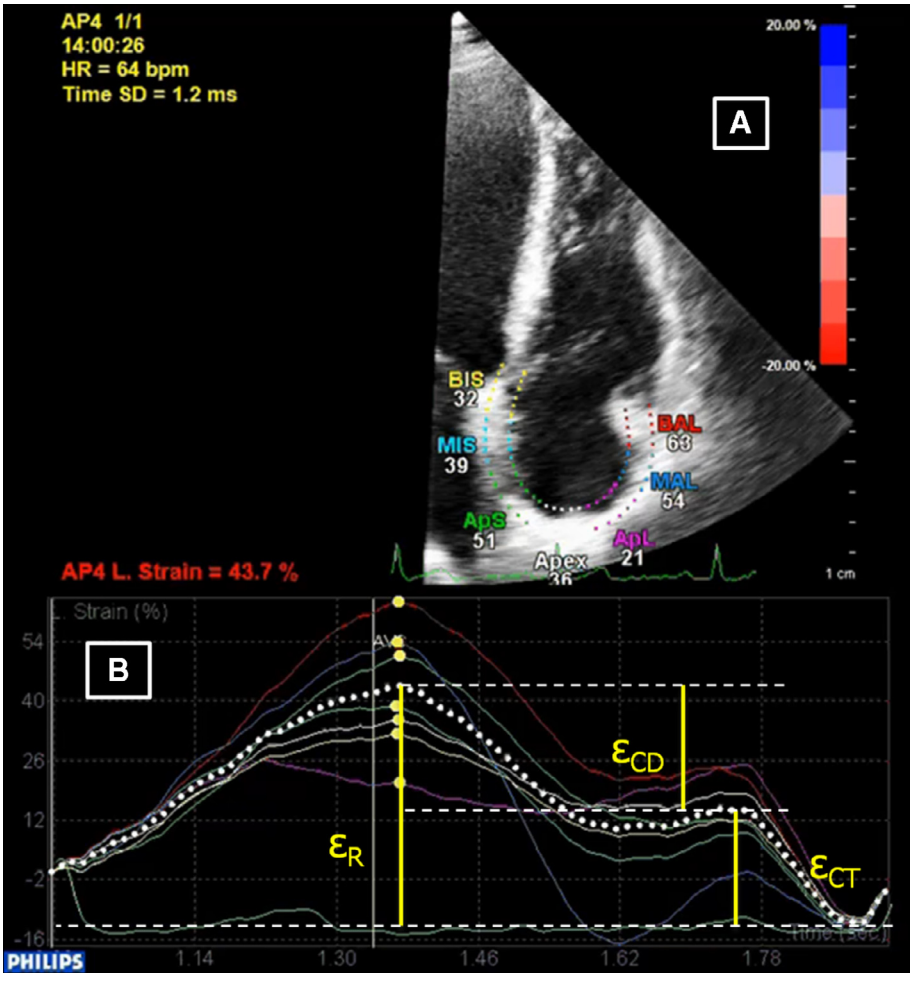

Figure 1. Speckle tracking analysis of RA strain: 4-chamber view depicting the region of interest created by the speckle tracking software (A). The global strain curve (dashed line) is obtained after averaging the seven regional strain curves (B). (ε_R: reservoir strain; ε_{CT}: contractile strain; ε_{CD}: conduit strain.)

Table 1
Baseline characteristics of the systemic sclerosis population

Clinical variable	Value
Disease duration (years)	7.2 ± 5.8
Limited cutaneous form	32 (46%)
Coronary artery disease	2 (3%)
Hypertension	36 (51%)
Angiotensin convertase enzyme inhibitors	33 (47%)
Calcium channel blockers	36 (51%)
Loop diuretics	31 (44%)
Mineralocorticoid receptor antagonists	18 (26%)
New York Heart Association functional class	
I	20 (28%)
II	32 (46%)
III	18 (26%)
6-minute walking distance (m)	391 ± 95
Modified Borg dyspnea index	1.7 ± 1.6
Erythrocyte sedimentation rate (mm/h)	21.9 ± 16.0
C-reactive protein (mg/l)	3.6 ± 5.5
Creatinine (μmol/l)	70.6 ± 23.7
NT-proBNP (pg/ml)	192 ± 163
Forced vital capacity (%)	100.5 ± 15.0
Diffusing capacity of carbon monoxide (%)	64.5 ± 15.1

Functional capacity of the patients was assessed by 6-minute walk test (6MWT), on the day of the echocardiographic measurements.[22]

Categorical data were expressed as frequencies and percentages; continuous data were expressed as mean ± SD. Comparisons of data were performed using independent-sample *t* tests for continuous variables and chi-square tests for categorical variables. Univariate predictors of 6MWT distance were assessed using linear regression analysis. A p value of <0.05 was considered significant. Multiple stepwise linear regression analysis was performed by entering those variables that were considered significant on univariate analysis. Variance inflation factor values above 2.5 were considered to have potential multicollinearity. Receiver operating characteristic (ROC) curve analysis was used to derive the optimal cut-off values for predicting 6MWT distance <300 m. Intraobserver variability was assessed by the intraclass correlation coefficient. IBM SPSS 22 statistical software was used.

Results

Of a total of 80 patients, 70 were eligible for the study. A total of 10 subjects were excluded due to inadequate acoustic window (5), or RA foreshortening (5). Detailed clinical data of the SSc patients are reported in Tables 1 and 2. The average frame rate was 89 frames/s. Intraclass correlation coefficients were 0.91, 0.96 and 0.91 for ε_R, ε_{CT}, and ε_{CD}, respectively.

Significant differences were found between the SSc group and control group in the parameters reflecting RV systolic function. Real RV systolic dysfunction, however, was rare in the SSc population: RVFAC $< 35\%$, TAPSE $<$ 16 mm and tricuspid S < 10 cm/s were found in 3 (4.6%), 1 (1.4%), and 8 (11.4%) patients, respectively. Tricuspid E/e' suggested elevated RV filling pressure in 22 (31.4%) SSc patients. RA ε_R and ε_{CD} values were significantly lower in the SSc population, while RA stiffness was significantly

Table 2
Clinical and echocardiographic data of the systemic sclerosis population and comparison with healthy subjects

Variable	Systemic sclerosis (n = 70)	Healthy subjects (n = 25)	p
Age (years)	57±12	54±7	0.239
Body surface area (m^2)	1.75±0.19	1.83±0.18	0.071
Women	63 (90%)	19 (76%)	0.082
Left ventricular ejection fraction (%)	60.8 ± 4.5	63.3 ± 2.5	**0.011**
Pulmonary arterial systolic pressure (mmHg)	26.2 ± 5.7	25.8 ± 2.9	0.724
Right ventricular basal diameter index (mm/m^2)	18.4 ± 2.4	17.5 ± 1.6	0.924
Right ventricular mid-cavity diameter index (mm/m^2)	13.5 ± 2.1	13.0 ± 1.5	0.175
Right ventricular longitudinal diameter index (mm/m^2)	31.7 ± 3.6	32.3 ± 2.8	0.392
Inferior vena cava (mm)	14.0 ± 3.8	14.8 ± 4.7	0.469
Collapsibility index (%)	55.5 ± 11.5	55.0 ± 13.4	0.874
Right ventricular wall thickness (mm)	5.0 ± 1.0	4.8 ± 0.8	0.329
Right ventricular fractional area change (%)	47.5 ± 7.2	54.1 ± 6.6	**0.000**
Tricuspid annular plane systolic excursion (mm)	21.1 ± 2.6	23.6 ± 1.6	**0.000**
Tricuspid E (cm/s)	47.5 ± 9.2	54.3 ± 8.9	**0.002**
Tricuspid A (cm/s)	39.5 ± 8.8	39.0 ± 5.6	0.771
Tricuspid e' (cm/s)	9.5 ± 2.3	11.7 ± 2.8	**0.002**
Tricuspid a' (cm/s)	13.2 ± 2.6	13.6 ± 3.3	0.533
Tricuspid S (cm/s)	12.4 ± 2.3	13.6 ± 2.3	**0.027**
Tricuspid E/e' ratio	5.3 ± 1.5	4.9 ± 1.4	0.278
Maximal right atrial volume index (ml/m^2)	19.4 ± 5.5	19.5 ± 5.9	0.943
Right atrial reservoir strain (%)	49.3 ± 10.7	59.6 ± 9.9	**0.000**
Right atrial contractile strain (%)	22.9 ± 5.8	25.3±5.7	0.082
Right atrial conduit strain (%)	26.8 ± 8.1	34.3 ± 7.3	**0.000**
Right atrial stiffness	0.11 ± 0.04	0.08 ± 0.02	**0.001**

Statistically significant p values are formatted in bold ($p < 0.05$).

Table 3
Predictors of the 6-minute walking distance in systemic sclerosis patients: univariate and multivariate regression analyses

Variables distance (m)	Associations with 6-minute walking			
	Univariate analysis		Multivariate analysis	
	r	p	β	p
Age (years)	−0.452	**0.000**		
Right ventricular wall thickness (mm)	−0.369	**0.002**	−0.289	**0.030**
Tricuspid annular plane systolic excursion (mm)	0.367	**0.002**		
Tricuspid e' (cm/s)	0.407	**0.001**		
Tricuspid E/e' ratio	−0.320	**0.008**		
Right atrial reservoir strain (%)	0.273	**0.024**		
Right atrial conduit strain (%)	0.327	**0.006**		
Right atrial stiffness	−0.401	**0.001**	−0.418	**0.002**

Statistically significant p values are formatted in bold ($p < 0.05$).

increased in SSc patients compared with the control group. Detailed echocardiographic data of the 70 patients compared with controls are reported in Table 2.

6MWT distance covered by the SSc patients was 391 ± 95 m. Univariate and multivariate predictors of the 6MWT distance are reported in Table 3. In stepwise multiple linear regression analysis RV wall thickness and RA stiffness became independent predictors of 6MWT distance (multiple r = 0.506; p = 0.001; F = 7.754). Variance inflation factor values for all variables were below 2.5. Main predictors of the 6MWT distance in SSc patients are reported in Figure 2.

6MWT distance <300 m was obtained in 11 patients. Using ROC analysis, RA stiffness ≥ 0.107 and RV wall thickness ≥ 5.2 mm were the best predictors of the 6MWT distance <300 m. ROC curves demonstrating the predictive power of these parameters are presented in Figure 3.

Discussion

The main findings of our study are the following: (1) RA ε_R and ε_{CD} are impaired, while RA stiffness is increased in SSc compared with healthy subjects. (2) RA stiffness is one of the main determinants of the functional capacity in SSc patients.

In SSc there are few data about RA size and function. Lindqvist et al found enlarged RA area in SSc patients with normal RV end-diastolic diameters and without manifest pulmonary hypertension.[11] Similarly, D'Andrea et al reported significant enlargement of the RA area compared with healthy subjects,[23] while Durmus et al found RA area index values similar to those in the healthy persons.[9] In the latter 2 studies RA function was also investigated, by the help of 2D speckle tracking technique. Significantly decreased segmental strain values were reported by D'Andrea et al in SSc patients, especially in those with pulmonary fibrosis.[23] Durmus et al found decreased ε_R and ε_{CD} values compared with a healthy control population. ε_{CT} was not investigated in their study.[9] Our findings are in line with the results of Durmus et al: although RA volume values were similar in our SSc patients and in the healthy group, we found significantly decreased ε_R and ε_{CD} values in the SSc group. ε_{CT} values did not differ between SSc group and healthy persons in our study.

We applied another parameter of the atrial performance, RA stiffness, which has never been investigated in SSc before. The role of this parameter was first reported in the left heart: it was proved to be an accurate index to distinguish diastolic heart failure patients from those with asymptomatic diastolic dysfunction.[13] Less is known, however,

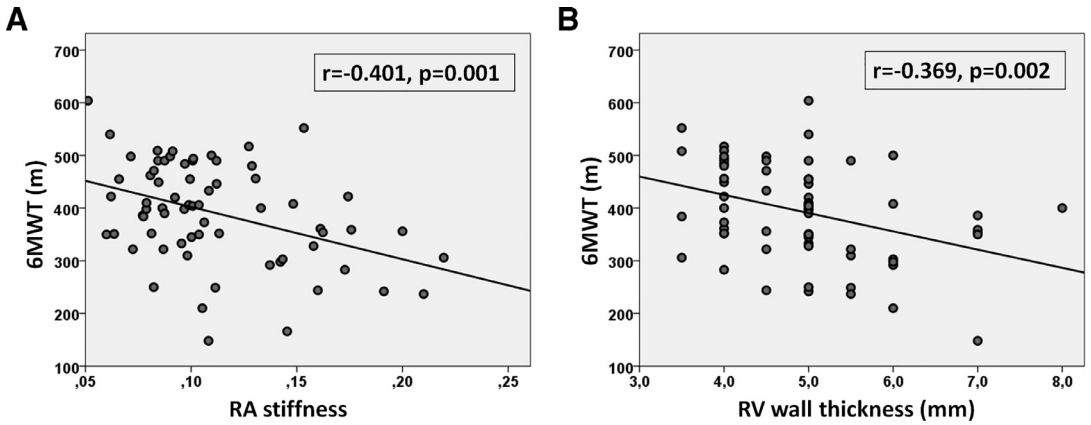

Figure 2. Main predictors of the 6MWT distance in patients with SSc are RA stiffness *(A)* and RV wall thickness *(B)*. RA = right atrial; RV = right ventricular; 6MWT = 6-minute walk test.

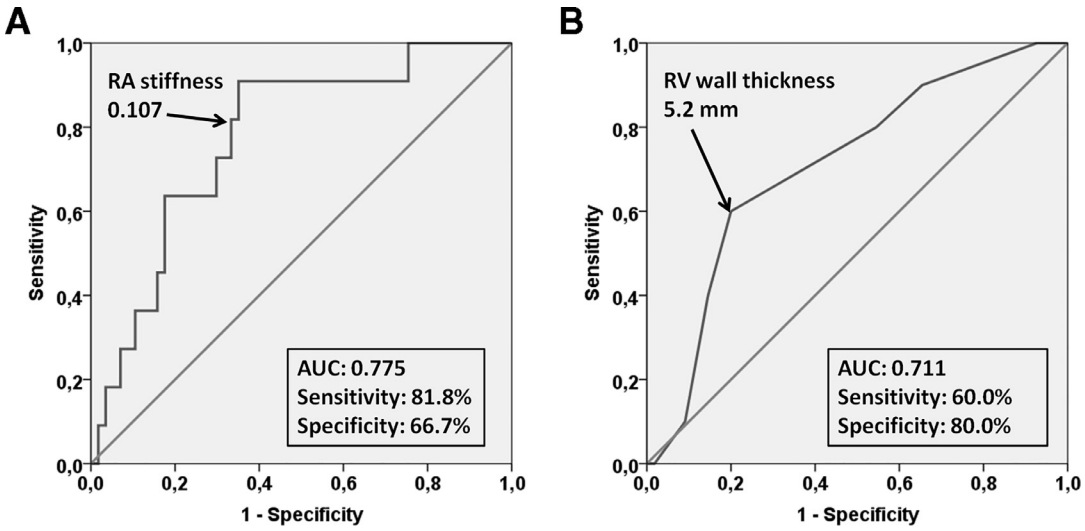

Figure 3. ROC curves demonstrating the sensitivity and specificity of RA stiffness *(A)* and RV wall thickness *(B)* in predicting poor functional capacity (6MWT distance <300 m). AUC = area under the curve; RA = right atrial; RV = right ventricular; 6MWT = 6-minute walk test.

about the use of the atrial stiffness in the right heart. Teixeira et al demonstrated increased RA stiffness in patients with left heart failure.[21] In our study, RA stiffness turned out to be significantly elevated in the SSc population, compared with healthy subjects.

In treatment-naive patients with idiopathic PAH Saha et al demonstrated significant correlation in RA ε_R and 6MWT distance.[15] As it was reported earlier by our group, RA area index was proved to be an independent predictor of the 6MWT distance in patients with chronic obstructive pulmonary disease.[16] These data suggest that RA size and mechanics may correlate with the functional capacity of the patients in conditions with known right heart involvement. The possible explanation for this phenomenon is the subclinical elevation of the pulmonary vascular resistance, which may be unmasked by exercise, when the pulmonary circulation no longer has the capacity to adapt and the pulmonary pressure increases parallel with the increasing cardiac output.[24] D'Andrea et al reported significant correlation between RA lateral segmental strain and pulmonary artery systolic pressure during effort, suggesting, that in SSc patients with exercise induced pulmonary hypertension the intermittent pressure overload may lead to ultrastructural changes in the RA wall.[23] It has been demonstrated that left atrial ε_R correlated significantly with the extent of left atrial wall fibrosis as assessed by cardiac magnetic resonance imaging and with left atrial interstitial fibrosis in patients with mitral valve disease in pathologic specimens.[25,26] Although similar histopathologic evidences are not available in the right heart, impaired RA function and elevated RA stiffness may represent the consequence the intermittent pressure overload due to stress induced elevation of the pulmonary artery pressure in SSc. This functional alteration reduces the capacity of the atrium to help maintain cardiac output during exercise. RA stiffness is a complex parameter reflecting atrial mechanics and RV filling pressure simultaneously. This may explain that it showed stronger correlation with the functional capacity of the patients than RA strain parameters.

Karna et al demonstrated the increased RV thickness as the single most important predictor of the prolonged myocardial performance index in SSc patients.[27] Lindqvist et al reported altered RV diastolic function in SSc patients, with an increase in RV wall thickness as early markers of RV dysfunction, probably in response to intermittent PAH.[11] RV dysfunction may contribute to reduced exercise tolerance through reduction in RV stroke volume. The physiologic cost of decreased RV stroke volume may be exacerbated by exercise, and may therefore explain the association of RV dysfunction with decreased 6MWT distance.[28] Although we could not prove significantly increased RV wall thickness in our population compared with healthy subjects, RV wall thickness became independent predictor of the functional capacity in SSc patients. Our data suggest, however, that for utilizing its predictive capabilities, RV wall thickness should be measured by 0.1 mm increments. Unfortunately, the accuracy of the echocardiographic measurements is limited at this level, making this parameter clinically less useful.

Some limitations of our study are to be acknowledged. For obtaining RA strain values, we used a software that was developed for left ventricular strain analysis because a dedicated software for atrial strain estimation is not available. Our patients did not undergo right heart catheterization, therefore pulmonary arterial pressure was estimated noninvasively, and no data were available about the pulmonary vascular resistance of the patients. Due to the lack of invasive measurements, RV filling pressures were also estimated by Doppler methods. It is important to note that the noninvasive approach used for the estimation of the RA stiffness has not been invasively validated in the right heart yet.

RA ε_R and ε_{CD} are impaired, while RA stiffness is increased in SSc compared with healthy subjects. The mechanism of the exercise intolerance is complex in SSc,

thus it is difficult to identify the true contributors. Nevertheless, our study suggests that speckle tracking-derived RA stiffness is a useful parameter of the RA function which has a strong influence on the functional capacity in patients with SSc. Further evaluation of RA stiffness is required to verify whether this parameter is able to identify patients with subclinical elevation of pulmonary vascular resistance and to elucidate its prognostic value in SSc patients.

Disclosures

The authors have no conflicts of interest to disclose.

1. Komocsi A, Vorobcsuk A, Faludi R, Pinter T, Lenkey Z, Kolto G, Czirjak L. The impact of cardiopulmonary manifestations on the mortality of SSc: a systematic review and meta-analysis of observational studies. *Rheumatology* 2012;51:1027–1036.
2. Faludi R, Kolto G, Bartos B, Csima G, Czirjak L, Komocsi A. Five-year follow-up of left ventricular diastolic function in systemic sclerosis patients: determinants of mortality and disease progression. *Semin Arthritis Rheum* 2014;44:220–227.
3. Kahan A, Allanore Y. Primary myocardial involvement in systemic sclerosis. *Rheumatology* 2006;45(Suppl 4). iv14-17.
4. Atas H, Kepez A, Tigen K, Samadov F, Ozen G, Cincin A, Sunbul M, Bozbay M, Direskeneli H, Basaran Y. Evaluation of left atrial volume and function in systemic sclerosis patients using speckle tracking and real-time three-dimensional echocardiography. *Anatol J Cardiol* 2016;16:316–322.
5. Agoston G, Gargani L, Miglioranza MH, Caputo M, Badano LP, Moreo A, Muraru D, Mondillo S, Moggi Pignone A, Matucci Cerinic M, Sicari R, Picano E, Varga A. Left atrial dysfunction detected by speckle tracking in patients with systemic sclerosis. *Cardiovasc Ultrasound* 2014;12:30.
6. Porpaczy A, Nogradi A, Kehl D, Strenner M, Minier T, Czirjak L, Komocsi A, Faludi R. Impairment of left atrial mechanics is an early sign of myocardial involvement in systemic sclerosis. *J Card Fail* 2018;24:234–242.
7. Yiu KH, Ninaber MK, Kroft LJ, Schouffoer AA, Stolk J, Scherer HU, Meijs J, de Vries-Bouwstra J, Tse HF, Delgado V, Bax JJ, Huizinga TW, Marsan NA. Impact of pulmonary fibrosis and elevated pulmonary pressures on right ventricular function in patients with systemic sclerosis. *Rheumatology* 2016;55:504–512.
8. Faludi R, Komocsi A, Bozo J, Kumanovics G, Czirjak L, Papp L, Simor T. Isolated diastolic dysfunction of right ventricle: stress-induced pulmonary hypertension. *Eur Respir J* 2008;31:475–476.
9. Durmus E, Sunbul M, Tigen K, Kivrak T, Ozen G, Sari I, Direskeneli H, Basaran Y. Right ventricular and atrial functions in systemic sclerosis patients without pulmonary hypertension: Speckle-tracking echocardiographic study. *Herz* 2015;40:709–715.
10. Mukherjee M, Chung SE, Ton VK, Tedford RJ, Hummers LK, Wigley FM, Abraham TP, Shah AA. Unique abnormalities in right ventricular longitudinal strain in systemic sclerosis patients. *Circ Cardiovasc Imaging* 2016;9:e003792.
11. Lindqvist P, Caidahl K, Neuman-Andersen G, Ozolins C, Rantapää-Dahlqvist S, Waldenström A, Kazzam E. Disturbed right ventricular diastolic function in patients with systemic sclerosis: a Doppler tissue imaging study. *Chest* 2005;128:755–763.
12. Vieira MJ, Teixeira R, Goncalves L, Gersh BJ. Left atrial mechanics: echocardiographic assessment and clinical implications. *J Am Soc Echocardiogr* 2014;27:463–478.
13. Kurt M, Wang J, Torre-Amione G, Nagueh SF. Left atrial function in diastolic heart failure. *Circ Cardiovasc Imaging* 2009;2:10–15.
14. Cameli M, Mandoli GE, Loiacono F, Dini FL, Henein M, Mondillo S. Left atrial strain: a new parameter for assessment of left ventricular filling pressure. *Heart Fail Rev* 2016;21:65–76.
15. Saha SK, Soderberg S, Lindqvist P. Association of right atrial mechanics with hemodynamics and physical capacity in patients with idiopathic pulmonary arterial hypertension: insight from a single-center cohort in Northern Sweden. *Echocardiography* 2016;33:46–56.
16. Faludi R, Hajdu M, Vertes V, Nogradi A, Varga N, Illes MB, Sarosi V, Alexy G, Komocsi A. Diastolic dysfunction is a contributing factor to exercise intolerance in COPD. *COPD* 2016;13:345–351.
17. van den Hoogen F, Khanna D, Fransen J, Johnson SR, Baron M, Tyndall A, Matucci-Cerinic M, Naden RP, Medsger TA Jr., Carreira PE, Riemekasten G, Clements PJ, Denton CP, Distler O, Allanore Y, Furst DE, Gabrielli A, Mayes MD, van Laar JM, Seibold JR, Czirjak L, Steen VD, Inanc M, Kowal-Bielecka O, Muller-Ladner U, Valentini G, Veale DJ, Vonk MC, Walker UA, Chung L, Collier DH, Ellen Csuka M, Fessler BJ, Guiducci S, Herrick A, Hsu VM, Jimenez S, Kahaleh B, Merkel PA, Sierakowski S, Silver RM, Simms RW, Varga J, Pope JE. 2013 classification criteria for systemic sclerosis: an American college of rheumatology/European league against rheumatism collaborative initiative. *Ann Rheum Dis* 2013;72:1747–1755.
18. Galiè N, Humbert M, Vachiery JL, Gibbs S, Lang I, Torbicki A, Simonneau G, Peacock A, Vonk Noordegraaf A, Beghetti M, Ghofrani A, Gomez Sanchez MA, Hansmann G, Klepetko W, Lancellotti P, Matucci M, McDonagh T, Pierard LA, Trindade PT, Zompatori M, Hoeper M. 2015 ESC/ERS Guidelines for the diagnosis and treatment of pulmonary hypertension. *Eur Heart J* 2016;37:67–119.
19. Rudski LG, Lai WW, Afilalo J, Hua L, Handschumacher MD, Chandrasekaran K, Solomon SD, Louie EK, Schiller NB. Guidelines for the echocardiographic assessment of the right heart in adults. *J Am Soc Echocardiogr* 2010;23:685–713.
20. Mor-Avi V, Lang RM, Badano LP, Belohlavek M, Cardim NM, Derumeaux G, Galderisi M, Marwick T, Nagueh SF, Sengupta PP, Sicari R, Smiseth OA, Smulevitz B, Takeuchi M, Thomas JD, Vannan M, Voigt JU, Zamorano JL. Current and evolving echocardiographic techniques for the quantitative evaluation of cardiac mechanics. *Eur J Echocardiogr* 2011;12:167–205.
21. Teixeira R, Monteiro R, Garcia J, Baptista R, Ribeiro M, Cardim N, Goncalves L. The relationship between tricuspid regurgitation severity and right atrial mechanics: a speckle tracking echocardiography study. *Int J Cardiovasc Imaging* 2015;31:1125–1135.
22. Laboratories ATSCoPSfCPF. ATS statement: guidelines for the six-minute walk test. *Am J Respir Crit Care Med* 2002;166:111–117.
23. D'Andrea A, D'Alto M, Di Maio M, Vettori S, Benjamin N, Cocchia R, Argiento P, Romeo E, Di Marco G, Russo MG, Valentini G, Calabro R, Bossone E, Grunig E. Right atrial morphology and function in patients with systemic sclerosis compared to healthy controls: a two-dimensional strain study. *Clin Rheumatol* 2016;35:1733–1742.
24. Lewis GD, Bossone E, Naeije R, Grünig E, Saggar R, Lancellotti P, Ghio S, Varga J, Rajagopalan S, Oudiz R, Rubenfire M. Pulmonary vascular hemodynamic response to exercise in cardiopulmonary diseases. *Circulation* 2013;128:1470–1479.
25. Kuppahally SS, Akoum N, Burgon NS, Badger TJ, Kholmovski EG, Vijayakumar S, Rao SN, Blauer J, Fish EN, Dibella EV, Macleod RS, McGann C, Litwin SE, Marrouche NF. Left atrial strain and strain rate in patients with paroxysmal and persistent atrial fibrillation: relationship to left atrial structural remodeling detected by delayed-enhancement MRI. *Circ Cardiovasc Imaging* 2010;3:231–239.
26. Her A-Y, Choi E-Y, Shim CY, Song BW, Lee S, Ha J-W, Rim S-J, Hwang KC, Chang BC, Chung N. Prediction of left atrial fibrosis with speckle tracking echocardiography in mitral valve disease: a comparative study with histopathology. *Korean Circ J* 2012;42:311–318.
27. Karna SK, Rohit MK, Wanchu A. Right ventricular thickness as predictor of global myocardial performance in systemic sclerosis: a Doppler tissue imaging study. *Indian Heart J* 2015;67:521–528.
28. Fenster BE, Holm KE, Weinberger HD, Moreau KL, Meschede K, Crapo JD, Make BJ, Bowler R, Wamboldt FS, Hoth KF. Right ventricular diastolic function and exercise capacity in COPD. *Respir Med* 2015;109:1287–1292.

Prognostic value of right atrial stiffness in systemic sclerosis

Á. Nógrádi[1], Z. Varga[1], M. Hajdu[1], L. Czirják[2], A. Komócsi[1], R. Faludi[1]

[1]Heart Institute, Medical School, University of Pécs; [2]Department of Rheumatology and Immunology, Medical School, University of Pécs, Hungary.

Abstract

Objective

We hypothesised that right atrial (RA) size and mechanics may have prognostic role in systemic sclerosis (SSc) patients without manifest pulmonary arterial hypertension (PAH), thus we aimed to investigate the prognostic power of RA volume, strain and stiffness parameters alone and when added to the echocardiographic marker of RV longitudinal systolic function.

Methods

Seventy SSc patients (57±12 years) were enrolled into our follow-up study. They underwent standard echocardiographic and tissue Doppler measurements at baseline. In addition to maximal RA volume index, RA reservoir, conduit and contractile strain were measured with 2D speckle tracking technique. RA stiffness was calculated as ratio of TriE/e' to reservoir strain. Survival was assessed after 5 years. All-cause mortality was chosen as outcome. Sequential χ^2 analysis was used to evaluate the incremental prognostic benefit of adding RA volume, strain or stiffness to tricuspid S (TriS).

Results

During the follow-up period of 4.7±0.9 years, 6 patients (8.6%) died. When added to TriS in sequential Cox model, RA stiffness significantly improved the diagnostic performance of the model ($\Delta\chi2$= 3.950; p=0.047) and remained independent predictor of the outcome (HR 2.460 (1.005-6.021); p=0.049). Vmax index and strain parameters did not show incremental prognostic value over TriS. Using ROC analysis, RA stiffness ≥0.156 was the best predictor of mortality (sensitivity=83.3%, specificity =89.1%, AUC=0.859).

Conclusion

RA stiffness is associated with all-cause mortality in SSc patients without PAH independent of and incremental to the RV longitudinal systolic function. It may be proposed as non-invasive marker for identifying patients with high mortality risk.

Key words

systemic sclerosis, prognosis, right atrial function, right atrial stiffness

Ágnes Nógrádi, MD
Zsuzsanna Varga, MD
Máté Hajdu, MD
László Czirják, MD, DSc
András Komócsi, MD, DSc
Réka Faludi, MD, PhD

Please address correspondence to:
Réka Falud,
Heart Institute,
University of Pécs,
Ifjúság u. 13.
H-7624 Pécs, Hungary.
E-mail: faludi.reka@pte.hu

Received on June 5, 2022; accepted in revised form on July 4, 2022.

Competing interests: none declared.

Introduction

Systemic sclerosis (SSc) is a connective tissue disease, characterised by inflammation, microvascular damage, and generalised fibrosis of the skin and various internal organs (1, 2). It has been proved that cardiac manifestation is present in a high proportion of patients and is recognised as powerful adverse prognostic factor (3, 4). Left ventricular diastolic dysfunction is associated with increased risk of mortality in SSc (5-7). Prognostic value of the subclinically impaired left ventricular systolic function has also been reported (8, 9). Predictive power of the right ventricular (RV) longitudinal systolic function is also evident in SSc (8, 9). Impaired right atrial (RA) function has also been reported in this disease, by the help of speckle tracking technique (10-12). Its prognostic value, however, remains to be seen. On the other hand, recent studies suggest, that RA size and mechanics are associated with unfavourable prognosis, not only in patients with idiopathic or connective tissue disease associated pulmonary arterial hypertension (PAH) (13, 14), but also in left heart failure, independently of the left ventricular ejection fraction (15). We thus aimed to investigate the prognostic power of the RA size and function alone and in combination with the RV longitudinal systolic function in SSc patients without manifest PAH.

Methods

Study population

Seventy consecutive patients diagnosed with SSc in the tertiary centre of the Department of Rheumatology and Immunology, Medical School, University of Pécs, Hungary, were enrolled into our follow-up study. They underwent echocardiography during a 9-month period in the year 2015. All cases complied with the updated ACR/EULAR classification criteria (16).

Patients were systematically screened for PAH. Right heart catheterisation was initiated in the presence of abnormalities suggestive of PAH (velocity of tricuspid regurgitation higher than 2.8 m/s or consistent with 2.5-2.8 m/s in the presence of unexplained dyspnoea, signs of right ventricular hypertrophy/dilatation, or a systolic D-sign; disproportional decrease of CO diffusion capacity (DLCO) compared with the forced vital capacity (FVC/DLCO >1.6), and/or DLCO<60% pred) (17). The diagnosis of PAH was based on results obtained by right heart catheterisation (mean pulmonary artery pressure ≥25 mmHg and pulmonary capillary wedge pressure ≤15 mmHg and pulmonary vascular resistance >3 Wood units) (18). Patients with PAH, atrial fibrillation or significant left sided valvular disease were excluded from the study. Detailed medical history was obtained.

Patients were followed for 5 years after the initial investigation with yearly scheduled visits. Patients refusing or not able to attend at the visit were consented for telephone visit for the assessment of the vital status. To avoid misclassification of the cause of death, all-cause mortality was selected as endpoint. Follow-up time was defined as the time between the date of echocardiography and the date of death or the last clinical visit.

The study complied with the Declaration of Helsinki. The institutional ethics committee approved of the study (ref.: 5338). All subjects had given written informed consent prior to inclusion.

Echocardiography

Echocardiography was performed using Philips EPIQ 7G ultrasound system (Philips Healthcare, Best, The Netherlands) by a single investigator. Left ventricular ejection fraction was measured by biplane Simpson's method. Basal, mid-cavity, and longitudinal dimensions of the RV were obtained at end-diastole in RV–focused apical 4-chamber view and corrected for body surface area (BSA). Tricuspid annular plane systolic excursion (TAPSE) and RV fractional area change (RVFAC) were measured, as parameters of the RV systolic function. Maximal and minimal diameters of the inferior vena cava were measured in subxiphoid view. Collapsibility index (the percent decrease in the diameter of inferior vena cava with inspiration) was calculated. RV wall thickness was obtained from subxiphoid view by 2D echocardiography at end-diastole. Se-

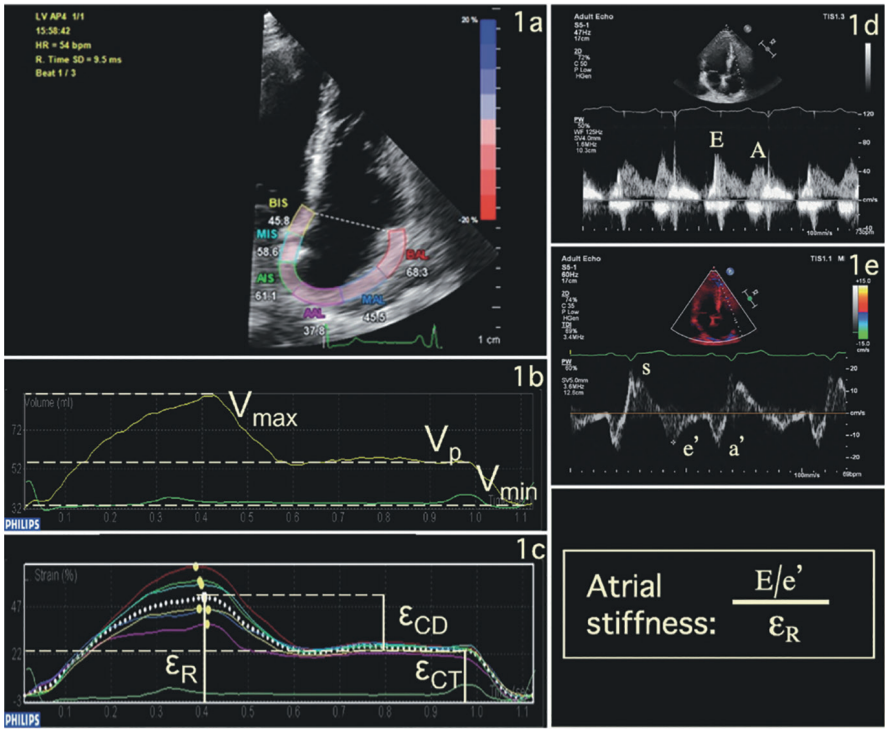

Fig. 1. RV-focused apical 4-chamber view depicting the region of interest **(1a)** and the RA strain curve created by the speckle-tracking software **(1c)**. Using the atrial borders created for speckle-tracking analysis, RA volume curves were generated by the same software **(1b)**. Spectral Doppler curve of the transtricuspid flow **(1d).** Pulsed tissue Doppler curve measured on the lateral border of the tricuspid annulus **(1e)**.
ε_R: RA reservoir strain; ε_{CD}: RA conduit strain; ε_{CT}: RA contractile strain; Vmax: maximal RA volume; Vmin: minimal RA volume; Vp: volume at the beginning of P-wave; E: early-diastolic wave of the tricuspid inflow; A: late-diastolic wave of the tricuspid inflow; systolic (S), early-(e') and late-(a') diastolic myocardial velocities.

verity of tricuspid regurgitation was assessed according to the current recommendations and classified as mild, moderate, or severe. Systolic pulmonary artery pressure was estimated as a sum of the pressure difference across the tricuspid valve (calculated using the modified Bernoulli equation) and an estimate of mean RA pressure (5 to 15 mmHg) using the diameter and collapsibility index of the inferior vena cava (19). In addition to the spectral Doppler parameters of the transmitral and transtricuspid flow (E, A) (Fig. 1d), myocardial systolic (S), early (e') and late (a') diastolic velocities were measured in apical 4-chamber view at the septal and lateral border of the mitral annulus as well as on the lateral border of the tricuspid annulus (Fig. 1e) using pulsed tissue Doppler imaging. Mitral and tricuspid E/A and E/e' ratios were calculated. Doppler measurements were obtained from ≥3 consecutive beats during end-expiratory apnoea. Left ventricular diastolic function was evaluated in accordance with the current recommendation (20). Impaired RV longitudinal systolic function was defined as TriS<10 cm/s (19). Elevated RV filling pressure was diagnosed if TriE/e'> 6 (19).

Right atrial strain and volume measurements

For atrial speckle tracking analysis, RV-focused apical 4-chamber view movies were obtained using 2D echocardiography. Care was taken to obtain true apical images to avoid foreshortening. Image contrast, depth and sector size were adjusted to achieve adequate frame rate (80 and 90 frames/s) and optimise RA border visualisation. Three consecutive heart cycles were recorded digitally. Recordings were processed by a single investigator blinded to standard echocardiographic and clinical data of the patients, using a dedicated software (QLab 10.5, Philips Healthcare, Andover, MA, USA), allowing off-line semi-automated analysis of speckle tracking-based strain (Fig. 1a). The beginning of the QRS was predefined by the software as reference point. The first positive peak of the curve was measured at the end of the reservoir phase, just before tricuspid valve opening (RA reservoir strain). This was followed by a plateau and a second late peak at the peak of the P wave on the electrocardiogram (RA contractile strain). RA conduit strain was defined as the difference between reservoir and contractile strain (21) (Fig. 1c). RA stiffness was calculated as ratio of TriE/e' to RA reservoir strain (22-24).

Using the atrial borders created for speckle tracking analysis, RA volume curves were generated by the same software (Fig. 1b). Volume calculation was based on Simpson's single plane method of disks. Maximal RA volume was measured at the end of T wave on electrocardiogram, just before the opening of the tricuspid valve, and indexed for BSA (RA Vmax index).

Statistical analysis

Categorical data were expressed as frequencies and percentages; continuous data were expressed as the mean ± SD. Comparisons of data between two groups were performed using independent-sample t-tests or Mann-Whitney test for continuous variables and χ^2 tests for categorical variables.

Univariable and multiple Cox proportional-hazards models were applied. Hazard ratios (HR) were calculated with 95% confidence intervals (CI). Models were set up based on variables with $p<0.1$ in univariable analysis. Sequential χ^2 analysis was used to evaluate the incremental prognostic benefit of adding RA volume, strain or stiffness to TriS. C-statistics were applied to compare multivariable Cox models, with values greater than 0.7 representing acceptable models. In order to input them into Cox models, RA stiffness and NT-proBNP data were standardised by calculating a z-score for each value.

Receiver-operating characteristic (ROC) curves were used to examine the diagnostic performance of RA stiffness in predicting all-cause mortality. Area un-

Table I. Clinical characteristics of the entire study population at baseline and data stratified by RA stiffness values.

Variable	All patients (n=70)	RA stiffness <0.156 (n=58)	RA stiffness ≥0.156 (n=12)	*p*
Age (years)	57 ± 12	56 ± 12	64 ± 7	**0.030**
Body surface area (m^2)	1.75 ± 0.19	1.76 ± 0.20	1.74 ± 0.14	0.781
Female gender n (%)	63 (90)	52 (90)	11 (92)	0.833
Disease duration (years)	7.2 ± 5.8	6.8 ± 5.0	8.8 ± 8.7	0.456
Limited cutaneous form n (%)	32 (46)	27 (46.5)	5 (42)	0.757
Modified Rodnan skin score	11.3 ± 8.0	10.8 ± 7.5	14.3 ± 10.1	0.187
Follow-up time (days)	1721 ± 344	1768 ± 234	1491 ± 623	0.155
Death n (%)	6 (9)	1 (2)	5 (42)	**<0.001**
Anti-Centromere Antibody n (%)	18 (26)	14 (24)	4 (33)	0.577
Anti-Topoisomerase I Antibody n (%)	20 (29)	14 (24)	6 (50)	**0.042**
Coronary artery disease n (%)	2 (3)	1 (2)	1 (8.5)	0.211
Systemic arterial hypertension n (%)	36 (51)	30 (52)	6 (50)	0.913
Angiotensin convertase enzyme inhibitors n (%)	33 (47)	29 (50)	4 (33)	0.378
Calcium channel blockers n (%)	36 (51)	28 (48)	8 (67)	0.246
Loop diuretics n (%)	31 (44)	24 (41)	7 (58)	0.282
Mineralocorticoid receptor antagonists n (%)	18 (26)	14 (24)	4 (33)	0.507
New York Heart Association I	20 (28)	19 (33)	1 (8.5)	**0.014**
functional class n (%) II	32 (46)	28 (48)	4 (33)	
III	18 (26)	11 (19)	7 (58.5)	
6-minute walking distance (m)	391 ± 95	405 ± 95	323 ± 61	**0.006**
Modified Borg dyspnoea index	1.7 ± 1.6	1.6 ± 1.6	2.1 ± 1.8	0.286
Erythrocyte sedimentation rate (mm/h)	21.9 ± 16.0	20.9 ± 15.8	26.6 ± 17.3	0.269
C-reactive protein (mg/l)	3.6 ± 5.5	3.3 ± 5.4	4.9 ± 5.9	0.357
Creatinine (μmol/l)	70.6 ± 23.7	70.8 ± 24.7	70.0 ± 18.4	0.919
NT-proBNP (pg/ml)	192.0 ± 163.0	164.4 ± 136.4	325.6 ± 217.6	**0.007**
Troponin-T (ng/l)	12.0 ± 11.2	9.3 ± 7.9	19.5 ± 15.6	0.090
Forced vital capacity (%)	100.5 ± 15.0	101.4 ± 15.4	96.1 ± 12.4	0.265
Diffusing capacity of carbon monoxide (%)	64.5 ± 15.1	67.2 ± 13.9	51.4 ± 14.8	**0.001**

Statistically significant *p*-values ($p<0.05$) are given in bold.

der the curve (AUC) value was calculated. Optimal cut-off value was chosen to maximise sensitivity and specificity. Based on this cut-off value, Kaplan-Meier survival curve was created and differences between groups were tested by Mantel-Cox log rank test.

Prognostic power of concordant *versus* discordant values for TriS and RA stiffness were also evaluated: three groups were created defined by dividing each variable at the cut-off value (high TriS AND low RA stiffness; low TriS OR high RA stiffness; low TriS AND high RA stiffness). Kaplan-Meier survival curve was created and differences between groups were tested by Mantel-Cox log rank test.

To determine intraobserver variability, assessment of RA strain and volume parameters was repeated 2 and 4 weeks after the index measurements in 30 randomly selected patients by the same investigator. To calculate interobserver variability, assessment of RA strain and volume parameters was repeated by another experienced cardiologist in 20 randomly selected patients. Intraobserver and interobserver variability was assessed by the intraclass correlation coefficient.

A *p*-value of <0.05 was considered significant. The data were analysed using IBM SPSS 27 statistical software.

Results

Clinical and echocardiographic characteristics

Seventy SSc patients were enrolled into the study. At baseline, mean age of the study cohort was 57±12 years. 32 (46%) patients had limited cutaneous while 38 (54%) patients had diffuse cutaneous form of the disease. Table I and Table II summarise the clinical and echocardiographic characteristics of the population. Comparison of the echocardiographic data with an age and gender matched healthy population has already been reported (12).

Left ventricular ejection fraction was preserved (≥55%) in 68 (97%) and mildly reduced (45–54%) in 2 (3%) patients. Left ventricular diastolic function was preserved in 20 (28.6%) patients whereas elevated left ventricular filling pressure was found in 15 (21.4%) patients. RV dimensions, RV wall thickness and pulmonary artery pressure values were within the normal range. TriS <10 cm/s were found in 8 (11.4%) patients. TriE/e' suggested elevated RV filling pressure in 22 (31.4%) patients.

Intra- and interobserver variability

Intraclass correlation coefficients for intraobserver variability were 0.91, 0.96, 0.91 and 0.93 for reservoir, contractile and conduit strain and for Vmax, respectively. Regarding interobserver variability, intraclass correlation coefficients for reservoir, contractile and conduit strain and for Vmax were 0.89, 0.88, 0.87 and 0.91, respectively.

Associations of outcome

During the follow-up period of 4.7±0.9 years, 6 patients (8.6%) died. No patient was lost to follow-up.

Among all clinical and laboratory parameters, known coronary artery disease, NT-proBNP, and troponin-T levels showed significant correlation with the outcome whereas 6-minute walking distance and diffusing capacity of carbon monoxide (DLCO) showed borderline significance. Left ventricular ejection fraction not, but the grade of left ventricular diastolic dysfunction showed significant association with all-cause mortality in univariate Cox regression analyses.

In addition to the systolic pulmonary artery pressure, parameters of the RV longitudinal systolic function (TAPSE and TriS) and RV filling pressure (TriE/e') became significant predictors of mortality. RA Vmax index showed significant association with outcome, whereas reservoir and conduit strain parameters of the RA function did not. Regarding contractile strain, the association showed borderline significance. RA stiffness, in contrast, became significant predictor of mortality in univariate analysis. Results of the univariate Cox regression analyses are reported in Table III.

Table II. Echocardiographic characteristics of the entire study population at baseline and data stratified by RA stiffness values.

Variable		All patients (n=70)	RA stiffness <0.156 (n=58)	RA stiffness ≥0.156 (n=12)	*p*
Left ventricular ejection fraction (%)		60.8 ± 4.5	60.7 ± 4.7	60.8 ± 3.8	0.949
Left ventricular diastolic function n (%)	Normal	20 (28.6)	20 (34.5)	0	0.052
	Impaired relaxation	35 (50)	27 (46.5)	8 (66.6)	
	Pseudonormal	15 (21.4)	11 (19)	4 (33.3)	
Grade of tricuspid regurgitation n (%)	Mild	63 (90)	53 (91)	10 (84)	0.445
	Moderate	5 (7)	4 (7)	1 (8)	
	Severe	2 (3)	1 (2)	1 (8)	
Pulmonary arterial systolic pressure (mm Hg)		26.2 ± 5.7	25.1 ± 5.0	30.2 ± 6.8	**0.008**
RV basal diameter index (mm/m^2)		18.4 ± 2.4	18.3 ± 2.6	19.1 ± 1.5	0.287
RV mid-cavity diameter index (mm/m^2)		13.5 ± 2.1	13.4 ± 2.2	13.9 ± 1.4	0.512
RV longitudinal diameter index (mm/m^2)		31.7 ± 3.6	31.8 ± 3.7	31.2 ± 3.2	0.606
Inferior vena cava (mm)		14.0 ± 3.8	14.3 ± 3.5	12.3 ± 4.7	0.119
Collapsibility index (%)		55.5 ± 11.5	55.6 ± 11.8	55.9 ± 9.6	0.910
RV wall thickness (mm)		5.0 ± 1.0	5.0 ± 1.0	5.0 ± 1.1	0.894
RVFAC (%)		47.5 ± 7.2	47.9 ± 6.0	46.0 ± 11.4	0.426
TAPSE (mm)		21.1 ± 2.6	21.6 ± 2.3	18.8 ± 3.0	**0.001**
Tricuspid E (cm/s)		47.5 ± 9.2	46.7 ± 9.7	51.4 ± 5.2	0.101
Tricuspid A (cm/s)		39.5 ± 8.8	38.0 ± 8.0	46.6 ± 9.2	**0.002**
Tricuspid e' (cm/s)		9.5 ± 2.3	10.1 ± 2.4	6.9 ± 1.2	**<0.001**
Tricuspid a' (cm/s)		13.2 ± 2.6	13.5 ± 2.5	12.0 ± 2.4	0.074
Tricuspid S (cm/s)		12.4 ± 2.3	12.8 ± 2.1	10.4 ± 2.2	**0.001**
Tricuspid E/e'		5.3 ± 1.5	4.8 ± 1.1	7.6 ± 1.2	**<0.001**
RA size and function					
RA Vmax index (mL/m^2)		19.4 ± 5.5	18.8 ± 4.8	22.6 ± 7.8	0.171
RA reservoir strain (%)		49.3 ± 10.7	50.5 ± 10.2	43.6 ± 11.4	**0.041**
RA contractile strain (%)		22.9 ± 5.8	23.0 ± 5.1	22.5 ± 8.4	0.770
RA conduit strain (%)		26.8 ± 8.1	27.6 ± 7.5	22.9 ± 10.0	0.066
RA stiffness		0.112 ± 0.039	0.098 ± 0.024	0.180 ± 0.021	**<0.001**

When added to TriS in sequential Cox model, RA stiffness significantly improved the diagnostic performance of the model ($\Delta\chi^2$= 3.950; p=0.047) and remained independent predictor of the outcome (HR 2.460 (1.005-6.021); p=0.049). In contrast, Vmax index and RA contractile strain did not show incremental prognostic value over TriS in the χ^2 model (Table IV).

Discriminative ability of RA stiffness

To demonstrate the performance of RA stiffness in predicting all-cause mortality, ROC curve was created, with an AUC of 0.859. The optimal cut-off point for predicting all-cause mortality was 0.156. Patients with RA stiffness equal or above this cut-off value had significantly higher risk for death (log-rank p<0.001). ROC curve and Kaplan-Meier cumulative survival curve demonstrating the predictive power of the RA stiffness are presented in Figure 2.

Clinical and echocardiographic characteristics of the study cohort stratified by the cut-off RA stiffness value are shown in Table I and Table II. Patients with elevated RA stiffness were significantly older and their walking distance was significantly shorter compared with the other subgroup. Significantly higher NT-proBNP levels whereas significantly lower DLCO values were found in these patients. Anti-topoisomerase I antibody positivity was also more common in this subgroup.

Left ventricular ejection fraction values were similar in the two subgroups. Patients with high RA stiffness exhibited worse left ventricular diastolic function, though this difference has borderline significance. Global RV systolic function (RVFAC) was preserved in both subgroups. Parameters reflecting the RV longitudinal systolic function (TAPSE, TriS), however, were significantly lower in patients with RA stiffness above the cut-off. Significantly lower Trie' and higher TriE/e' values were also found in these patients. Systolic pulmonary artery pressure was significantly higher in this subgroup, but still within the normal range.

Incremental prognostic value of RA stiffness

When evaluated by comparing groups above and below the cut-off value (10 cm/s for TriS and 0.156 for RA stiffness) for each parameter, patients with high TriS AND low RA stiffness (n=55) showed the lowest mortality rate (1 event (1.8%)). Compared with this reference group, patients with low TriS OR high RA stiffness (n=10) had significantly higher mortality rate (2 events (20%); log-rank p=0.008) whereas the highest mortality rate was observed in patients with low TriS AND elevated RA stiffness (n=5, 3 events (60%), log-rank p<0.001) (Fig. 3).

Discussion

SSc is a connective tissue disease characterised by vascular abnormalities and diffuse fibrosis of the skin and various internal organs (1, 2). Cardiac involvement implies poor prognosis in SSc (3, 4), thus its early recognition would be crucial, with non-invasive tools allowing pre-clinical identification of the damages. Novel echocardiographic techniques, such as tissue Doppler imaging or speckle tracking based strain measurements may provide useful information about the early myocardial involvement in this disease.

Myocardial fibrosis may lead to left ventricular diastolic dysfunction, which is highly prevalent in SSc and is associated with increased risk of mortality (5-7). Prognostic value of the increased left atrial volume was also reported (6). Myocardial fibrosis may also eventuate in subclinically impaired left ventricular systolic function (9, 25, 26). Both speckle tracking-derived left ventricular global longitudinal (9) and circumferential strain (8) showed significant associations with the outcome in this condition. Nevertheless, in SSc myocardial mechanics is impaired not only in the left, but also in the right heart (27). Both TriS (8) and TAPSE (9) showed significant, independent association with the adverse outcome.

After decades of focusing on ventricular function, nowadays more attention

Table III. Univariate Cox regression analysis of associations with all-cause mortality in patients with SSc.

Variable	HR (95% CI)	*p*
Clinical characteristics		
Age (years)	1.029 (0.951-1.113)	0.472
Body surface area (m^2)	0.278 (0.003-28.131)	0.587
Female gender	0.502 (0.059-4.298)	0.529
Disease duration (years)	1.049 (0.935-1.177)	0.415
Limited cutaneous form	0.350 (0.063-1.940)	0.229
Modified Rodnan skin score	1.047 (0.957-1.146)	0.314
Anti-Centromere Antibody positivity	1.490 (0.273-8.140)	0.645
Anti-Topoisomerase I Antibody positivity	2.136 (0.427-10.676)	0.355
Coronary artery disease	10.170 (1.171-88.354)	**0.035**
Systemic arterial hypertension	1.082 (0.215-5.442	0.923
Angiotensin convertase enzyme inhibitor use	0.844 (0.169-4.216)	0.837
Calcium channel blocker use	5.244 (0.612-44.952)	0.131
Loop diuretics use	1.469 (0.269-8.024)	0.657
Mineralocorticoid receptor antagonist use	2.939 (0.593-14.569)	0.187
New York Heart Association functional class	2.380 (0.714-7.938)	0.158
6-minute walking distance (m)	0.993 (0.985-1.001)	*0.079*
Modified Borg dyspnoea index	1.171 (0.763-1.798)	0.469
Erythrocyte sedimentation rate (mm/h)	0.996 (0.945-1.050)	0.885
C-reactive protein (mg/l)	0.979 (0.824-1.163)	0.809
Creatinine (μmol/l)	0.999 (0.963-1.037)	0.969
NT-proBNP (pg/ml)	2.447 (1.299-4.609)	**0.006**
Troponin-T (ng/l)	1.070 (1.024-1.118)	**0.003**
Forced vital capacity (%)	0.972 (0.911-1.036)	0.382
Diffusing capacity of carbon monoxide (%)	0.956 (0.912-1.002)	*0.061*
Echocardiographic characteristics		
Left ventricular ejection fraction (%)	1.007 (0.840-1.206)	0.942
Grade of left ventricular diastolic dysfunction	6.751 (1.428-31.909)	**0.016**
Grade of tricuspid regurgitation	3.113 (1.330-7.283)	**0.009**
Pulmonary arterial systolic pressure (mm Hg)	1.130 (1.003-1.272)	**0.044**
RV basal diameter index (mm/m^2)	1.167 (0.862-1.579)	0.318
RV mid-cavity diameter index (mm/m^2)	1.154 (0.792-1.682)	0.455
RV longitudinal diameter index (mm/m^2)	1.111 (0.897-1.376)	0.334
Inferior vena cava (mm)	1.026 (0.812-1.295)	0.832
Collapsibility index (%)	1.053 (0.961-1.153)	0.272
RV wall thickness (mm)	0.953 (0.436-2.080)	0.903
RVFAC (%)	0.976 (0.867-1.099)	0.689
TAPSE (mm)	0.638 (0.445-0.914)	**0.014**
Tricuspid E (cm/s)	1.039 (0.969-1.114)	0.282
Tricuspid A (cm/s)	1.049 0.976-1.127)	0.192
Tricuspid e' (cm/s)	0.735 (0.492-1.100)	0.134
Tricuspid a' (cm/s)	0.676 (0.439-1.043	*0.077*
Tricuspid S (cm/s)	0.548 (0.355-0.848)	**0.007**
Tricuspid E/e'	2.002 (1.220-3.285)	**0.006**
RA size and function		
RA Vmax index (mL/m^2)	1.202 (1.061-1.362)	**0.004**
RA reservoir strain (%)	0.952 (0.874-1.036)	0.253
RA contractile strain (%)	0.839 (0.690-1.020)	*0.079*
RA conduit strain (%)	0.978 (0.877-1.091)	0.690
RA stiffness	3.185 (1.544-6.570)	**0.002**

Statistically significant *p*-values ($p<0.05$) are given in bold. $0.05 \leq p < 0.1$ values are given in italics.

is given to the atrial size and mechanics. Lindqvist *et al*. found enlarged RA area in SSc patients without manifest PAH (28). Similarly, D'Andrea *et al*. reported significant enlargement of the RA area compared with healthy subjects (11), while Durmus *et al*. found RA area index values similar to those in healthy persons (10). Significantly decreased RA segmental strain values were reported by D'Andrea *et al*. in SSc patients, especially in those with pulmonary fibrosis (11). Durmus *et al*. found decreased reservoir and conduit strain values compared to a healthy control population (10). The previous findings of our group were in line with the results of Durmus *et al*.: RA volume values were similar in SSc patients without manifest PAH and in the control group, but significantly decreased reservoir and conduit strain values were found in the SSc group. Contractile strain values did not differ between SSc group and healthy persons (12). Despite these data, the prognostic value of RA size and mechanics has never been investigated in SSc.

Recent studies suggested, however, that RA size and mechanics are associated with unfavourable prognosis in patients with idiopathic or connective tissue disease associated PAH (13, 14). In addition, Jain *et al*. proved, that RA reservoir and conduit strain are independent predictors of mortality in left heart failure with both preserved and reduced ejection fraction (15).

Thus, we hypothesised that RA size and mechanics may have prognostic role even in SSc patients without manifest PAH and aimed to investigate the prognostic power of the RA volume, strain and stiffness parameters alone and when added to the echocardiographic marker of the RV longitudinal systolic function.

In univariate Cox regression analysis RA Vmax index and RA stiffness showed significant association with 5-year all-cause mortality, whereas RA contractile strain showed borderline significance with the outcome. When added to TriS in sequential Cox model, RA stiffness significantly improved the diagnostic performance of the model and remained independent predictor of the outcome. Our data support the strong prognostic value of RA stiffness in SSc patients without manifest PAH. RA stiffness is a complex parameter reflecting atrial mechanics and RV filling pressure simultaneously. This may explain its superiority over the RA volume and strain parameters.

Atrial stiffness is a novel echocardiographic parameter of the atrial performance. It represents the change in pressure required to increase the volume of the atrium in a given measure (22, 23). The diagnostic role of this parameter was first described in the left heart: Kurt *et al*. reported left atrial stiffness as an accurate index to distinguish diastolic heart failure patients from those with

Table IV. Models of sequential Cox regression analysis for predicting outcome in SSc.

		Model 1	Model 2	Model 3
C-statistics	0.721	0.737	0.820	0.849
$\Delta\chi^2$		2.376; p=0.123	2.536; p=0.111	3.950; ***p*=0.047**
Variables in model	**HR (95%CI) *p*-value**	**HR (95%CI) *p*-value**	**HR (95%CI) *p*-value**	**HR (95%CI) *p*-value**
Tricuspid S (cm/s)	0.548 (0.355-0.848); ***p*=0.007**	0.687 (0.421-1.122); p=0.134	0.599 (0.399-0.901); ***p*=0.014**	0.768 (0.464-1.271); p=0.304
RA Vmax index (ml/m^2)		1.114 (0.967-1.283); p=0.135		
RA contractile strain (%)			0.867 (0.716-1.049); p=0.141	
RA stiffness				2.460 (1.005-6.021); ***p*=0.049**

C-statistics represents the overall performance of the predictive model. $\Delta\chi^2$ reflects the incremental prognostic value of the RA variables over TriS, when added to the model. Statistically significant p-values (p<0.05) are given in bold.

asymptomatic diastolic dysfunction (22). In the study of Porpáczy *et al*. left atrial stiffness was superior to left atrial Vmax index and reservoir strain in predicting elevated NT-proBNP levels in SSc patients (29). In the right heart, Teixeira et al. demonstrated increased RA stiffness in patients with left heart failure (24). Besides, in our previous study, RA stiffness was proved to be significantly elevated in SSc patients, compared with healthy subjects, and showed significant correlation with the functional capacity of the patients (12). In the study of Pilichowska-Paszkiet *et al*. fibrosis of the left atrial wall was detected by electroanatomical mapping. Left atrial stiffness showed robust correlation with the extent of this fibrosis in patients with atrial fibrillation (30). Similar histopathologic evidence is not available in the right heart. Still, elevated RA stiffness may represent the extent of the replacement fibrosis affecting the RA wall, as it was reported in the left heart (31).

In SSc, impairment of the RV function and the subsequent RA dysfunction and dilatation are traditionally attributed to the development of PAH or PH due to severe pulmonary fibrosis (32). Similar findings, however, has been proved in SSc patients even without the resting elevation of the pulmonary pressure (8-10, 12, 27, 28). In SSc patients without resting PAH, RV myocardial dysfunction may be considered as the sign of the primary myocardial involvement of the disease (27). On the other hand, in SSc patients with interstitial lung disease or subclinical pulmonary vascular disease, the subclinical elevation of the pulmonary vascular resistance may be unmasked by exercise, when pulmonary circulation no longer has the capacity to adapt, and the pulmonary pressure increases parallel with the increasing cardiac output (33). This exercise-induced, intermittent pressure overload may also lead to ultrastructural changes in the right heart (27, 28). In addition, independently from the aetiology, left ventricular diastolic dysfunction is often associated with impaired mechanics of the right heart. This phenomenon is thought to be explained by the exercise-induced elevation of left ventricular filling pressure and the con-

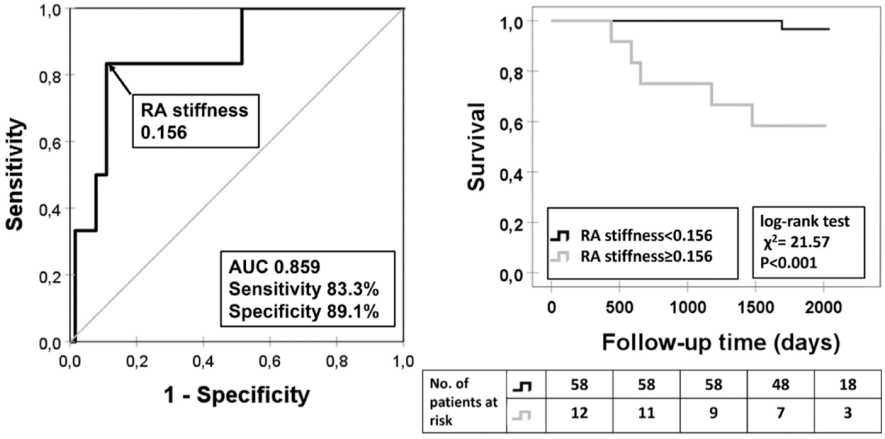

Fig. 2. ROC curve and Kaplan-Meier survival curve demonstrating the performance of RA stiffness in predicting all-cause mortality.

Fig. 3. Kaplan-Meier survival curve demonstrating the incremental prognostic value of RA stiffness when added to TriS in predicting all-cause mortality. The cohort was stratified by the TriS and RA stiffness profile of the patients.

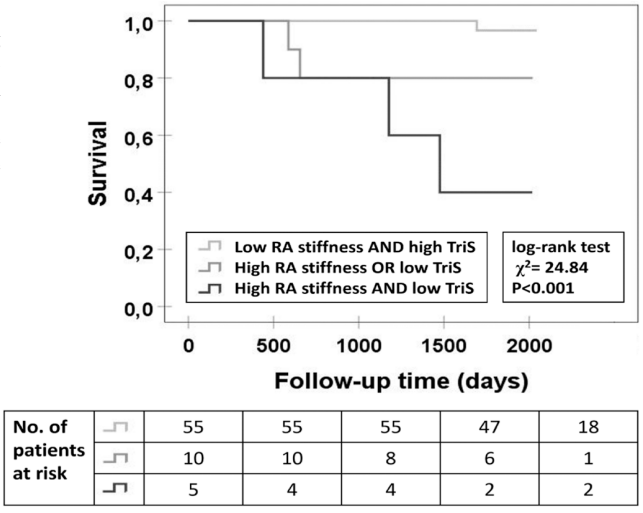

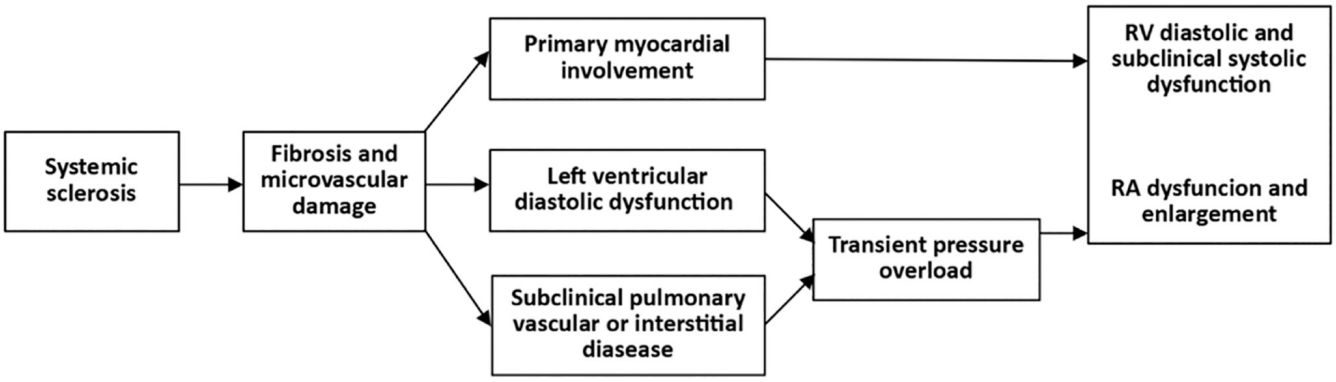

Fig. 4. Mechanisms involved in the development of RA dysfunction and enlargement in SSc patients without manifest PAH.

sequential elevation of the pulmonary artery pressure (34) (Fig. 4).

When stratified by RA stiffness cut-off, our data may support all these hypotheses: high risk patient with RA stiffness above the cut-off exhibited significantly higher pulmonary arterial systolic pressure (but still within the normal range) and significantly lower DLCO values. Besides, there was a clear tendency suggesting worse left ventricular diastolic function in the high-risk subgroup, though the difference was not statistically significant. Diagnostic and prognostic utility of the well know cardiac biomarkers, NT-proBNP and troponin-T has already been proved in SSc (35-37). Patient with RA stiffness above the cut-off showed significantly higher NT-proBNP values. Troponin-T level was also higher in this subgroup, albeit the differences were not statistically significant. Anti-topoisomerase I antibody positivity was also significantly more common in the high-risk subgroup. The potential clinical significance of this antibody level has been reported in evaluating disease severity and prognosis in SSc (38, 39).

Limitations of the study

Our data should be interpreted in the context of their limitations. First, the statistical power of our analysis is limited by the relatively low number of participants and events. Our results require further validation in a larger SSc population. For obtaining RA strain values, we used a software that was developed for left ventricular strain analysis because a dedicated software for atrial strain estimation was not available. RV strain may better reflect the subclinical impairment of the RV systolic function than our traditional and tissue Doppler parameters. Nevertheless, in the lack of appropriate analytical software, RV strain analysis was not performed in our study.

Conclusion

RA stiffness is associated with all-cause mortality in SSc patients without PAH independent of and incremental to the RV longitudinal systolic function. It may be proposed as a non-invasive marker for identifying SSc patients with high mortality risk.

Acknowledgments

The authors would like to thank József Kiss-Meirosu for his help in editing graphs and pictures.

References

1. GABRIELLI A, AVVEDIMENTO EV, KRIEG T: Scleroderma. *N Engl J Med* 2009; 360: 1989-2003. https://doi.org/10.1056/NEJMra0806188.
2. DI BATTISTA M, BARSOTTI S, ORLANDI M *et al*.: One year in review 2021: systemic sclerosis. *Clin Exp Rheumatol* 2021; 39 (Suppl. 131): S3-12. https://doi.org/10.55563/clinexprheumatol/izadb8.
3. KOMÓCSI A, VOROBCSUK A, FALUDI R *et al*.: The impact of cardiopulmonary manifestations on the mortality of SSc: a systematic review and meta-analysis of observational studies. *Rheumatology* (Oxford) 2012; 51: 1027-36. https://doi.org/10.1093/rheumatology/ker357.
4. HSU VM, CHUNG L, HUMMERS LK *et al*.: Risk factors for ortamlity and cardiopulmonary hospitalization in systemic sclerosis patients at risk for pulmonary hypertension, in the PHAROS Registry. *J Rheumatol* 2019; 46: 176-83. https://doi.org/10.3899/jrheum.180018.
5. HINCHCLIFF M, DESAI CS, VARGA J, SHAH SJ: Prevalence, prognosis, and factors associated with left ventricular diastolic dysfunction in systemic sclerosis. *Clin Exp Rheumatol* 2012; 30 (Suppl. 71): S30-7.
6. FALUDI R, KÖLTŐ G, BARTOS B, CSIMA G, CZIRJÁK L, KOMÓCSI A: Five-year follow-up of left ventricular diastolic function in systemic sclerosis patients: determinants of mortality and disease progression. *Semin Arthritis Rheum* 2014; 44: 220-7. https://doi.org/10.1016/j.semarthrit.2014.04.001.
7. TENNØE AH, MURBRÆCH K, ANDREASSEN JC *et al*.: Left ventricular diastolic dysfunction predicts mortality in patients with systemic sclerosis. *J Am Coll Cardiol* 2018; 72: 1804-13. https://doi.org/10.1016/j.jacc.2018.07.068.
8. SAITO M, WRIGHT L, NEGISHI K, DWYER N, MARWICK TH: Mechanics and prognostic value of left and right ventricular dysfunction in patients with systemic sclerosis. *Eur Heart J Cardiovasc Imaging* 2018; 19: 660-7. https://doi.org/10.1093/ehjci/jex147.
9. TENNØE AH, MURBRÆCH K, ANDREASSEN JC *et al*.: Systolic dysfunction in systemic sclerosis: Prevalence and prognostic implications. *ACR Open Rheumatol* 2019; 1: 258-66. https://doi.org/10.1002/acr2.1037.
10. DURMUS E, SUNBUL M, TIGEN K *et al*.: Right ventricular and atrial functions in systemic sclerosis patients without pulmonary hypertension: Speckle-tracking echocardiographic study. *Herz* 2015; 40: 709-15. https://doi.org/10.1007/s00059-014-4113-2.
11. D'ANDREA A, D'ALTO M, DI MAIO M *et al*.: Right atrial morphology and function in patients with systemic sclerosis compared to healthy controls: a two-dimensional strain study. *Clin Rheumatol* 2016; 35: 1733-42. https://doi.org/10.1007/s10067-016-3279-9
12. NÓGRÁDI A, PORPÁCZY A, PORCSA L *et al*.: Relation of right atrial mechanics to functional capacity in patients with systemic sclerosis. *Am J Cardiol* 2018; 122: 1249-54. https://doi.org/10.1016/j.amjcard.2018.06.021.
13. BAI Y, YANG J, LIU J, NING H, ZHANG R: Right atrial function for the prediction of prognosis in connective tissue disease-associated pulmonary arterial hypertension: a study with two-dimensional speckle tracking. *Int J Cardiovasc Imaging* 2019; 35: 1637-49. https://doi.org/10.1007/s10554-019-01613-w.
14. HASSELBERG NE, KAGIYAMA N, SOYAMA Y *et al*.: The prognostic value of right atrial

strain imaging in patients with precapillary pulmonary hypertension. *J Am Soc Echocardiogr* 2021; 34: 851-861.e1. https://doi.org/10.1016/j.echo.2021.03.007.
15. JAIN S, KURIAKOSE D, EDELSTEIN I *et al*.: Right atrial phasic function in heart failure with preserved and reduced ejection fraction. *JACC Cardiovasc Imaging* 2018; 12: 1460-70. https://doi.org/10.1016/j.jcmg.2018.08.020.
16. VAN DEN HOOGEN F, KHANNA D, FRANSEN J *et al*.: 2013 classification criteria for systemic sclerosis: an American College of Rheumatology/European League Against Rheumatism collaborative initiative. *Ann Rheum Dis* 2013; 72: 1747-55. https://doi.org/10.1136/annrheumdis-2013-204424.
17. SCHWAIGER JP, KHANNA D, GERRY COGHLAN J: Screening patients with scleroderma for pulmonary arterial hypertension and implications for other at-risk populations. *Eur Respir Rev* 2013; 22: 515-25. https://doi.org/10.1183/09059180.00006013.
18. GALIÈ N, HUMBERT M, VACHIERY JL *et al*.: 2015 ESC/ERS Guidelines for the diagnosis and treatment of pulmonary hypertension. *Eur Heart J* 2016; 37: 67-119. https://doi.org/10.5603/KP.2015.0242.
19. RUDSKI LG, LAI WW, AFILALO J *et al*.: Guidelines for the echocardiographic assessment of the right heart in adults. *J Am Soc Echocardiogr* 2010; 23: 685-713. https://doi.org/10.1016/j.echo.2010.05.010.
20. NAGUEH SF, SMISETH OA, APPLETON CP *et al*.: Recommendations for the evaluation of left ventricular diastolic function by echocardiography. *J Am Soc Echocardiogr* 2016; 29: 277-314. https://doi.org/10.1016/j.echo.2016.01.011.
21. BADANO LP, KOLIAS TJ, MURARU D *et al*.: Standardization of left atrial, right ventricular, and right atrial deformation imaging using two-dimensional speckle tracking echocardiography: a consensus document of the EACVI/ASE/Industry Task Force to standardize deformation imaging. *Eur Heart J Cardiovasc Imaging* 2018; 19(6): 591-600. https://doi.org/10.1093/ehjci/jey042.
22. KURT M, WANG J, TORRE-AMIONE G, NAGUEH SF: Left atrial function in diastolic heart failure. *Circ Cardiovasc Imaging* 2009; 2: 10-5. https://doi.org/10.1161/CIRCIMAGING.108.813071.
23. CAMELI M, MANDOLI GE, LOIACONO F, DINI FL, HENEIN M, MONDILLO S: Left atrial strain: a new parameter for assessment of left ventricular filling pressure. *Heart Fail Rev* 2016; 21: 65-76. https://doi.org/10.1007/s10741-015-9520-9.
24. TEIXEIRA R, MONTEIRO R, GARCIA J *et al*.: The relationship between tricuspid regurgitation severity and right atrial mechanics: a speckle tracking echocardiography study. *Int J Cardiovasc Imaging* 2015; 31: 1125-35. https://doi.org/10.1007/s10554-015-0663-5.
25. SPETHMANN S, DREGER H, SCHATTKE S *et al*.: Two-dimensional speckle tracking of the left ventricle in patients with systemic sclerosis for an early detection of myocardial involvement. *Eur Heart J Cardiovasc Imaging* 2012; 13: 863-70. https://doi.org/10.1093/ehjci/jes047.
26. VAN WIJNGAARDEN SE, BEN SAID-BOUYERI S, NINABER MK *et al*.: Progression of left ventricular myocardial dysfunction in systemic sclerosis: A speckle-tracking strain echocardiography study. *J Rheumatol* 2019; 46: 405-15. https://doi.org/10.3899/jrheum.171207.
27. MEUNE C, KHANNA D, ABOULHOSN J *et al*.: A right ventricular diastolic impairment is common in systemic sclerosis and is associated with other target-organ damage. *Semin Arthritis Rheum* 2016; 45: 439-45. https://doi.org/10.1016/j.semarthrit.2015.07.002.
28. LINDQVIST P, CAIDAHL K, NEUMAN-ANDERSEN G *et al*.: Disturbed right ventricular diastolic function in patients with systemic sclerosis: A Doppler tissue imaging study. *Chest* 2005; 128: 755-63. https://doi.org/10.1378/chest.128.2.755.
29. PORPÁCZY A, NÓGRÁDI Á, VÉRTES V *et al*.: Left atrial stiffness is superior to volume and strain parameters in predicting elevated NT-proBNP levels in systemic sclerosis patients. *Int J Cardiovasc Imaging* 2019; 35: 1795-802. https://doi.org/10.1007/s10554-019-01621-w.
30. PILICHOWSKA-PASZKIET E, BARAN J, SYGITOWICZ G *et al*.: Noninvasive assessment of left atrial fibrosis. Correlation between echocardiography, biomarkers, and electroanatomical mapping. *Echocardiography* 2018; 35: 1326-34. https://doi.org/10.1111/echo.14043.
31. BISBAL F, BARANCHUK A, BRAUNWALD E, BAYÉS DE LUNA A, BAYÉS-GENÍS A: Atrial failure as a clinical entity. *J Am Coll Cardiol* 2020; 75: 222-32. https://doi.org/10.1016/j.jacc.2019.11.013.
32. YIU KH, NINABER MK, KROFT LJ *et al*.: Impact of pulmonary fibrosis and elevated pulmonary pressures on right ventricular function in patients with systemic sclerosis. *Rheumatology* (Oxford) 2016; 55: 504-12. https://doi.org/10.1093/rheumatology/kev342.
33. LEWIS GD, BOSSONE E, NAEIJE R *et al*.: Pulmonary vascular hemodynamic response to exercise in cardiopulmonary diseases. *Circulation* 2013; 128: 1470-9. https://doi.org/10.1161/CIRCULATIONAHA.112.000667.
34. BRAND A, BATHE M, OERTELT-PRIGIONE S *et al*.: Right heart function in impaired left ventricular diastolic function: 2D speckle tracking echocardiography-based and Doppler tissue imaging-based analysis of right atrial and ventricular function. *Echocardiography* 2018; 35: 47-55. https://doi.org/10.1111/echo.13745.
35. ALLANORE Y, KOMÓCSI A, VETTORI S *et al*.: N-terminal pro-brain natriuretic peptide is a strong predictor of mortality in systemic sclerosis. *Int J Cardiol* 2016; 223: 385-9. https://doi.org/10.1016/j.ijcard.2016.08.246.
36. KÖLTŐ G, VUOLTEENAHO O, SZOKODI I *et al*.: Prognostic value of N-terminal natriuretic peptides in systemic sclerosis: a single centre study. *Clin Exp Rheumatol* 2014; 32 (Suppl. 86): S75-81.
37. PAIK JJ, CHOI DY, MUKHERJEE M *et al*.: Troponin elevation independently associates with mortality in systemic sclerosis. *Clin Exp Rheumatol* 2022; 40(10): 1933-40. https://doi.org/10.55563/clinexprheumatol/fytfmy.
38. SATO S, HAMAGUCHI Y, HASEGAWA M, TAKEHARA K: Clinical significance of anti-topoisomerase I antibody levels determined by ELISA in systemic sclerosis. *Rheumatology* (Oxford) 2001; 40: 1135-40. https://doi.org/10.1093/rheumatology/40.10.1135.
39. VAN LEEUWEN NM, WORTEL CM, FEHRES CM *et al*.: Association between centromere- and topoisomerase-specific immune responses and the degree of microangiopathy in systemic sclerosis. *J Rheumatol* 2021; 48: 402-9. https://doi.org/10.3899/jrheum.191331.